Oncology Treatment Discovery

Editors-in-Chief

Vincent J. Cogliano

U.S. Environmental Protection Agency, USA

Chong Li

Chinese Academy of Sciences, China

BIO-BYWORD SCIENTIFIC PUBLISHING PTY LTD
(619 649 400)
Level 10
50 Clarence Street
SYDNEY NSW 2000
Copyright © 2026. Bio-Byword Scientific Publishing Pty Ltd.
Complimentary Copy

Oncology Treatment Discovery

Focus and Scope

Oncology Treatment Discovery is a peer-reviewed, open access journal. It accepts manuscripts relevant to experimental and clinical cancer research. The journal publishes the latest findings in cancer research, including preliminary results, repeated argumentation studies and negative results. The journal welcomes various types of submissions, e.g. research papers, clinical research reports, review articles. Content covers topics that advance clinical practice, challenge the status quo, advocate change in health policy, genomic instability, growth promoting signals, growth inhibitory signals, cell death, tumour microenvironment, carcinogenesis and cancer prevention and tackle issues related to global oncology.

About Publisher

Bio-Byword Scientific Publishing is a fast-growing, peer-reviewed and open access journal publisher, which is located in Sydney, Australia. As a dependable and credible corporation, it promotes and serves a broad range of subject areas for the benefit of humanity. By informing and educating a global community of scholars, practitioners, researchers and students, it endeavors to be the world's leading independent academic and professional publisher. To realize it, it keeps creative and innovative to meet the range of the authors' needs and publish the best of their work.

By cooperating with University of Sydney, University of New South Wales and other world-famous universities, Bio-Byword Scientific Publishing has established a huge publishing system based on hundreds of academic programs, and with a variety of journals in the subjects of medicine, construction, education and electronics.

Publisher Headquarter

BIO-BYWORD SCIENTIFIC PUBLISHING PTY LTD
Level 10
50 Clarence Street
Sydney NSW 2000
Website: www.bbwpublisher.com
Email: info@bbwpublisher.com

2026, Volume 4, Issue 3

Table of Contents

1 **A Study on the Quantitative Evaluation of the Invasiveness of Lung Adenocarcinoma Based on the Texture Features of Pulmonary Nodules Using United Imaging uCT968 Ultra-High-End CT**
Man Zhang

9 **Mutational Landscape and Clinicopathological Correlates of 553 Chinese Colorectal Cancer Cases Assessed by 116-Gene Targeted Sequencing**
Yitong Liu, Jianglin Li, Mingfeng Wu, Zidan Luo, Yiyun Sun, Xinyu Chen, Enle Zhou

23 **Research on the High-quality Development Path of Tumor Prevention and Control in Frontier Minority Counties under the Background of Public Hospital Reform-based on the Empirical Analysis of Lufeng City**
Ruyan Liu, Manchang Li, Fayuan Pu, Guolin Li, Jiantao Dong, Yinting Lu

33 **Research Progress of TMEM2 in Extracellular Matrix Remodeling and Tumor Microenvironment Regulation**
Yiyun Sun, Mingfeng Wu, Zidan Luo, Xinyu Chen, Enle Zhou, Ping Dong

48 **Artificial Intelligence Risk Prediction Model for PICC Catheter-related Venous Thrombosis in Cancer Patients: A Systematic Review**
Xi Yang, Rui Wang, Qinglan Fu, Lanying Qiu, Xiaowei Fu

62 **Mechanisms of Lactate and Targeted Therapeutic Strategies in the Colorectal Cancer Microenvironment**
Zijie Yang, Chao Chen, Yinhua Zhang

70 **A Study on the Diagnostic Value of Multimodal MRI in Assessing Early Radiation-Induced Brain Injury Following Intensity-Modulated Radiation Therapy for Nasopharyngeal Carcinoma**
Jingyin Ma, Xueping Zheng, Ning Zhai, Chengtong Zhu, Ying Wang, Yun Ren, Feifei Lu

79 **A Study on the Patterns of Recurrence of Liver Metastases after Curative Surgery for Gastric Cancer, Based on the SEER Database**
Wei Xu , Yue Qiu, Shiqi Zhang, Caiyue Gao, Xiaoyan Wang, Changfeng Man, Yu Fan

89 **Study on the Application Value of Teleradiology in Primary-Level Imaging Services Under the Medical Alliance Model**
Chungeng Tang, Xingxiong Zou, Jie Zhang, Menghong Zou, Ruohan Feng, Tao Li, Kang Zhou, Hui Li, Chunlei Jia, Hongwei Li

99 **Application of an MMHEM-Based Postoperative Transitional Care Program in Patients After Laryngeal Cancer Surgery**
Qingsi Chen, Liqin Lin

Oncology Treatment Discovery, 2026, Volume 4, Issue 3
https://bbwpublisher.com/journal/OTD
Online ISSN: 2981-8079
Print ISSN: 3083-4996

A Study on the Quantitative Evaluation of the Invasiveness of Lung Adenocarcinoma Based on the Texture Features of Pulmonary Nodules Using United Imaging uCT968 Ultra-High-End CT

Man Zhang*

Xiangyang Hospital of Traditional Chinese Medicine, Xiangyang 441000, Hubei, China

****Author to whom correspondence should be addressed.***

Copyright: © 2026 Author(s). This is an open-access article distributed under the terms of the Creative Commons Attribution License (CC BY 4.0), permitting distribution and reproduction in any medium, provided the original work is cited.

Abstract: *Objective*: To explore the quantitative evaluation of the invasiveness of lung adenocarcinoma based on the texture features of pulmonary nodules using United Imaging uCT968 ultra-high-end CT. *Methods*: A total of 100 patients with pulmonary mixed ground-glass nodules confirmed by pathological examination after lung surgery in our hospital from December 2024 to December 2025 were selected. Based on whether the lesion invaded the surrounding tissues, minimally invasive cancer and invasive cancer were classified into the invasive group, while benign lesions and carcinoma in situ were classified into the non-invasive group. Both groups underwent CT examinations in our hospital. Clinical data and CT texture features were compared between the two groups. Logistic regression analysis was used to identify factors influencing the invasiveness of pulmonary nodules and to predict the diagnostic efficacy for pulmonary nodule invasion. *Results*: There were no statistically significant differences between the two groups in terms of gender, clinical stage, maximum lesion diameter, spiculation sign, lobulation sign, air bronchogram, and average CT value of the lesion ($P > 0.05$). Statistically significant differences were observed in pleural indentation sign, vacuole sign, and texture features, including entropy, correlation, contrast, energy, and homogeneity, between the two groups ($P < 0.05$). Logistic regression analysis revealed that pleural indentation sign, vacuole sign, and texture features including entropy, correlation, contrast, energy, and homogeneity were risk factors influencing the invasiveness of pulmonary nodules clinically. Compared to individual texture features, the combined use of texture features demonstrated higher diagnostic value for detecting the invasiveness of lung adenocarcinoma. *Conclusion*: The quantitative texture features (entropy, correlation, contrast, energy, and homogeneity) of pulmonary nodules obtained using United Imaging uCT968 ultra-high-end CT have good diagnostic value for the invasiveness of lung adenocarcinoma and possess high clinical application value.

Keywords: CT detection; Texture features of pulmonary nodules; Lung adenocarcinoma; Invasiveness

Online publication: October 20, 2026

1. Introduction

Lung adenocarcinoma, as the most predominant pathological subtype of lung cancer, poses a significant global public health threat due to its high incidence and mortality rates. Different pathological subtypes of lung adenocarcinoma exhibit marked differences in biological behavior and invasiveness, directly influencing the choice of treatment regimen and the prognosis of patients [1]. Although traditional CT examinations play an indispensable role in the diagnosis of lung adenocarcinoma, they remain inadequate in assessing its invasiveness. Traditional CT signs, such as nodule size, shape, and edge characteristics, often rely heavily on the subjective interpretation of physicians and struggle to fully reveal the complex internal heterogeneity of lesions. While lung puncture biopsy can provide definitive pathological diagnosis, its inherent sampling bias and requirements for lesion location may result in assessment outcomes that do not fully represent the true invasive state of the entire lesion [2-3]. Therefore, there is an urgent need for a more objective and quantifiable assessment method to overcome the limitations of traditional approaches. The United Imaging uCT968 ultra-high-end CT demonstrates significant advantages in the detection and fine characterization of pulmonary nodules, thanks to its outstanding spatial resolution and extremely low image noise. This device not only clearly presents the subtle internal structures of ground-glass nodules (GGNs) but also extracts rich and high-fidelity texture features through its advanced post-processing techniques [4-5]. However, the current challenge lies in how to fully utilize the imaging data from the United Imaging uCT968, particularly its texture features, to assess the invasiveness of lung adenocarcinoma quantitatively. This study employs texture features extracted from chest plain scan images obtained using the United Imaging uCT968 ultra-high-end CT to predict the invasiveness of pulmonary nodules, providing a foundational basis for subsequent research.

2. Subjects and methods

2.1. Study subjects

This prospective study included 240 patients with pulmonary mixed ground-glass nodules confirmed by pathological examination after lung surgery in our hospital from December 2025 to December 2026. Based on whether the lesions invaded the surrounding tissues, minimally invasive cancer and invasive cancer were classified into the invasive group (n = 120), while benign lesions and carcinoma in situ were classified into the non-invasive group (n = 120). Clinical and pathological information, including age, gender, smoking status, and pathological diagnosis, was obtained from the electronic medical record system of our hospital.

Inclusion Criteria: (1) Pathological confirmation of lung adenocarcinoma following surgery; (2) All patients had pulmonary nodules detected and underwent lung resection treatment; (3) Received low-dose chest CT scans and quantitative analysis after admission; (4) Complete CT quantitative parameters.

Exclusion Criteria: (1) Presence of nodules or malignant tumors in other parts of the body; (2) History of preoperative radiotherapy or chemotherapy; (3) The time interval between CT examination and surgery exceeded 3 months; (4) Motion artifacts present in CT scan images; (5) Incomplete clinical data.

2.2. Imaging examination

All enrolled patients underwent plain chest CT scans using the United Imaging uCT968 ultra-high-end multi-slice spiral CT. Prior to the scan, patients were instructed to lie supine with their arms raised above their heads and to breathe quietly during the procedure. The scan positioning line started horizontally from the bilateral lung apices (thoracic inlet) and continued downward to the bilateral lung bases (above the

diaphragm), ensuring complete coverage of the entire lung fields. The scanning parameters were set as follows: tube voltage of 120 kV, reference tube current of 50 mAs under automatic tube current modulation technology, pitch of 0.609, field of view (FOV) of 350 mm × 350 mm, acquisition slice thickness of 5 mm, reconstruction slice thickness of 5 mm, and reconstruction matrix of 512 × 512. After transferring the raw image data to the workstation, high-resolution (HR) reconstruction algorithms were used for processing, generating images in both lung window (window level: -450 HU, window width: 1500 HU) and mediastinal window (window level: 40 HU, window width: 400 HU) settings for subsequent observation and analysis of the lesions.

Plain Chest CT Scan Interpretation: Two radiologists with more than 5 years of experience independently interpreted the plain chest CT scan images.

Plain Chest CT Scan Texture Feature Interpretation: The specific steps are shown in the following figure.

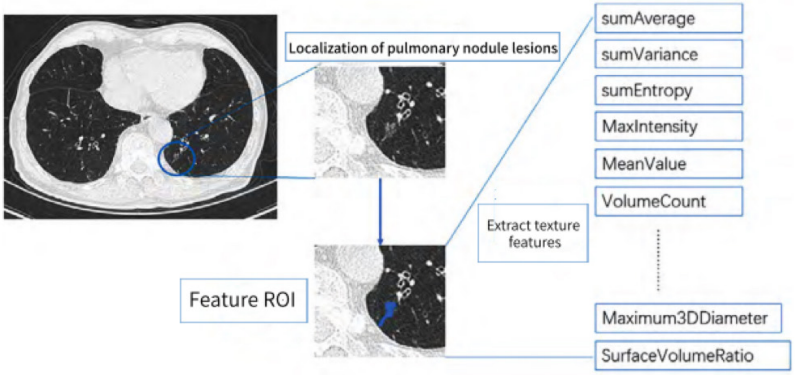

Figure 1 Flowchart of pulmonary nodule delineation and texture feature extraction

Figure 1. Flowchart of pulmonary nodule delineation and texture feature extraction.

$$(1)\ \textbf{contrast}: \text{contrast} = \sum_{i=1}^{Ng}\sum_{j=1}^{Ng}|i-j|^2 P(i,j)$$

$$(2)\ \textbf{Related}: \text{correrelation} = \frac{\sum_{i=1}^{Ng}\sum_{j=1}^{Ng} ijP(i,j) - \mu_t(i)\mu_j(j)}{\sigma_x(i)\sigma_y(j)}$$

$$(3)\ \textbf{Energy}: \text{energy} = \sum_{i=1}^{Ng}\sum_{j=1}^{Ng}\left[P(i,j)\right]^2$$

$$(4)\ \textbf{Consistency}: \text{homogeneity} = \sum_{i=1}^{Ng}\sum_{j=1}^{Ng}\frac{P(i,j)}{1+|i-j|^2}$$

$$(5)\ \textbf{Entropy}: \text{entropy} = \sum_{i=1}^{Ng}\sum_{j=1}^{Ng}P(i,j)\log\left[P(i,j)\right]$$

Figure 2. Formulas for calculating texture features.

2.3. Pathological evaluation

Pathological evaluations of frozen sections during or after surgery were conducted based on the International Association for the Study of Lung Cancer/American Thoracic Society/European Respiratory Society classification, which includes atypical adenomatous hyperplasia, adenocarcinoma in situ, minimally invasive adenocarcinoma, lepidic-predominant adenocarcinoma (LPA), acinar-predominant adenocarcinoma, papillary-predominant adenocarcinoma, micropapillary-predominant adenocarcinoma, solid-predominant adenocarcinoma with mucin production, and four other variant subtypes. Atypical adenomatous hyperplasia, adenocarcinoma in situ, minimally invasive adenocarcinoma, and LPA are considered less invasive nodules due to their higher 5-year survival rates, whereas other subtypes of invasive adenocarcinoma are regarded as invasive nodules due to their aggressive biological behavior.

2.4. Index analysis

2.4.1. Collection of general patient information

This includes age, gender, disease duration, smoking history, family history, and history of benign pulmonary diseases.

2.4.2. Factor analysis

Multivariate logistic regression analysis was performed to identify factors influencing the invasiveness of pulmonary nodules.

2.4.3. CT texture features

Using postoperative pathological results as the gold standard, the sensitivity, specificity, and accuracy of direct interpretation of plain chest CT scans and interpretation based on CT texture features were compared.

2.5. Statistical analysis

Statistical analysis was performed using SPSS 26.0 software. For univariate analysis, the chi-square test was used to compare the composition of categorical data between groups. Non-normally distributed continuous data were described using mean ± standard deviation (SD), and comparisons between groups with homogeneous variance were conducted using the *t*-test. Categorical data were expressed as cases or percentages. Multivariate analysis was performed using a logistic regression model. The significance level was set at $\alpha = 0.05$, with a P-value < 0.05 considered statistically significant.

3. Results

3.1. Baseline and texture feature analysis of the two groups

As shown in **Table 1**, there were no statistically significant differences between the two groups in terms of gender, clinical stage, maximum lesion diameter, spiculation sign, lobulation sign, air bronchogram, and average CT value of the lesion ($P > 0.05$). Statistically significant differences were observed in pleural indentation sign, vacuole sign, and texture features including entropy, correlation, contrast, energy, and homogeneity between the two groups ($P < 0.05$).

Table 1. Baseline and texture feature analysis of the two groups

Item		Invasive Group (n=120)	Non-invasive Group (n=120)	χ^2/t value	*P* value
Gender	Male	73	70	0.156	0.693
	Female	47	50		
Clinical Stage	Stage I	59	55	0.124	0.637
	Stage II	38	43		
	Stage III	23	22		
Texture Features	Entropy	2.56 ± 0.19	2.10 ± 0.12	22.420	0.001
	Correlation	0.31 ± 0.05	0.58 ± 0.11	24.480	0.001
	Contrast	6.81 ± 1.35	5.19 ± 1.03	10.450	0.001
	Energy	0.10 ± 0.02	0.16 ± 0.04	14.700	0.001
	Homogeneity	0.38 ± 0.03	0.49 ± 0.10	11.540	0.001
Maximum Lesion Diameter (cm)		2.91 ± 0.10	2.93 ± 0.09	1.628	0.105
Pleural Indentation Sign		61	35	11.730	0.001
Spiculation Sign		59	53	1.069	0.301
Lobulation Sign		61	58	0.150	0.698
Vacuole Sign		66	39	12.340	0.001
Air Bronchogram Sign		53	51	0.068	0.794
Mean CT Value of Lesion		0.71 ± 0.03	0.72 ± 0.02	2.031	0.063

3.2. Logistic regression analysis of factors influencing the invasiveness of pulmonary nodules

As shown in **Table 2**, pleural indentation sign, vacuole sign, and texture features including entropy, correlation, contrast, energy, and homogeneity are risk factors clinically influencing the invasiveness of pulmonary nodules.

Table 2. Logistic regression analysis of factors influencing the invasiveness of pulmonary nodules

Factor	β	SE	Wald χ^2 value	*P* value	OR	95% CI
Pleural indentation sign	0.516	0.037	3.195	0.001	2.675	1.345~4.861
Vacuole sign	0.318	0.061	2.415	0.001	1.946	1.063~3.946
Entropy	0.152	0.084	3.842	0.001	1.842	1.013~4.761
Correlation	0.216	0.391	5.673	0.001	1.639	1.269~3.175
Contrast	0.311	0.277	4.812	0.001	2.946	1.765~5.137
Energy	0.219	0.294	4.913	0.001	2.758	1.346~5.976
Homogeneity	0.137	0.372	2.948	0.001	2.791	1.338~5.729

3.3. Predictive value of pulmonary nodule texture features for the invasiveness of lung adenocarcinoma

As shown in **Table 3**, compared to individual texture features, the combined use of texture features demonstrates higher diagnostic value for detecting the invasiveness of lung adenocarcinoma.

Table 3. Predictive value of pulmonary nodule texture features for the invasiveness of lung adenocarcinoma

Index	*P* value	Youden's Index	Cut-off value	Sensitivity (%)	Specificity (%)	Accuracy (%)	95% CI
Entropy	0.001	0.533	0.394	84.59	81.50	81.26	0.419~0.913
Correlation	0.001	0.501	0.371	81.76	82.76	86.49	0.412~0.811
Contrast	0.001	0.475	0.519	79.67	81.09	84.91	0.467~0.916
Energy	0.001	0.496	0.317	85.43	86.74	83.59	0.138~0.721
Homogeneity	0.001	0.518	0.421	81.26	84.19	85.49	0.167~0.946
Combined	0.001	0.913	0.728	96.53	93.47	96.72	0.175~0.837

4. Discussion

The invasiveness of lung adenocarcinoma is closely related to its pathological basis. The degree of tumor cell infiltration determines the malignancy and clinical manifestations of the lesion, while the complex microenvironment regulatory network not only affects tumor growth rate but also determines its invasive capacity toward surrounding tissues. In recent years, texture feature analysis based on CT images has demonstrated significant application value in the diagnosis of pulmonary nodules. As a quantitative tool for describing the gray-level distribution and spatial structure of images, texture features can effectively reflect the internal heterogeneity of pulmonary nodules, thereby aiding in the differentiation between benign and malignant lesions. Previous studies have shown that CT image texture parameters such as energy, entropy, and standard deviation are significantly higher in malignant pulmonary nodules compared to benign ones, and these parameters also exhibit good performance in distinguishing subsolid nodules with different degrees of infiltration [6,7]. Furthermore, the development of radiomics technology has enabled the extraction of more high-dimensional texture features, providing new insights for the precise diagnosis of pulmonary nodules. However, existing research has primarily focused on the application of texture features in differentiating between benign and malignant lesions, with insufficient exploration of their value in assessing the invasiveness of lung adenocarcinoma, particularly their performance in subsolid nodules with varying degrees of infiltration, which still requires in-depth validation.

This study found that the quantitative evaluation of the invasiveness of lung adenocarcinoma using texture features from United Imaging uCT968 ultra-high-end CT has considerable value. Statistically significant differences were observed between the two groups in terms of pleural indentation sign, vacuole sign, and texture features including entropy, correlation, contrast, energy, and homogeneity ($P < 0.05$). Logistic regression analysis revealed that pleural indentation sign, vacuole sign, and texture features including entropy, correlation, contrast, energy, and homogeneity are risk factors clinically influencing the invasiveness of pulmonary nodules. Compared to individual texture features, the combined use of texture features demonstrates higher diagnostic value for detecting the invasiveness of lung adenocarcinoma. These findings suggest that United Imaging uCT968 ultra-high-end CT holds significant value in assessing the invasiveness of lung adenocarcinoma, which can be attributed to its advanced technological characteristics that provide unique advantages in the field of pulmonary disease diagnosis. The device employs a wide-detector design and an intelligent scanning platform, enabling rapid, low-dose, large-scale imaging while delivering high-resolution and high-clarity image quality, laying the foundation for precise detection and feature extraction of pulmonary nodules [8,9]. In practical applications, United Imaging uCT968 has been

successfully used for the early diagnosis and treatment efficacy evaluation of various pulmonary diseases, particularly excelling in the qualitative analysis and quantitative measurement of pulmonary nodules. For instance, an artificial intelligence-assisted system can automatically segment pulmonary nodules and extract their morphological features and texture parameters, enabling a preliminary assessment of lesion nature. Additionally, United Imaging uCT968 offers significant advantages in texture feature extraction, with its high sensitivity and resolution facilitating the capture of subtle changes in the internal microstructure of pulmonary nodules, providing reliable data support for subsequent texture analysis.

5. Conclusion

In conclusion, the application of United Imaging uCT968 ultra-high-end CT for diagnosing the invasiveness of lung adenocarcinoma demonstrates high diagnostic efficacy. Through dynamic monitoring of texture features, it can predict disease progression risk and guide the formulation of follow-up plans.

Funding

Quantitative Evaluation of the Invasiveness of Lung Adenocarcinoma Based on Texture Features of Pulmonary Nodules Using the United Imaging uCT968 Ultra-High-End CT (Project No.: XYZY2025Y10)

Disclosure statement

The author declares no conflict of interest.

References

[1] Zhou C, Ren W, Chen J, et al., 2025, Predicting the Aggressiveness of Different Pathological Grades in Stage IA Lung Adenocarcinoma Based on CT Radiomics Models. Doctor Online, 15(11): 54–57.

[2] Cai X, Wang P, Zhou H, et al., 2023, CT-Based Radiomics Nomogram for Predicting Visceral Pleural Invasion in Peripheral T1-Sized Solid Lung Adenocarcinoma. American Journal of Cancer Research, 13(12): 5901–5913.

[3] Zuo Z, Li Y, Peng K, et al., 2022, CT Texture Analysis-Based Nomogram for the Preoperative Prediction of Visceral Pleural Invasion in cT1N0M0 Lung Adenocarcinoma: An External Validation Cohort Study. Clinical Radiology, 77(3): e215–e221.

[4] Zeng L, 2024, The Value of Predicting the Aggressiveness of Ground-Glass Nodule-Type Lung Adenocarcinoma Based on CT Morphology and Quantitative Parameters, thesis, Medical School of Nanchang University.

[5] Xu Q, Cheng H, 2025, The Predictive Value of Different Metabolic Parameters from 18F-FDG PET/CT for the Aggressiveness of Lung Adenocarcinoma. Imaging Diagnosis and Interventional Radiology, 34(3): 191–197.

[6] Zuo YQ, Gao D, Cui JJ, et al., 2025, Peritumoral and Intratumoral Radiomics for Predicting Visceral Pleural Invasion in Lung Adenocarcinoma Based on Preoperative Computed Tomography (CT). Clinical Radiology, 80: 106729.

[7] Song Y, Chen D, Lian D, et al., 2022, Study on the Correlation Between CT Features and Vascular Tumor Thrombus Together With Nerve Invasion in Surgically Resected Lung Adenocarcinoma. Frontiers in Surgery, 9: 931568.

[8] Han C, Shi G, Liu D, et al., 2025, The Predictive Value of CT for the Aggressiveness of Sub-Centimeter Pure Ground-Glass Nodule Lung Adenocarcinoma. Journal of Guizhou Medical University, 50(12): 1854–1860.

[9] Huang Y, Tan Y, Lin L, et al., 2025, The Predictive Value of Quantitative Parameters from Dual-Energy CT for the Differential Diagnosis and Pathological Aggressiveness of Lung Adenocarcinoma. Journal of Practical Radiology, 41(3): 394–398.

Publisher's note

Bio-Byword Scientific Publishing remains neutral with regard to jurisdictional claims in published maps and institutional affiliations.

Oncology Treatment Discovery, 2026, Volume 4, Issue 3
https://bbwpublisher.com/journal/OTD
Online ISSN: 2981-8079
Print ISSN: 3083-4996

Mutational Landscape and Clinicopathological Correlates of 553 Chinese Colorectal Cancer Cases Assessed by 116-Gene Targeted Sequencing

Yitong Liu†, Jianglin Li†, Mingfeng Wu, Zidan Luo, Yiyun Sun, Xinyu Chen, Enle Zhou*

Department of Pathology, Chongqing University Cancer Hospital, Chongqing 400030, China
† These authors contributed equally to this work and share the first authorship.

***Corresponding author*:** Enle Zhou, zhouenle@163.com

Copyright: © 2026 Author(s). This is an open-access article distributed under the terms of the Creative Commons Attribution License (CC BY 4.0), permitting distribution and reproduction in any medium, provided the original work is cited.

Abstract: *Objective*: Comprehensive molecular profiling of colorectal cancer (CRC) can inform precision oncology, yet real-world data from Chinese cohorts based on clinical targeted panels remain limited. This study aimed to characterize the mutational landscape of Chinese CRC using a 116-gene targeted next-generation sequencing (NGS) panel and to evaluate associations between key genomic alterations and clinicopathological features. *Method*: We retrospectively enrolled 553 patients with pathologically confirmed colorectal adenocarcinoma or its histological subtypes who underwent 116-gene targeted sequencing. Single-nucleotide variants (SNV)/short insertions and deletions (InDel), copy number amplifications, and gene fusions were identified using a standardized bioinformatics pipeline. Somatic variants were annotated using both AMP/ASCO/CAP oncogenicity labels and laboratory ACMG-style pathogenicity labels. Gene-level analyses were based on a nonsynonymous variant set. Associations with clinicopathological features were assessed using Fisher's exact test with Benjamini-Hochberg correction. Potentially actionable molecular events were stratified into three evidence-based tiers. *Results*: Among 553 CRC patients, 343 (62.0%) were male and 210 (38.0%) were female, with a median age of 62 years (range, 17-94 years). The rectum was the most common tumor site (53.3%), followed by the left colon (24.8%) and right colon (21.9%). A total of 4,725 SNV/InDel variants were identified, of which 3,107 were nonsynonymous (involving 102 genes); the median number of nonsynonymous mutations per patient was 4 (range, 1-60). The five most frequently mutated genes were TP53 (78.1%), KRAS (53.0%), APC (49.4%), PIK3CA (22.4%), and FBXW7 (20.6%). Copy number amplification was detected in 12.7% of patients (70/553), most commonly involving MYC (2.9%) and FGFR3 (2.5%). Gene fusions were identified in 7 patients (1.3%). Co-mutation analysis revealed significant co-occurrence of TP53 and APC (OR = 2.07, 95% CI: 1.36-3.14, adjusted $p = 0.005$) and mutual exclusivity between KRAS and BRAF (OR = 0.10, 95% CI: 0.04-0.25, adjusted $p < 0.001$). By evidence-based tiering, 19.9% (110/553) of patients harbored at least one Tier 1 molecular event, and 66.7% (369/553) harbored at least one Tier 1 or Tier 2 event. *Conclusion*: This study delineates the 116-gene mutational landscape of 553 Chinese CRC patients, characterizing the TP53-KRAS-APC core mutation pattern, hotspot distributions, low-frequency copy number amplifications and fusion events, and a tiered map of potentially actionable molecular events, providing real-world

regional data to inform precision oncology in CRC.

Keywords: Colorectal neoplasms; Targeted sequencing; Mutational landscape; Copy number amplification; Gene fusion; Molecular stratification

Online publication: October 20, 2026

1. Introduction

Colorectal cancer (CRC) is the third most commonly diagnosed malignancy and the second leading cause of cancer-related mortality worldwide [1]. Despite advances in surgical resection, chemoradiotherapy, and targeted therapy, the 5-year survival rate for advanced CRC remains suboptimal, underscoring the need for deeper molecular characterization to guide individualized treatment strategies.

The Cancer Genome Atlas (TCGA) performed whole-exome sequencing on 276 CRC cases, revealing high-frequency mutated genes and core signaling pathways [2]. However, TCGA primarily represents Western populations, whereas China bears a substantial and rising CRC burden [3], with Chinese patients exhibiting distinct tumor site distributions and molecular features compared with Western cohorts [4-6]. Although several large-scale studies have characterized the genomic landscape of Chinese CRC [4-6], systematic mutational profiling using clinical targeted panels with standardized somatic variant interpretation remains limited. In this study, we analyzed 116-gene targeted sequencing data from 553 Chinese CRC patients to characterize mutation frequencies, copy number amplifications, gene fusions, and variant classification patterns, and to explore associations between key genomic alterations and clinicopathological features, thereby providing real-world regional data to inform precision oncology in CRC.

2. Materials and methods

2.1. Study population

A total of 561 patients with CRC who underwent tumor tissue NGS testing at Chongqing University Cancer Hospital between August 2024 and July 2026 (last case tested on July 9, 2026) were retrospectively enrolled.

The inclusion criteria were:

(1) pathologically confirmed colorectal adenocarcinoma or its histological subtypes (including mucinous adenocarcinoma and signet ring cell carcinoma components);

(2) successful completion of 116-gene targeted NGS;

(3) availability of core clinicopathological data.

The exclusion criteria were:

(1) NGS failure or substandard sequencing quality;

(2) non-colorectal primary tumors;

(3) histological types not meeting adenocarcinoma definitions.

Based on criterion (3), 8 patients were excluded (2 neuroendocrine carcinomas, 5 adenomas with focal malignant transformation, and 1 mixed carcinoma with a neuroendocrine component), yielding a final cohort of 553 patients. This study was approved by the Ethics Committee of Chongqing University Cancer Hospital (Approval No.: CZLL2026-278-002), with the requirement for informed consent waived.

2.2. Clinicopathological data collection

Clinical data collected included sex, age, tumor site (right colon, left colon, or rectum), histological type, differentiation grade, specimen type (surgical or biopsy), neoadjuvant treatment status, and TNM stage. Tumor site classification followed Chinese CRC diagnostic guidelines: the right colon comprises the cecum, ascending colon, hepatic flexure, and transverse colon; the left colon comprises the splenic flexure, descending colon, sigmoid colon, and rectosigmoid junction; and the rectum refers to the segment below the peritoneal reflection.

2.3. NGS testing

All tumor tissue specimens were formalin-fixed and paraffin-embedded (FFPE), and genomic DNA was extracted. A custom 116-gene targeted capture panel (Pan116, capture region 0.25 Mb) covering genes commonly mutated in CRC, DNA damage repair genes, targeted therapy-related genes, and core signaling pathway genes was used. Paired-end sequencing was performed on the Illumina NextSeq platform with an average sequencing depth exceeding 500x. The bioinformatics pipeline included BWA alignment, GATK-based preprocessing, Mutect2 for SNV/InDel calling, ANNOVAR annotation, CNVkit for copy number analysis, and FACTERA for fusion detection. Microsatellite instability (MSI) status was determined by the NGS panel based on microsatellite locus instability counting, with at least 8 unstable loci classified as MSI-H (laboratory-established threshold). Fusion events were confirmed by manual review using the Integrative Genomics Viewer (IGV). Amplification was determined by CNVkit-estimated copy number with a laboratory-established threshold of 3.5 or greater. Nineteen genes were included in the copy number analysis module: AKT2, AURKA, CCND1, CCNE1, CD274, CDK6, EGFR, ERBB2, FGF19, FGF3, FGFR1, FGFR3, IGF1R, MYC, PGR, PSMD4, RET, RSF1, and TOP2A.

2.4. Variant classification and analysis set definition

Somatic variants retained two reporting label systems:

(1) AMP/ASCO/CAP oncogenicity labels (Oncogenic/Likely oncogenic) per the 2017 joint guidelines [7];

(2) laboratory-issued ACMG-style pathogenicity labels [8] (Pathogenic/Likely pathogenic/Uncertain/Likely benign/Benign).

These two systems differ in scope and were used solely to describe reporting distributions, not for cross-conversion or combined interpretation. It should be noted that the ACMG framework was originally designed for germline variants; this study employed a tumor-only somatic workflow without paired normal controls, and these labels reflect laboratory reporting conventions only. Variant functional annotation referenced the COSMIC database [9] and cBioPortal [10].

Two variant sets were defined:

(1) All detected variants: all SNV/InDel variants reported by the panel, used only for describing variant type composition and overall pathogenicity distribution;

(2) Nonsynonymous analysis set: after excluding synonymous mutations, intronic variants (except splice sites), UTR, and flanking region variants, missense, nonsense, frameshift, in-frame insertion/deletion, and splice site variants were included.

All gene-level analyses (mutation frequency, hotspot mutations, co-mutation, clinicopathological associations, and potentially actionable molecular events) were based on the nonsynonymous analysis set.

During quality control, 5 samples were found to have duplicate bioinformatics analysis records; 22 fully duplicate variant entries were removed by sample-gene-transcript-HGVS deduplication, and all statistics were based on deduplicated, sample-level variant events. Additionally, as this study employed a tumor-only clinical somatic testing workflow without paired normal controls, germline-origin variants cannot be fully excluded; therefore, clinical interpretation of DNA damage repair gene mutations (e.g., BRCA1/2, PALB2) requires caution.

2.5. Statistical methods

Categorical variables were described as frequencies (percentages), and continuous variables as medians (ranges). Associations between gene mutations and clinicopathological features were analyzed using Fisher's exact test: tumor site was compared as colon (right and left combined) versus rectum in 2 x 2 tests; differentiation was compared as poorly differentiated (including poor-to-moderate, 48 cases) versus moderately differentiated (including moderate-to-well, 334 cases) in 2 x 2 tests, with well-differentiated (6 cases) and missing records (165 cases) excluded; and sex was compared as male versus female. Copy number amplification associations were analyzed using the same methods. Multiple comparisons were corrected using the Benjamini-Hochberg method (BH-FDR) per clinical variable across 30 genes (30 tests per variable), with adjusted $p < 0.05$ considered statistically significant. The association between BRAF mutation and tumor site was prespecified based on prior literature as a right colon versus rectum pairwise comparison, with uncorrected p-values reported. Co-mutation analysis was performed using pairwise Fisher's exact tests on the 15 most frequently mutated genes (105 pairs), reporting odds ratios (OR), 95% confidence intervals (CI), and BH-FDR-adjusted *p*-values. Statistical analyses were performed using Python 3.13.

2.6. Potentially actionable molecular event definition and evidence tiering

Referencing the NCCN Colon Cancer Guidelines (Version 3.2025) [11], potentially actionable molecular events were stratified into three evidence-based tiers as a research classification (not ESCAT/OncoKB standard):

(1) Tier 1 (guideline-recommended or relatively high-level evidence molecular events): Tier 1A includes CRC guideline-recommended events: MSI-H/dMMR status (an independent biomarker phenotype guiding immunotherapy), BRAF p.V600E mutation, KRAS p.G12C mutation, ERBB2 (HER2) amplification, and NTRK1 gene fusion; Tier 1B includes pan-cancer approved or rare high-level evidence events in CRC: ERBB2 mutation, ALK fusion, and RET fusion, where ERBB2 mutation classification is based on anti-HER2 response evidence from pan-cancer basket trials (evidence level below that of ERBB2 amplification in CRC guidelines) and ALK/RET fusion evidence is mostly from case reports or small series;

(2) Tier 2 (predictive/resistance markers): markers that are not direct therapeutic targets but guide treatment decisions, including KRAS non-G12C mutations and NRAS mutations (anti-EGFR resistance prediction);

(3) Tier 3 (exploratory molecular events): events with no approved drugs in CRC but with clinical trial or preclinical evidence, including PIK3CA, MET, BRCA1/2, and BRAF non-V600E mutations, and FGFR1/FGFR3, MYC, and CCND1 amplifications. EGFR amplification was not included in the tiering analysis owing to insufficient evidence.

3. Results

3.1 Patient characteristics

Among the 553 CRC patients, 343 (62.0%) were male and 210 (38.0%) were female, with a median age of 62 years (range, 17-94 years). The rectum was the most common tumor site (295 cases, 53.3%), followed by the left colon (137 cases, 24.8%) and right colon (121 cases, 21.9%). Adenocarcinoma was the predominant histological type (509 cases, 92.0%), with 34 cases (6.1%) containing mucinous adenocarcinoma components and 5 cases (0.9%) containing signet ring cell carcinoma components; histological type was not recorded in 5 cases (0.9%). Surgical specimens accounted for 363 cases (65.6%) and biopsy specimens for 157 cases (28.4%), with specimen type not recorded in 33 cases (6.0%). Fifty-seven cases (10.3%) were post-neoadjuvant treatment. NGS testing revealed MSI-H in 35 cases (6.3%) and MSS in 518 cases (93.7%) (**Table 1**). Pathological TNM staging was available for only 144 cases (26.0%) and was therefore not included in subsequent association analyses.

Table 1. Clinicopathological and molecular characteristics of 553 colorectal cancer patients

Characteristic	Value
Total cases	553
Sex (Male/Female)	343 (62.0%) / 210 (38.0%)
Age, median (range)	62 (17-94)
Tumor site (Rectum/Left colon/Right colon)	295 (53.3%) / 137 (24.8%) / 121 (21.9%)
Specimen type (Surgical/Biopsy/Not recorded)	363 / 157 / 33
Post-neoadjuvant cases	57 (10.3%)
MSI status (MSI-H/MSS)	35 (6.3%) / 518 (93.7%)
Total SNV/InDel variants detected	4725
Nonsynonymous analysis set	3107 (excluding synonymous/intronic/UTR/flanking: 1618)
Genes with variants (all/nonsynonymous)	105 / 102
Nonsynonymous mutations/case, median (range)	4 (1-60)
Cases with copy number amplification	70 (12.7%)
Cases with fusion events	7 (1.3%)
Cases with >=1 Tier 1 / Tier 1+2 / any tier event	110 (19.9%) / 369 (66.7%) / 435 (78.7%)
AMP/ASCO/CAP Oncogenic/Likely oncogenic	608 (12.9%)
ACMG-style P/LP/Uncertain/LB/B	404 (8.6%) / 675 (14.3%) / 2015 (42.6%) / 937 (19.8%) / 86 (1.8%)

Note: Pathogenicity and tier rows merged for brevity; full classification detail in Section 3.6.

3.2. Gene mutation profile

The 116-gene panel detected 4,725 SNV/InDel variants (involving 105 genes) across the 553 CRC cases, of which 3,107 were nonsynonymous variants (involving 102 genes), with 1,618 synonymous, intronic, UTR, and flanking region variants excluded. The median number of nonsynonymous mutations per patient was 4 (range, 1-60), with a median of 4 mutated genes per patient (range, 1-38).

Based on the nonsynonymous analysis set, the 10 most frequently mutated genes were TP53 (78.1%, 432/553), KRAS (53.0%, 293/553), APC (49.4%, 273/553), PIK3CA (22.4%, 124/553), FBXW7 (20.6%, 114/553), SMAD4 (17.2%, 95/553), ARID1A (17.0%, 94/553), BRCA2 (13.2%, 73/553), TSC2 (11.6%, 64/553), and MSH6 (11.2%, 62/553) (**Figure 1**). The patient-level mutational landscape of the 15 most

frequently mutated genes is shown in **Figure 2**.

By gene function, tumor suppressor genes (TP53, APC, SMAD4, FBXW7, ARID1A) showed high mutation frequencies; KRAS, PIK3CA, and BRAF represented oncogenes; and DNA damage repair genes (BRCA1, BRCA2, ATM) had relatively lower mutation frequencies with potential relevance for molecular stratification or exploratory investigation in selected contexts. Notably, a substantial proportion of variants in certain genes, particularly TSC2, were classified as VUS and are further addressed in the Discussion.

Codon-level variant analysis was performed for 6 high-frequency genes (KRAS, TP53, BRAF, PIK3CA, APC, and NRAS). KRAS mutations predominantly affected codon 12, with p.G12D (83 cases, 15.0%), p.G12V (66 cases, 11.9%), and p.G13D (55 cases, 9.9%) being the most common hotspots, collectively accounting for 69.6% of KRAS mutations; p.G12C (17 cases, 3.1%) is noteworthy as the target of KRAS G12C inhibitors. TP53 mutations were relatively dispersed, with p.R175H (50 cases, 9.0%) being the most common hotspot, followed by p.R282W (21 cases, 3.8%), p.R273C (20 cases, 3.6%), and p.R273H (18 cases, 3.3%), concentrated in the DNA-binding domain (exons 5-8). Among BRAF mutations, p.V600E accounted for 70.5% (31/44), while non-V600E variants accounted for 29.5% (13/44). PIK3CA hotspot mutations clustered at p.E545K (22 cases, 4.0%), p.H1047R (17 cases, 3.1%), and p.E542K (16 cases, 2.9%). APC mutations were predominantly truncating (nonsense and frameshift), with p.R1450* (29 cases, 5.2%) being the most common truncation site, concentrated in the exon 16 mutation cluster region. NRAS mutations (19 cases, 3.4%) were predominantly p.G12D (6 cases) and p.Q61K/R (8 cases combined).

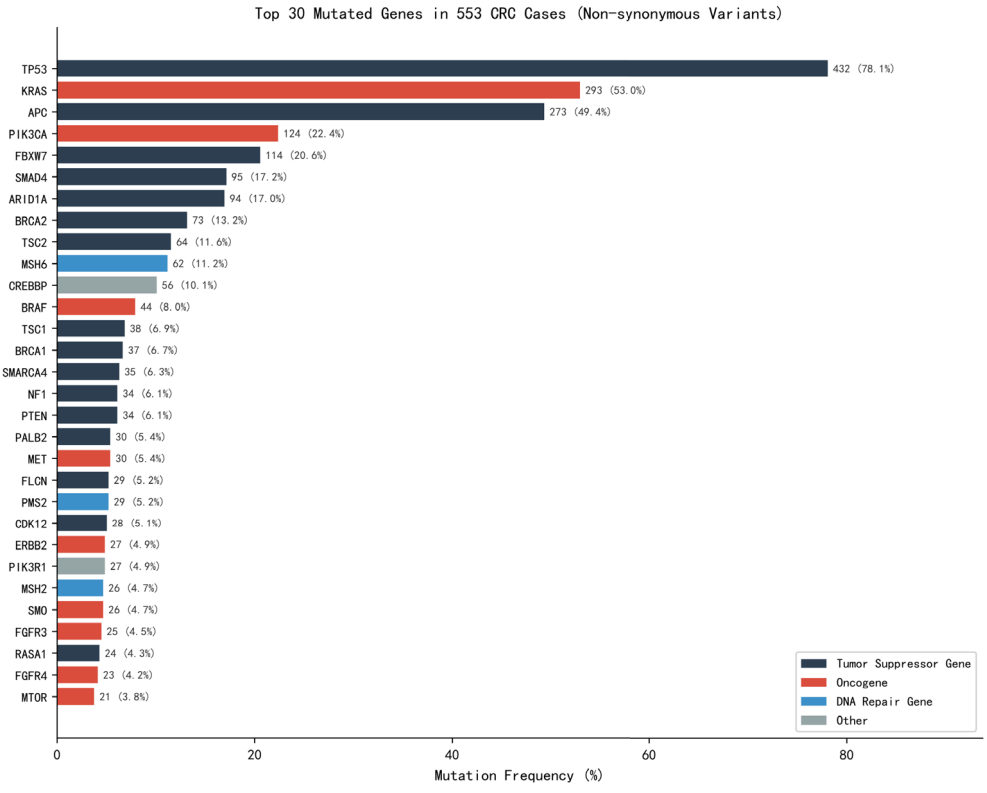

Figure 1. Mutation frequencies of the 30 most frequently mutated genes in 553 colorectal cancer cases (nonsynonymous variant analysis set; descriptive mutational profile, not driver gene ranking). Bars show mutation frequency (%); bar-end labels indicate case count and frequency; colors distinguish gene functional types (tumor suppressor/oncogene/DNA repair/other, classified by dominant biological function; categories are not mutually exclusive).

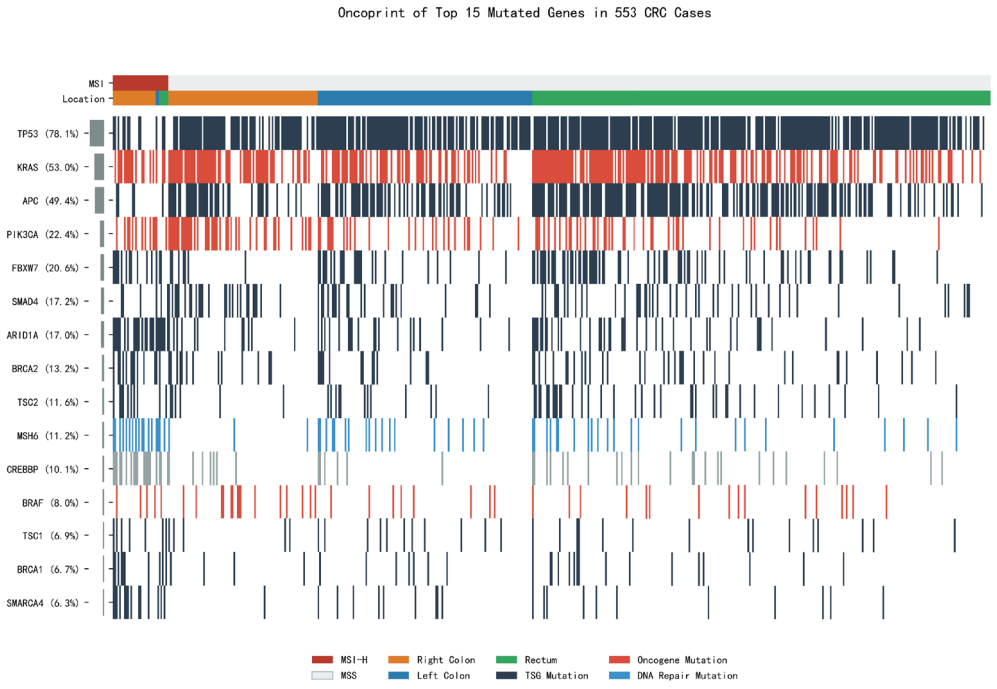

Figure 2. Patient-level mutational landscape of the 15 most frequently mutated genes in 553 colorectal cancer cases. Each column represents a single patient; multiple variant events in the same gene are recorded as a single cell (presence/absence). Patients are sorted by MSI status (top track, red = MSI-H) and tumor site (bottom track, orange = right colon, blue = left colon, green = rectum); genes are colored by functional type with mutation frequencies on the left.

3.3. Copy number amplification

Among the 553 CRC cases, 70 (12.7%) harbored at least one gene copy number amplification (the CNV analysis assessed amplification events only; homozygous deletions were not evaluated). Among the 19 CNV detection genes (see Section 2.3), the five most frequently amplified genes were MYC (2.9%, 16/553), FGFR3 (2.5%, 14/553), FGFR1 (2.0%, 11/553), ERBB2 (1.6%, 9/553), and AURKA (1.4%, 8/553). CCND1, FGF19, and FGF3 amplification frequencies were each 1.3% (7/553), and CD274 and EGFR amplification frequencies were each 0.9% (5/553), with the remaining genes below 0.5%.

Association analysis showed that ERBB2 amplification frequencies were similar across the right colon (1.7%), left colon (1.5%), and rectum (1.7%) (p = 1.000). MYC amplification was more frequent in the rectum (3.7%) and left colon (2.9%) than in the right colon (0.8%), although the difference was not statistically significant (p = 0.309).

3.4. Gene fusions

Seven patients (1.3%) harbored fusion events: 2 ALK fusions (EML4-ALK), 1 RET fusion (NCOA4-RET), and 4 NTRK1-related fusions. The 4 NTRK1-related fusions involved 3 distinct structures: TPM3-NTRK1 (2 cases, breakpoints at ex9-ex9 and ex8-ex9), TPR-NTRK1 (1 case, ex9-ex9), and NTRK1-TPR (1 case, ex10-ex21). In the first three, NTRK1 was the 3' gene with an intact kinase domain, representing canonical oncogenic NTRK fusions; in NTRK1-TPR, NTRK1 was the 5' gene with the kinase domain not retained, of uncertain oncogenic significance. Among fusion-positive patients, 4 were female and 3 were male, with a median age of 68 years (range, 54-80 years); by original anatomical site, 5 were located in the ileocecal

region, 1 in the ascending colon, and 1 in the rectum; by the study's site grouping, the first 6 were classified as right colon. Given the small sample size, site distribution is presented descriptively. Four fusion-positive patients were MSI-H (3 kinase domain-intact NTRK1 fusions and 1 EML4-ALK fusion).

3.5. Co-mutation analysis

Pairwise Fisher's exact tests with BH-FDR correction on the 15 most frequently mutated genes revealed 21 significantly co-mutated or mutually exclusive gene pairs (adjusted $p < 0.05$). Key findings included: significant co-occurrence of TP53 and APC (OR = 2.07, 95% CI: 1.36-3.14, $p = 6.61$ x 10-4, adjusted $p = 0.005$), consistent with their synergistic driver roles in CRC tumorigenesis; significant mutual exclusivity between KRAS and BRAF (OR = 0.10, 95% CI: 0.04-0.25, adjusted $p < 0.001$) and between APC and BRAF (OR = 0.20, 95% CI: 0.09-0.45, adjusted $p < 0.001$), suggesting alternative activation patterns within the MAPK pathway; and significant co-occurrence of KRAS and PIK3CA (OR = 2.32, 95% CI: 1.52-3.54, adjusted $p = 0.001$). Additionally, co-mutation clustering of MSH6 with CREBBP (OR = 5.42, 95% CI: 2.87-10.24), SMARCA4 (OR = 4.20), BRCA1 (OR = 4.47), and ARID1A (OR = 2.45) primarily reflects the high mutational burden phenotype of MSI-H tumors (**Figure 3**).

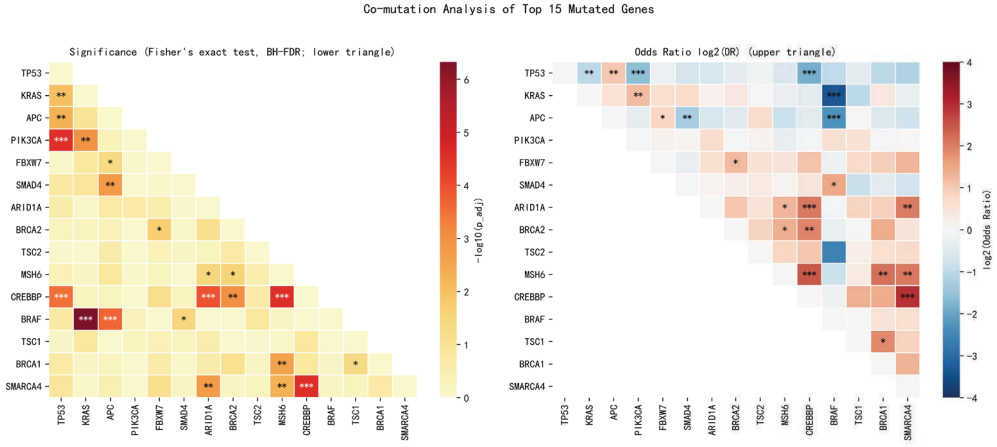

Figure 3. Co-mutation analysis of the 15 most frequently mutated genes. Left panel (lower triangle): Fisher's exact test significance after BH-FDR correction (-log10 adjusted p); right panel (upper triangle): log2(OR), red for co-mutation (OR > 1), blue for mutual exclusivity (OR < 1). Significance symbols shown only for adjusted $p < 0.05$ (* adjusted $p < 0.05$, ** adjusted $p < 0.01$, *** adjusted $p < 0.001$); cells without asterisks indicate non-significance after BH-FDR correction, not missing values. OR estimates for low-frequency events (fewer than 5 co-mutated cases) are unstable and should be interpreted as association signals only. Note: MSH6-related co-mutation clustering primarily reflects the high mutational burden background of MSI-H tumors.

3.6. Variant classification

All 4,725 detected SNV/InDel variants were described using two label systems (see Section 2.4). In ACMG-style pathogenicity labels, Uncertain was the most prevalent category (42.6%, 2,015), followed by Likely benign (19.8%, 937), Likely pathogenic (14.3%, 675), Pathogenic (8.6%, 404), and Benign (1.8%, 86), with Pathogenic/Likely pathogenic totaling 22.8% (1,079). In AMP/ASCO/CAP oncogenicity labels, Likely oncogenic accounted for 9.4% (443) and Oncogenic for 3.5% (165), totaling 12.9% (608).

The variant type distribution (all detected variants) showed missense mutations as the most common (2,197, 46.5%), followed by intronic variants (896, 19.0%), synonymous mutations (680, 14.4%), nonsense

mutations (424, 9.0%), and frameshift deletions (239, 5.1%). Synonymous, intronic, and UTR/flanking region variants were used for descriptive statistics only and were not included in gene-level analyses.

3.7. Potentially actionable molecular event tiering

Per the evidence tiering criteria in Section 2.6 (Figure 4), patient-level prevalence was: Tier 1A, 15.9% (88/553); Tier 1B, 5.4% (30/553); and their union, 19.9% (110/553, with 8 patients harboring both Tier 1A and 1B events). In Tier 1A, MSI-H was the most common event (6.3%), followed by BRAF p.V600E (5.6%), KRAS p.G12C (3.1%), ERBB2 amplification (1.6%), and NTRK1 fusion (0.5%, kinase domain-intact); Tier 1B included ERBB2 mutation (4.9%), ALK fusion (0.4%), and RET fusion (0.2%).

Tier 2: KRAS non-G12C mutations (49.9%) and NRAS mutations (3.4%), with 369 patients (66.7%) harboring at least one Tier 1 or Tier 2 event.

Tier 3: PIK3CA mutations (22.4%), BRCA2 mutations (13.2%), BRCA1 mutations (6.7%), MET mutations (5.4%), BRAF non-V600E mutations (2.4%), and amplifications of MYC (2.9%), FGFR3 (2.5%), FGFR1 (2.0%), and CCND1 (1.3%). Including Tier 3, 435 patients (78.7%) harbored at least one event of any tier. It should be noted that BRCA1/2 mutations are mostly passenger events and are not equivalent to homologous recombination deficiency; MET mutations differ fundamentally from MET amplification or exon 14 skipping in targetability; and these Tier 3 events should be regarded as exploratory.

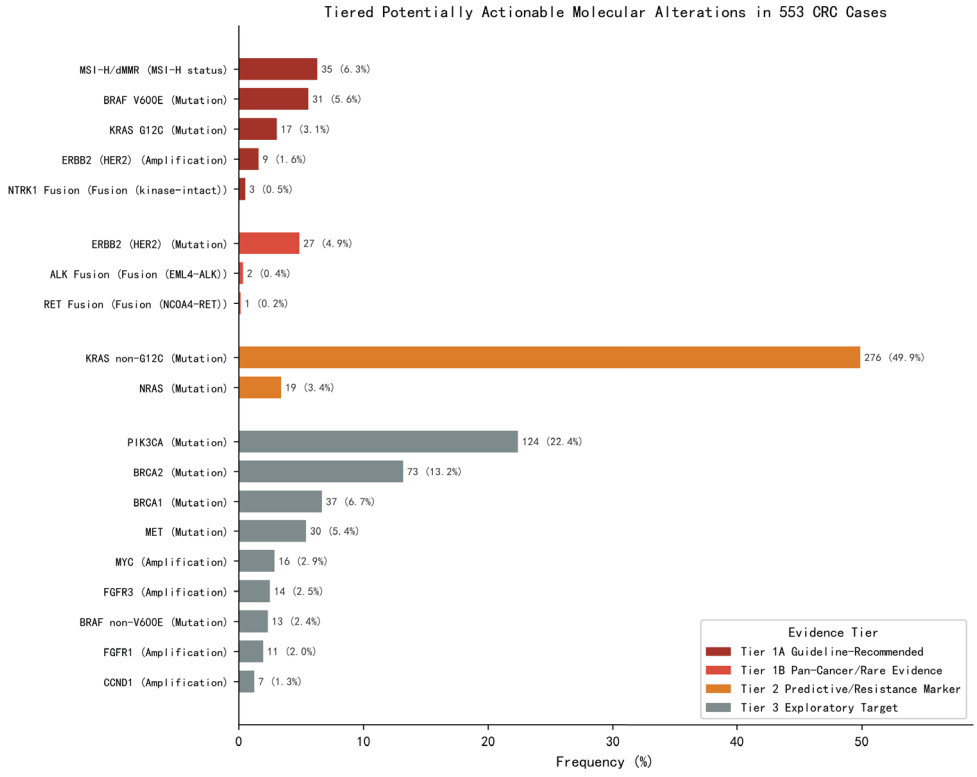

Figure 4. Tiered potentially actionable molecular events in 553 colorectal cancer cases. Classification is a research framework based on NCCN guidelines and literature evidence (not ESCAT/OncoKB standard): Tier 1A (dark red) = CRC guideline-recommended molecular events (88 cases, 15.9%), Tier 1B (light red) = pan-cancer approved or rare events with relatively high-level evidence (30 cases, 5.4%), Tier 2 (orange) = predictive/resistance markers, Tier 3 (gray) = exploratory molecular events; patient-level deduplication across tiers: Tier 1A+1B = 19.9% (110/553, with 8 patients harboring both Tier 1A and 1B events), Tier 1+2 = 66.7% (369/553), all tiers = 78.7% (435/553). Note: BRCA1/2, MET, and other Tier 3 events are exploratory and not equivalent to proven CRC therapeutic targets.

3.8. Associations between gene mutations and clinicopathological features

Association analysis results for the 30 most frequently mutated genes with tumor site, differentiation, and sex. Tumor site *p*-values correspond to 2 x 2 Fisher's exact tests comparing colon (right and left combined) versus rectum (BH-FDR corrected, 30 tests per variable), with subgroup frequencies shown as descriptive breakdowns. PIK3CA mutations were significantly enriched in colon (right colon 43.0%, left colon 19.7% vs. rectum 15.3%, adjusted $p < 0.001$); TP53 was enriched in rectum (rectum 83.1% vs. colon combined 72.5%, adjusted $p = 0.022$; right colon 64.5%, left colon 79.6%); APC was enriched in rectum (rectum 55.6% vs. colon combined 43.0%, adjusted $p = 0.022$; right colon 35.5%, left colon 48.2%); and CDK12 (right colon 12.4%, left colon 4.4% vs. rectum 2.4%, adjusted $p = 0.022$) and SMO (right colon 13.2%, left colon 2.2% vs. rectum 2.4%, adjusted $p = 0.047$) mutations were enriched in colon. A prespecified pairwise comparison (not additionally corrected) showed BRAF mutation enrichment in the right colon (15.7% vs. rectum 5.8%, uncorrected $p = 0.002$), consistent with prior literature. In poorly differentiated tumors, SMAD4 (31.2% vs. moderately differentiated 12.3%, adjusted $p = 0.012$), ARID1A (37.5% vs. 15.6%, adjusted $p = 0.012$), BRAF (22.9% vs. 4.8%, adjusted $p = 0.003$), CDK12 (16.7% vs. 3.6%, adjusted $p = 0.012$), and PALB2 (14.6% vs. 3.3%, adjusted $p = 0.021$) mutations were significantly enriched. APC mutations were more common in males (54.8% vs. females 40.5%, adjusted $p = 0.036$). Given the high proportion of missing differentiation records (29.8%, 165/553), differentiation-related results should be interpreted as exploratory. Additionally, CDK12, SMO, and PALB2 mutations are predominantly variants of uncertain significance (VUS), and their associations with clinicopathological features may be influenced by VUS inclusion, requiring cautious interpretation in conjunction with pathogenicity classification.

4. Discussion

This study systematically analyzed 116-gene targeted sequencing data from 553 Chinese CRC patients, delineating the mutational landscape across SNV/InDel, copy number amplification, gene fusion, and variant classification dimensions based on a well-defined nonsynonymous variant analysis set, providing real-world regional data for CRC precision oncology.

4.1. Comparison of high-frequency mutated genes with TCGA and Chinese studies

The mutation frequencies of TP53 (78.1%), KRAS (53.0%), and APC (49.4%) in this study differ from TCGA reports (TP53, 50%-60%; KRAS, 40%-45%; APC, 70%-80%) [2]. The higher TP53 frequency may reflect:

(1) population differences, as this cohort has a higher proportion of rectal cancer (53.3%), in which both TP53 and APC were enriched;

(2) the high panel sequencing depth (>500x) increasing sensitivity for low-abundance TP53 variants, whereas APC large fragment deletions may be underestimated;

(3) the 28.4% biopsy specimens potentially affecting tumor purity. Additionally, TP53 detection included splice site variants, which may contribute to the elevated apparent frequency.

Compared with other Chinese large-scale studies, Guo et al. [5] (887-gene panel, 869 cases) reported TP53 (72%), APC (63%), and KRAS (42%) as the most frequent mutations, consistent with our ranking; Cheng et al. [6] (73-gene panel, 414 cases) reported lower mutation frequencies overall, likely reflecting the smaller panel size. Zhao et al. [4] (whole-exome sequencing, 1,015 cases) similarly confirmed TP53-KRAS-

APC as the core driver combination. The TSC2 mutation frequency of 11.6% in this study exceeds TCGA's approximately 5%-6% [2]; however, 94.0% (63/67) of TSC2 variants were VUS missense mutations, with only 4 patients (0.7%) harboring pathogenic or likely pathogenic TSC2 variants, consistent with TCGA's truncation-dominated inactivation pattern, indicating that the difference primarily stems from variant inclusion criteria.

4.2. Clinical significance of copy number amplifications and gene fusions

Copy number amplification events were relatively infrequent (12.7%), but some carry therapeutic significance: ERBB2 amplification (1.6%) is a potential target for anti-HER2 therapy [12], MYC amplification (2.9%) suggests aberrant WNT pathway activation [13], and EGFR amplification (0.9%) has unclear treatment guidance value and was not included in the tiering analysis.

Gene fusions were rare (1.3%), but some fusion-positive patients may benefit from targeted therapy: kinase domain-intact NTRK1 fusions (0.5%, 3 cases) represent established targets for larotrectinib [14], and ALK fusions (0.4%) and RET fusions (0.2%) also have corresponding targeted agents [15-16]. Breakpoint structure analysis revealed that the same "NTRK1 fusion" designation can correspond to different molecular structures (3 kinase domain-intact versus 1 kinase domain-not-retained), underscoring the importance of evaluating fusion direction and kinase domain integrity in clinical report interpretation. All 3 kinase domain-intact NTRK1 fusions were found in MSI-H patients, but the small sample size precludes further inference.

4.3. Challenges in somatic variant classification

This study retained both AMP/ASCO/CAP oncogenicity labels [7] and laboratory ACMG-style pathogenicity labels [8] for somatic variants (see Section 2.4). The high proportion of variants classified as Uncertain (42.6%) reflects the practical difficulty of somatic variant interpretation in solid tumor panel testing: unlike germline variants, clinical interpretation evidence for somatic variants is more limited, particularly for missense mutations lacking functional experimental validation. Pathogenic/likely pathogenic variants accounted for 22.8% under the ACMG framework. In contrast, oncogenic/likely oncogenic variants accounted for 12.9% under the AMP/ASCO/CAP framework (the two systems partially overlap and cannot be simply summed), indicating that a considerable proportion of variants receive some interpretive label in clinical testing reports. However, their clinical significance requires context-specific interpretation. For genes dominated by VUS such as TSC2, apparent mutation frequency alone may overestimate clinical significance, and pathogenicity-stratified interpretation is essential.

4.4. Co-mutation patterns and pathway interactions

TP53-APC co-mutation (OR = 2.07) is one of the canonical synergistic driver combinations in CRC, with both genes functioning as tumor suppressors in the p53 and WNT pathways, respectively, and their co-mutation accelerating adenoma-to-carcinoma progression [17]. The significant mutual exclusivity of KRAS-BRAF (OR = 0.10) and APC-BRAF (OR = 0.20) is consistent with alternative activation of MAPK pathway driver events: BRAF-mutant CRC constitutes a molecularly distinct subgroup (often associated with MSI-H and serrated pathway origin) that rarely overlaps with classical KRAS or APC driver events [18]. KRAS-PIK3CA co-mutation (OR = 2.32) suggests that synergistic activation of the MAPK and PI3K pathways confers a selective advantage in some CRC cases, consistent with prior reports [18]. The co-mutation clustering of MSH6 with CREBBP, SMARCA4, BRCA1, and ARID1A primarily reflects the high mutational burden

background of MSI-H tumors rather than specific pathway interactions, and interpretation should account for MSI status as a confounder.

4.5. Potentially actionable molecular events and precision treatment

This study stratified potentially actionable molecular events into three evidence-based tiers to avoid overestimating clinical actionability. At the Tier 1 level, 19.9% of patients harbored at least one Tier 1 molecular event. MSI-H patients are a well-defined population that benefits from immune checkpoint inhibition: pembrolizumab is established as first-line standard therapy for MSI-H advanced CRC [19], nivolumab plus ipilimumab has shown durable benefit [20], and PD-1 blockade has demonstrated remarkably high complete response rates in dMMR locally advanced rectal cancer [21]. Patients with BRAF p.V600E mutations can benefit from encorafenib plus cetuximab [22]; those with KRAS p.G12C (3.1%) from sotorasib or adagrasib combined with anti-EGFR therapy [23]; and those with ERBB2 amplification from tucatinib plus trastuzumab [24]. ERBB2 mutation evidence is primarily derived from basket trials and does not have the same guideline-level support as ERBB2 amplification in CRC. NTRK1/ALK/RET fusions, although rare, have clearly effective targeted agents, highlighting the value of multigene panel testing.

At the Tier 2 level, KRAS non-G12C mutations (49.9%) and NRAS mutations (3.4%) are negative predictive markers for anti-EGFR therapy, with decisive influence on first-line treatment decisions. At the Tier 3 level, PIK3CA, MET, BRCA1/2, and other variants have no approved drugs in CRC and represent exploratory directions for later-line treatment. It should be specifically noted that BRAF non-V600E mutations (29.5% of BRAF mutations) are mostly class II or III variants that are insensitive to BRAF monomer inhibitors, whereas class III mutations may instead benefit from MEK inhibitors or combined anti-EGFR strategies [25], and should not be equated with V600E in clinical interpretation.

4.6. Limitations

This study has several limitations:

(1) the retrospective single-center design with low TNM staging completeness (26.0%) precluded analysis of gene-stage associations;

(2) the limited panel coverage (0.25 Mb) is unsuitable for standard tumor mutational burden calculation and may miss off-panel variants (e.g., POLE proofreading domain [26]);

(3) the lack of paired normal controls means that some variants may be of germline origin, and certain genes have high VUS proportions (e.g., TSC2), requiring functional validation;

(4) the amplification threshold (3.5 or greater copies) is lower than high-level amplification criteria used in some studies (e.g., 6 or greater copies), necessitating caution in cross-study comparisons, and the low amplification and fusion detection rates limit statistical power;

(5) the lack of follow-up data and consensus molecular subtype analysis precludes assessment of gene-prognosis and gene-transcriptomic subtype associations. Nevertheless, this study reflects real-world clinical sequencing practice at a provincial cancer center and remains representative of routine molecular diagnostic workflows.

5. Conclusion

This study delineates the 116-gene mutational landscape of 553 Chinese CRC patients, characterizing

the TP53-KRAS-APC core mutation pattern, classic hotspot distributions, low-frequency copy number amplification and fusion events, and a tiered map of potentially actionable molecular events (19.9% of patients harboring Tier 1 events), providing real-world regional data to inform precision oncology in CRC.

Disclosure statement

The author declares no conflict of interest.

References

[1] Sung H, Ferlay J, Siegel RL, et al., 2021, Global Cancer Statistics 2020: GLOBOCAN Estimates of Incidence and Mortality Worldwide for 36 Cancers in 185 Countries. CA: A Cancer Journal for Clinicians, 71(3): 209–249.

[2] Cancer Genome Atlas Network, 2012, Comprehensive Molecular Characterization of Human Colon and Rectal Cancer. Nature, 487(7407): 330–337.

[3] Chen W, Zheng R, Baade PD, et al., 2016, Cancer Statistics in China, 2015. CA: A Cancer Journal for Clinicians, 66(2): 115–132.

[4] Zhao Q, Wang F, Chen YX, et al., 2022, Comprehensive Profiling of 1015 Patients' Exomes Reveals Genomic-Clinical Associations in Colorectal Cancer. Nature Communications, 13: 2342.

[5] Guo L, Wang Y, Yang W, et al., 2023, Molecular Profiling Provides Clinical Insights Into Targeted and Immunotherapies as Well as Colorectal Cancer Prognosis. Gastroenterology, 165(2): 414–428.

[6] Cheng B, Xu L, Zhang Y, et al., 2024, Correlation Between NGS Panel-Based Mutation Results and Clinical Information in Colorectal Cancer Patients. Heliyon, 10(7): e29299.

[7] Li MM, Datto M, Duncavage EJ, et al., 2017, Standards and Guidelines for the Interpretation and Reporting of Sequence Variants in Cancer: A Joint Consensus Recommendation of the Association for Molecular Pathology, American Society of Clinical Oncology, and College of American Pathologists. Journal of Molecular Diagnostics, 19(1): 4–23.

[8] Richards S, Aziz N, Bale S, et al., 2015, Standards and Guidelines for the Interpretation of Sequence Variants: A Joint Consensus Recommendation of the American College of Medical Genetics and Genomics and the Association for Molecular Pathology. Genetics in Medicine, 17(5): 405–424.

[9] Tate JG, Bamford S, Jubb HC, et al., 2019, COSMIC: The Catalogue Of Somatic Mutations In Cancer. Nucleic Acids Research, 47(D1): D941–D947.

[10] Cerami E, Gao J, Dogrusoz U, et al., 2012, The cBio Cancer Genomics Portal: An Open Platform for Exploring Multidimensional Cancer Genomics Data. Cancer Discovery, 2(5): 401–404.

[11] National Comprehensive Cancer Network, 2025, NCCN Clinical Practice Guidelines in Oncology: Colon Cancer (Version 3.2025), visited on July 20, 2026, https://www.nccn.org.

[12] Sartore-Bianchi A, Trusolino L, Martino C, et al., 2016, Dual-Targeted Therapy With Trastuzumab and Lapatinib in Treatment-Refractory, KRAS Codon 12/13 Wild-Type, HER2-Positive Metastatic Colorectal Cancer (HERACLES): A Proof-of-Concept, Multicentre, Open-Label, Phase 2 Trial. The Lancet Oncology, 17(6): 738–746.

[13] Blank A, Schenk L, Moch H, 2021, The Impact of MYC Alterations in Colorectal Cancer. Der Pathologe, 42(3): 255–261.

[14] Drilon A, Laetsch TW, Kummar S, et al., 2018, Efficacy of Larotrectinib in TRK Fusion-Positive Cancers in

Adults and Children. New England Journal of Medicine, 378(8): 731–739.

[15] Lin JJ, Riely GJ, Shaw AT, 2019, Targeting ALK: Precision Medicine Takes on Drug Resistance. Cancer Discovery, 9(7): 899–915.

[16] Subbiah V, Gainor JF, Rahal R, et al., 2018, Precision Targeted Therapy With BLU-667 for RET Fusion-Positive Solid Tumors. Cancer Discovery, 8(7): 836–849.

[17] Fearon ER, Vogelstein B, 1990, A Genetic Model for Colorectal Tumorigenesis. Cell, 61(5): 759–767.

[18] Yaeger R, Chatila WK, Lipsyc MD, et al., 2018, Clinical Sequencing Defines the Genomic Landscape of Metastatic Colorectal Cancer. Cancer Cell, 33(1): 125–136.

[19] Andre T, Shiu KK, Kim TW, et al., 2020, Pembrolizumab in Microsatellite-Instability-High Advanced Colorectal Cancer. New England Journal of Medicine, 383(23): 2207–2218.

[20] Overman MJ, Lonardi S, Wong KYM, et al., 2018, Durable Clinical Benefit With Nivolumab Plus Ipilimumab in DNA Mismatch Repair-Deficient/Microsatellite Instability-High Metastatic Colorectal Cancer. Journal of Clinical Oncology, 36(8): 773–779.

[21] Cercek A, Lumish M, Sinopoli J, et al., 2022, PD-1 Blockade in Mismatch Repair-Deficient, Locally Advanced Rectal Cancer. New England Journal of Medicine, 386(25): 2363–2376.

[22] Kopetz S, Grothey A, Yaeger R, et al., 2019, Encorafenib, Binimetinib, and Cetuximab in BRAF V600E-Mutated Colorectal Cancer. New England Journal of Medicine, 381(17): 1632–1643.

[23] Fakih MG, Kopetz S, Kuboki Y, et al., 2022, Sotorasib for Previously Treated Colorectal Cancers With KRAS G12C Mutation (CodeBreaK100): A Prespecified Analysis of a Single-Arm, Phase 2 Trial. The Lancet Oncology, 23(1): 115–124.

[24] Strickler JH, Cercek A, Siena S, et al., 2023, Tucatinib Plus Trastuzumab for Chemotherapy-Refractory, HER2-Positive, RAS Wild-Type Unresectable or Metastatic Colorectal Cancer (MOUNTAINEER): A Multicentre, Open-Label, Phase 2 Study. The Lancet Oncology, 24(5): 496–508.

[25] Yaeger R, Corcoran RB, 2019, Targeting Alterations in the RAF-MEK Pathway. Cancer Discovery, 9(3): 329–341.

[26] Palles C, Cazier JB, Howarth KM, et al., 2013, Germline Mutations Affecting the Proofreading Domains of POLE and POLD1 Predispose to Colorectal Adenomas and Carcinomas. Nature Genetics, 45(2): 136–144.

Publisher's note

Bio-Byword Scientific Publishing remains neutral with regard to jurisdictional claims in published maps and institutional affiliations.

Oncology Treatment Discovery, 2026, Volume 4, Issue 3
https://bbwpublisher.com/journal/OTD
Online ISSN: 2981-8079
Print ISSN: 3083-4996

Research on the High-quality Development Path of Tumor Prevention and Control in Frontier Minority Counties under the Background of Public Hospital Reform-based on the Empirical Analysis of Lufeng City

Ruyan Liu[1], Manchang Li[2], Fayuan Pu[1], Guolin Li[1], Jiantao Dong[1], Yinting Lu[1]

[1]Lufeng City People's Hospital, Lufeng 651299, Yunnan, China
[2]Anning First People's Hospital, Anning 650399, Yunnan, China

Copyright: © 2026 Author(s). This is an open-access article distributed under the terms of the Creative Commons Attribution License (CC BY 4.0), permitting distribution and reproduction in any medium, provided the original work is cited.

Abstract: *Objective:* To analyze the shortcomings of tumor prevention and control in multi-ethnic counties in border areas, explore the construction path of mutual adaptation, and provide a reference for the coordinated reform of medical prevention and control in similar areas. *Methods:* Taking Lufeng City as an empirical case, using the configuration perspective and the resource integration theory of multiple medical institutions, the qualitative configuration analysis was carried out from six aspects: organizational coordination, talent allocation, information construction, technical resources, service process and performance incentive. Combined with the data on tumor registration, screening, and medical community operation, the relationship between various elements was analyzed. *Results:* The hardware equipment for tumor diagnosis and treatment in Lufeng City improved significantly, but the multi-factor configuration mismatch was prominent, showing "strong hardware and weak system". It is mainly manifested in the lack of cross-agency coordination mechanisms, the concentration of talents at the county level, the obvious data barriers of business systems, the emphasis on hardware investment, the unsmooth full-cycle service chain of "prevention, screening, treatment, management and health", and the imperfect assessment and incentive mechanism. It is difficult to improve the overall service efficiency by upgrading hardware. *Conclusion:* The prevention and treatment of tumors in border ethnic counties cannot simply copy the reform model of focusing on equipment and attracting talent in the central and eastern regions. We should start from the aspects of system priority, talent-ability sinking and information-process reengineering based on local reality, promote the coordinated integration of multiple factors, and build a full-cycle closed-loop management system of tumors suitable for border ethnic counties.

Keywords: Public hospital reform; Border ethnic counties; Tumor prevention and treatment; Resource integration; Configuration perspective; Tight medical community; Lufeng City

Online publication: October 20, 2026

1. Introduction

Cancer has become a major public health issue threatening the life and health of ethnic minority populations in border regions. National policies such as the Cancer Prevention and Treatment Action, the construction of compact county-level medical communities, and the Thousand-County Project all explicitly require that tumor prevention and control efforts be shifted to an earlier stage [1-5]. County-level public hospitals serve as the key vehicle for implementing healthcare reform policies and safeguarding the health of grassroots populations. At present, many ethnic minority counties have equipped themselves with large-scale devices such as linear accelerators, afterloading treatment machines, and PETCT scanners. However, the service system still operates inefficiently: grassroots tumor screening mobilization is insufficient, postoperative rehabilitation and followup are inadequate, and patients are referred to provincial and prefectural hospitals, leading to increased outofcounty consumption of medical insurance funds. This indicates that tumor prevention and control are not merely a matter of hardware facilities, but rather a systemic problem involving intertwined institutional, human, informational, technical, procedural, and assessment dimensions. Most existing studies focus on the internal specialty capacity building of county-level hospitals, with few empirical studies on county-level tumor prevention and control in border ethnic regions from a multiinstitutional collaborative perspective [6]. Configuration theory holds that the effectiveness of public services depends on the coordinated matching of multiple factors; optimizing a single condition alone is insufficient to achieve overall system improvement. This offers a new analytical perspective for the construction of county-level tumor prevention and control systems [2].

Lufeng City, a multiethnic county in central Yunnan where ethnic minorities account for 27.8% of the population, was among the first batch of national pilot sites for compact countylevel medical community construction. Leveraging the ThousandCounty Project, Lufeng established the first countylevel tumor radiotherapy center in Chuxiong Prefecture, integrated tumor management into the “four highs and seven diseases” medicalprevention integrated fullcycle management framework, and simultaneously built a management information system. It has preliminarily achieved tumor chronic diseaseoriented and informationbased management, thereby providing a typical case for research. Taking Lufeng City as an example, this paper, from the perspectives of resource integration and configuration, analyzes the existing dilemmas, distills replicable construction pathways, and offers references for similar countylevel reforms.

2. Realistic logic of resource integration driving countylevel tumor prevention and control construction in border ethnic regions

Tumor prevention and control require the integration of clinical diagnosis and treatment with public health efforts. Highrisk interventions and screening fall under public health services, diagnosis and treatment are concentrated in countylevel hospitals, and postoperative rehabilitation and followup rely on township and village health centers for implementation. In the health system of border counties, these functions are dispersed across multiple institutions, including countylevel hospitals, CDC, maternal and child health hospitals, township health centers, and village clinics. Medical and health service resources are fragmented. Therefore, the highquality development of countylevel health services should emphasize the promotion of systematic crossinstitutional resource integration [3].

2.1. Countylevel public hospitals serve as the hub for countylevel tumor prevention and control

County-level hospitals function as the central node, undertaking the transfer of technical support from higherlevel institutions, referral of complex cases upward, and guidance of townshiplevel services. In border mountain areas, patients face long travel distances and high transportation costs. Highrisk interventions, early screening mobilization, postoperative rehabilitation, and routine followup rely heavily on rural medical institutions. If the countylevel fullchain service system operates poorly, many patients are forced to travel long distances to provincial or prefectural hospitals. This not only contradicts the original intention of hierarchical diagnosis and treatment reform but also increases the financial burden on patients' families.

2.2. Resource fragmentation constrains service efficiency improvement

Tumor prevention and control resources are distributed across different institutions such as countylevel public hospitals, CDC, maternal and child health hospitals, and township health centers, each with inconsistent assessment objectives. This leads to issues such as poor communication, ambiguous rights and responsibilities, and redundant work [3]. Additionally, ethnic regions face practical challenges including difficulties in attracting and retaining talent, large service radii in mountainous areas, and differences in ethnic health perceptions. No single institution can independently accomplish the fullcycle management of tumors; it is necessary to promote crossinstitutional coordination of multiple factors—human resources, funding, information, technology, and institutions. In Lufeng, all 21 oncology specialists are concentrated in the countylevel hospital. After hardware improvements, followup efforts in talent deployment, health education, and public health followup services have been insufficient. Overall service efficiency has not achieved expected results, and hardware advantages have not translated into accessible services for the public.

2.3. Fulllifecycle health management is an essential requirement for effective prevention and control

Traditional countylevel medical care has emphasized inhospital treatment, prioritizing surgery, radiotherapy, and chemotherapy, while paying insufficient attention to predisease highrisk intervention, postoperative rehabilitation, and psychological counseling. Many ethnic minority populations have limited awareness of tumors [4]. Health education needs to be adapted to local folk customs. It is necessary to rely on the integrated medical community to consolidate resources and, in conjunction with public hospital reform in ethnic regions, extend services from hospitals to rural areas outside the hospital. This should cover the complete cycle of highrisk intervention, early cancer screening, standardized diagnosis and treatment, postoperative rehabilitation, psychological intervention, and routine followup, matching the health needs of the population.

3. Theoretical framework and research methods

3.1. Theoretical framework

This study constructs an analytical framework combining configuration theory and multiinstitutional resource integration theory. Configuration theory posits that the effectiveness of complex public health systems arises from the coordination of multiple conditions, with complementarity, substitution, and constraint relationships among elements; no single condition can independently achieve highquality system operation [2].

Incorporating multiinstitutional resource integration theory, this paper takes the countylevel tumor prevention and control system as the subject and examines the integration pathways of multifactor coordination and adaptation across six core dimensions: organizational collaboration, workforce allocation, information infrastructure, technical resources, service processes, and performance incentives [3].

3.2. Research methods

An embedded singlecase study design is adopted, using the Lufeng experience for empirical analysis with qualitative configurational logical interpretation, without conducting fsQCA operations, to identify factor interactions and practical dilemmas. Meanwhile, policy documents on public hospital reform, the ThousandCounty Project, cancer prevention and treatment, and compact countylevel medical community construction are reviewed to identify gaps between policy and grassroots practice.

3.3. Data sources

Data sources include: national, provincial, and prefectural policy documents; Lufeng tumor management monitoring data, medical community operational data, medical insurance system data, health statistics annual reports, and twoway referral business data; annual tumor management work reports; and onsite observation and analysis materials.

3.4. Analytical dimensions

The six conditions are assessed in terms of completeness, practical shortcomings, configurational interactions among factors, and existing dilemmas.

4. Current state of configurational conditions and dilemmas of Lufeng's tumor prevention and control system

4.1. Organizational collaboration: Organizations established but institutional constraints insufficient

Based on the joint management requirements of "responsibility, management, service, and benefit" within the compact medical community, Lufeng has established a countylevel tumor prevention and control organizational structure led by the municipal government, coordinated by the Municipal Health Bureau, guided by the Municipal Tumor Prevention and Treatment Center, and involving collaborative participation from the Traditional Chinese Medicine Hospital, CDC, Maternal and Child Health Hospital, and township health centers. However, crossdepartmental tasks are mostly coordinated on an ad hoc basis without clear collaborative mechanisms, and the overall planning and assessment of each institution remain independent. Organizational collaboration is a prerequisite condition; the absence of collaborative institutions directly hinders talent deployment and data sharing [7].

4.2. Workforce allocation: Countylevel concentration with weak grassroots capacity

All 21 countylevel oncology professionals (including those recruited from provincial and prefectural levels) are concentrated at the county hospital. Services from regular "senior physician" assistance and workstation experts are essentially provided only at the county level. Townships have no fulltime oncology staff, and grassroots medical personnel lack standardized training in tumor risk identification, rehabilitation

assessment, and followup. Township health centers have multiple competing tasks, and tumor prevention and control accounts for only 4.2% of the public health assessment, resulting in low work motivation [8]. Although telemedicine can compensate for some operational shortcomings, it cannot replace homebased health education and onsite followup. Insufficient grassroots service capacity makes it difficult to accept downward referrals of postoperative patients, limiting the reach of reform benefits to remote mountainous areas.

4.3. Information infrastructure: Basic platforms exist, but data silos are prominent

Lufeng has established a population health information platform and a chronic disease management system. However, HIS, tumor registry, maternal and child screening, and resident electronic health records remain independent of each other. There are still issues such as inconsistent data standards, duplicate data entry, delayed information updates, difficulty in tracking screenpositive individuals, and difficulties in achieving closedloop followup.

4.4. Technical resources: Hardware advantages evident, but funding structure imbalanced

Lufeng has established a tumor radiotherapy center, with investment in tumorrelated hardware equipment accounting for 77.45% of total spending, whereas investment in education, training, and rehabilitation services accounts for only 22.55%. Mutual recognition of examination and test results across counties has not been fully realized, and appropriate screening technologies have been insufficiently deployed to mountain townships. Grassroots medical staff have considerable room for improvement in basic service capabilities, and patient guidance toward grassroots facilities is inadequate.

4.5. Service processes: Breaks in the full chain and insufficient services adapted to ethnic populations

Lufeng has implemented highrisk screening, MDT multidisciplinary diagnosis and treatment, and fullcycle management for highrisk (red), mediumrisk (yellow), and lowrisk (green) tumor patients. Twoway referral channels have been established, along with countytownship onestop service centers and a central pharmacy within the medical community to optimize service processes. However, breaks remain in the service chain: the downward referral rate for stable postoperative patients is only 18.7%, and the supply of rehabilitation and psychological intervention at the township level is inadequate. Some ethnic minority highrisk populations living in mountainous areas, affected by transportation and cognitive factors, show low screening willingness and poor followup compliance. The transformation of service processes is not synchronized with the needs of ethnic regional populations.

4.6. Performance incentives: Emphasis on task volume, lacking outcome orientation

Lufeng's current assessment focuses mainly on the quantity of screening tasks completed, lacking targetoriented indicators such as early diagnosis rate, screening participation rate, patient referral rate, followup completeness rate, and quality of life measures [9]. The linkage between assessment and institutional and individual incentives is weak, with insufficient binding on grassroots followup and highrisk interventions, leading to low motivation among medical staff.

Table 1. Current status of configurational conditions across six elements of Lufeng's tumor prevention and control system

Analytical Element	Condition Completeness	Lufeng Real-world Data Support	Main Shortcomings	Configurational Interaction Among Elements
Organizational Coordination	Moderate	Multi-agency collaborative framework is complete	Lack of clear authorityresponsibility coordination mechanism	Prerequisite, systematic linkage across institutions
Talent Allocation	Moderate	Countylevel talents sufficient; township basic capacity weak	No fulltime staff at primary level; extremely low weight of performance incentive	Affects implementation of primary basic health services
Information System Construction	Moderate	Built national health information platform and chronic disease management system	Existence of information system barriers, difficulty in efficient data governance	Information barriers weaken the effect of hardware and manpower investment
Technical Resources	Moderate	Built tumor radiotherapy center	High proportion of hardware investment, insufficient investment in soft services	Resource allocation constrains basic universal medical services
Service Process	Moderate	Conduct screening, MDT, graded and dynamic management with clear indicators; smooth upward referral	Low downward referral rate, weak primary health service capacity	Various systemic shortcomings ultimately manifest as service process breaks
Performance Incentive	Moderate	Has assessment mechanism	Lacks health outcome indicator assessment	Weakens the actual effectiveness of various reforms

5. Empirical analysis of configurational effectiveness

From the perspective of empirical outcomes in county-level medical operations, the benign configuration and alignment of the six key elements have effectively driven the formation of a closed-loop tumor diagnosis and treatment service system at the county level. This has directly led to the return flow of tumor patients for local care, the retention of medical insurance funds within the county, and increased revenue from enhanced primary-level diagnostic and treatment capacity, thereby significantly reversing the previous situation of large-scale outreferral of tumor patients, outflow of quality medical resources, and underutilization of specialized primarylevel services. In contrast, the earlier development model—which emphasized optimization of individual conditions and fragmented resource allocation—lacked comprehensive support in terms of organization, talent, mechanisms, and informatization. As a result, the advantages of hardware investment could not be translated into actual diagnostic and treatment service capacity, making it difficult to effectively retain patients and medical insurance resources within the county and failing to meet the convenient healthcare needs of remote ethnic populations, thus constraining the highquality development of countylevel public hospitals. The comparative configurational findings fully confirm that highquality development of tumor prevention and treatment in border ethnic counties is not achieved through singleresource input alone, but rather represents a systemic outcome resulting from the synergistic alignment and configurational optimization of the six core elements. The relevant comparative indicators are presented below.

Table 2. Comparison of core performance indicators before and after the reform of the tumor prevention and treatment system in Lufeng City

Core Evaluation Indicators	Inefficient Configuration Stage	Moderate Adaptation Stage	Change
TNM staging rate (%)	61%	77.7%	+16.7%, notable improvement in standardized service
CMI value	1.1328	1.28	+0.1472, improvement in diagnosis and treatment service capacity
Number of oncology inpatients transferred out (person-times)	2483	2407	Outbound transfers decreased by 3.06%; mild and stable patients returning to local medical care
Medical insurance funds consumed by oncology patients outside the city (10,000 yuan)	1939	1687	Out-of-region medical insurance fund consumption decreased by 2.52 million yuan
Proportion of primary care visits	71.27%	74.11%	+2.84%, improvement in primary care service capacity
Per capita income of primary healthcare institutions (yuan)	80456.5	85258.06	+4801.56, increase in primary care income

6. Pathways for building a county-level tumor prevention and treatment system in border ethnic regions guided by resource integration

Based on configuration theory, the quality of county-level tumor prevention and treatment is a systemic process requiring multi-element coordination, complementarity, and substitution. Optimizing a single condition is insufficient to achieve overall system improvement, nor is it necessary to pursue optimal performance across all elements. A differentiated combination model of "one main pathway supplemented by others" can be adopted [2].

6.1. Organizational integration: Consolidating cross-institutional collaborative responsibilities.

Relying on the compact county-level medical community, the responsibility and authority lists for tumor prevention and treatment among county-level hospitals, CDC, maternal and child health institutions, and township health centers should be refined, breaking down barriers of fragmented governance and independent assessment [7]. Mechanisms for regular meetings, special supervision, and annual joint evaluation should be established, with high-risk population tracking, positive screening disposition, and closed-loop referral management incorporated into mandatory assessments. Institutionalized coordination should resolve ad hoc cross-departmental coordination and operational disconnection issues, laying a solid institutional foundation for talent deployment, data interoperability, and business linkage.

6.2. Talent empowerment

Consolidating Primary-Level Service Capacity. A mechanism should be established whereby county-level teams assume responsibility for designated townships with regular deployment to grassroots levels. Practical rotational training should be conducted on tumor initial screening and identification, post-operative

rehabilitation assessment, and high-risk follow-up [8], addressing gaps in primary-level professional capacity. The public health assessment system should be optimized by increasing the incentive weight for tumor prevention and control to over 10%, thereby enhancing grassroots work motivation. This addresses the challenges of mountainous-area household mobilization, home-based follow-up, and insufficient patient acceptance capacity, thereby strengthening the primary-level service foundation.

6.3. Data empowerment

Breaking Down Information Silos. Relying on the county-level universal health information platform, data from diagnosis and treatment, tumor registries, maternal and child screening, and resident health records should be integrated, with unified data entry and update standards. A dynamic database for high-risk tumor populations should be established, enabling a digital closed loop of screening alerts, case tracking, and follow-up management, while reducing duplicate reporting, improving follow-up control quality and efficiency, and fully unleashing the potential of hardware and human resources.

6.4. Resource reciprocity

Addressing Gaps in Soft Services. While ensuring the operation and maintenance of large-scale radiotherapy equipment, the funding structure should be adjusted to increase the proportion of funding allocated to soft services—including health education, professional training, rehabilitation nursing, and technology deployment—to over 30% [3]. Appropriate screening technologies should be promoted at the grassroots level, and county-level mutual recognition of examinations and tests, along with telemedicine services, should be deepened to reduce healthcare costs, curb the outflow of medical insurance funds, and ensure that quality resources benefit mountain communities.

6.5. Service coordination

Improving Service Chains Adapted to Ethnic Characteristics. The criteria for graded referral of tumor patients should be refined, with clear indications for referring stable-phase and rehabilitation-phase patients to primary-level facilities, and the proportion of post-operative patients referred downward should be continuously increased [10]. Gaps in rehabilitation nursing, psychological counseling, and palliative care services at the township level should be addressed. Culturally appropriate bilingual health education materials should be developed based on ethnic characteristics, and innovative communication methods should be adopted. At the same time, convenience measures for mountainous areas should be enhanced, including paired assistance for key populations, green channels for elderly patients, home visits to remote villages, and local notification of screening results, thereby narrowing service gaps in mountainous regions and enhancing the public's sense of healthcare access.

6.6. Outcome benefits

Establishing a Health-Oriented Assessment System. The performance evaluation system should be optimized by reducing process-oriented indicators and focusing on outcome measures such as tumor early diagnosis rate, screening participation rate, follow-up completeness rate, out-of-county referral rate, quality of life, and patient satisfaction. The linkage between assessment results and funding allocation, awards and recognition, and individual performance should be strengthened, balancing positive incentives with negative constraints. This will drive primary-level institutions to shift from "completing tasks" to "delivering effective health

management", fully leveraging the guiding role of performance assessment and activating work momentum across the board.

There is no strict sequential order among the six pathways. Organizational integration provides the underlying rules, talent empowerment provides the implementing agents, data empowerment provides the technical tools, resource reciprocity provides material support, service coordination provides the ultimate vehicle, and performance assessment provides incentive and restraint mechanisms. The pathways interact and mutually reinforce one another, aligning with the differentiated and compound reform needs of border ethnic counties.

7. Conclusion

The high-quality development of public hospitals in border ethnic counties is not equivalent to hardware upgrades at the county hospital level; its essence lies in the multi-institutional resource reconfiguration serving multi-ethnic populations. Lufeng County has made progress in supplementing tumor diagnosis and treatment hardware through the medical community model, yet it still faces configurational challenges including the absence of collaborative systems, imbalanced talent structures, information barriers, imbalanced funding allocation, insufficient adapted services, and a lack of outcome-oriented incentives, resulting in a phenomenon of "strong hardware, weak system". Such regions should not simply replicate the linear reform models of central and eastern China that emphasize heavy equipment acquisition. Instead, they should leverage local resource endowments, rely on the resource integration facilitated by the compact medical community, and adopt a multi-dimensional synergistic approach encompassing institutionalized organization, grassroots-oriented talent deployment, digital information systems, balanced resources, accessible services, and effective performance assessment. This will enable the seamless integration of the full-cycle service chain of "prevention, screening, treatment, management, and rehabilitation" for tumors, optimize the accessible and welfare-enhancing service system adapted to ethnic and mountainous characteristics, and transform the county's hardware advantages in tumor prevention and treatment into tangible, perceptible, and sustainable health service benefits for all ethnic groups. This effectively meets the healthcare needs of remote ethnic populations for convenient and nearby services, and provides a replicable practical paradigm for the high-quality development of public hospitals and integrated tumor prevention-treatment governance in southwestern border counties.

Funding

Research Project on Modernization of Governance System and Governance Capacity in Medical Institutions (EvidenceBased) of the Institute of Hospital Administration, National Health Commission (Project No.: YLZLXZ25G069)

Disclosure statement

The authors declare no conflict of interest.

References

[1] National Health Commission, National Development and Reform Commission, Ministry of Education, et al., 2023, Implementation Plan for the Cancer Prevention and Treatment Action under the Healthy China Initiative (2023–2030). National Health Commission Disease Control Document No. 23 [2023].

[2] Li X, Zhang LF, 2024, Pathways for Realizing the Integration of Medical Treatment and Prevention in County-Level Medical Communities from a Configuration Perspective. Chinese Journal of Health Policy, 17(04): 45–52.

[3] Lyu L, Li J, Wang LS, 2024, Resource Integration Mechanisms in the Context of Compact County-Level Medical Community Development. Chinese Rural Health Service Administration, 44(05): 313–317.

[4] You LL, Zhao PY, Liu YL, 2022, Realistic Dilemmas and Promotion Strategies for the Integration of Medical Treatment and Prevention at the County Level in China. Chinese Journal of Public Health, 38(02): 129–133.

[5] General Office of the National Health Commission, 2021, Notice on Issuing the Work Plan for Improving the Comprehensive Capacity of County Hospitals under the "Thousand Counties Project". National Health Commission Medical Administration Document No. 538 [2021].

[6] Liu LF, Yao L, 2024, An Analysis of the Connotations of High-Quality Development in Primary Health Care. Chinese Journal of Health Policy, 17(01): 17–23.

[7] Chen XY, Zhou ZW, Yang XQ, 2025, Innovative Practice of Medical-Preventive Integration in Tightly-Knit County Medical Communities from the Perspective of Collaborative Governance. Journal of Sichuan University (Medical Sciences), 56(03): 412–417.

[8] Cao CL, Cao WW, Meng FY, 2024, Research on the Path of Continuous Improvement in Primary Health Care Service Quality from the Perspective of Empowerment. Chinese General Practice, 27(01): 9–14, 26.

[9] Hao M, Li CY, 2023, The Logic and Direction of Public Hospital Performance Assessment Reform in China. Chinese Journal of Hospital Administration, 39(07): 529–533.

[10] Breast Cancer Expert Committee of the National Cancer Quality Control Center, Cancer Prevention and Treatment Expert Committee of the Healthy China Initiative, 2024, Expert Consensus on the Management Pathway for County-Level Breast Cancer Prevention and Treatment in China (2023 Edition). Chinese Journal of Oncology, 46(02): 113–120.

Publisher's note

Bio-Byword Scientific Publishing remains neutral with regard to jurisdictional claims in published maps and institutional affiliations.

Oncology Treatment Discovery, 2026, Volume 4, Issue 3
https://bbwpublisher.com/journal/OTD
Online ISSN: 2981-8079
Print ISSN: 3083-4996

Research Progress of TMEM2 in Extracellular Matrix Remodeling and Tumor Microenvironment Regulation

Yiyun Sun, Mingfeng Wu, Zidan Luo, Xinyu Chen, Enle Zhou, Ping Dong*

Department of Pathology, Chongqing University Cancer Hospital, Chongqing400030, China

***Corresponding author*: Ping Dong, 1713819345@qq.com

Copyright: © 2026 Author(s). This is an open-access article distributed under the terms of the Creative Commons Attribution License (CC BY 4.0), permitting distribution and reproduction in any medium, provided the original work is cited.

Abstract: Remodeling of the extracellular matrix (ECM) and regulation of the tumor microenvironment (TME) are essential processes in tumorigenesis and tumor progression. Transmembrane protein 2 (TMEM2), a recently identified cell surface hyaluronidase, participates in various physiological and pathological processes by degrading hyaluronan (HA) in the ECM. This review summarizes the molecular structure and enzymatic properties of TMEM2, the current evidence and controversy regarding its intrinsic catalytic activity, and the mechanisms by which TMEM2 mediates ECM remodeling. Emphasis is placed on recent advances in TMEM2 research in a variety of solid tumors, including its roles in tumor cell proliferation and migration, epithelial-mesenchymal transition, chemoresistance, and regulation of the tumor microenvironment through HA metabolism. Current evidence is mainly derived from bioinformatics analyses, cell-based experiments, and limited animal studies, and further prospective validation is still needed. The potential of TMEM2 as a prognostic biomarker and therapeutic target is also discussed, together with current limitations and future directions, with the goal of providing a reference for basic research and clinical translation in this field.

Keywords: TMEM2; Hyaluronidase; Hyaluronan; Extracellular Matrix; Tumor Microenvironment

Online publication: October 20, 2026

1. Introduction

The tumor microenvironment (TME) plays an important role in tumor initiation, progression, invasion, and drug resistance. As an important component of the TME, the extracellular matrix (ECM) directly influences the biological behavior of tumor cells through changes in its composition and mechanical properties [1,2]. Hyaluronan (HA) is one of the most abundant glycosaminoglycans in the ECM; it is synthesized on the inner side of the plasma membrane by hyaluronan synthases 1-3 (HAS1-3) and directly extruded into the extracellular space, forming a highly hydrated gel-like matrix that participates in key processes such as cell proliferation, migration, differentiation, and signal transduction [3,4]. In a variety of solid tumors, abnormal accumulation of HA is

closely associated with tumor progression, therapeutic resistance, and poor prognosis [5,6].

The metabolic balance of HA is jointly maintained by hyaluronan synthases (HASs) and hyaluronidases (HYALs). Traditionally, the hyaluronidase family members HYAL1 and HYAL2 are considered primarily responsible for HA catabolism: HYAL2 cleaves high-molecular-weight HA (HMW-HA) into intermediate fragments of approximately 20 kDa, which are then further degraded by HYAL1 into small oligosaccharides [7]. However, this classical model cannot fully account for all features of HA turnover in vivo; in particular, the mechanism underlying local HA degradation at the cell surface long remained elusive. In 2017, Yamamoto et al. [8] identified TMEM2 (transmembrane protein 2, also known as CEMIP2) as a novel cell-surface hyaluronidase, filling a knowledge gap in the field of HA metabolism and providing a new perspective for understanding cell-surface HA degradation and its role in tumors [9,10].

In recent years, research on TMEM2 has advanced rapidly, revealing that it not only plays an important role in physiological HA metabolism but also participates in tumor initiation and progression. By degrading cell-surface HA, TMEM2 regulates cell adhesion and migration [11,12], promotes epithelial-mesenchymal transition (EMT) [13], mediates chemoresistance [13], and remodels the mechanical properties of the ECM to alter drug delivery efficiency [5,6]; it may exert tumor-promoting effects in various malignancies, including breast cancer [11,14], pancreatic cancer [12,32], and glioblastoma (GBM) [13]. However, several issues still require systematic review and in-depth discussion, including the controversy over species differences in the catalytic activity of TMEM2 [16,17,18], its differential mechanisms of action across tumor types, and its feasibility as a therapeutic target. This review focuses on three main themes: (1) whether TMEM2 is a bona fide hyaluronidase: current evidence and controversy; (2) how TMEM2 affects tumor biological behavior and the tumor microenvironment through HA metabolism and ECM remodeling; and (3) whether TMEM2 can serve as a prognostic biomarker or therapeutic target for tumors. On this basis, the limitations of existing research and future directions are discussed.

2. Molecular structure and biological functions of TMEM2

2.1. Gene and protein structure

The TMEM2 gene is located on human chromosome 9q21.13 and encodes a type II transmembrane protein with a relative molecular mass of approximately 154 kDa; its gene symbol is CEMIP2 (cell migration-inducing hyaluronidase 2) [8,15]. Its ectodomain contains a conserved β-helix fold domain together with SD1 and SD2 domains, which are closely related to the recognition and binding of polysaccharide substrates [15,36]. In 2023, Niu et al. [36] resolved its high-resolution three-dimensional structure by cryo-electron microscopy, laying a structural foundation for understanding its catalytic mechanism.

The TMEM2 orthologs of humans, mice, and naked mole-rats share high sequence similarity, but their catalytic activities differ markedly: mouse TMEM2 exhibits strong HA-degrading activity, whereas naked mole-rat TMEM2, whose sequence features are closer to those of humans, has almost no physiological HA-degrading function [18]. These species differences provide important clues for understanding the functional adaptation of TMEM2.

2.2. Research progress and controversy regarding the hyaluronidase activity of TMEM2

Evidence supporting the HA-degrading enzymatic activity of TMEM2 mainly comes from classic functional studies. In the initial report in 2017, Yamamoto et al. [8] demonstrated through in vitro and in vivo experiments

that TMEM2 possesses HA-degrading activity, preliminarily establishing the research foundation of this field. In 2023, Narita et al. [17] provided further evidence through recombinant protein experiments, concluding that TMEM2 is a bona fide hyaluronidase with intrinsic catalytic activity that degrades HA via a catalytic mechanism distinct from that of traditional HYAL family enzymes. In addition, using conditional knockout mouse models, Tobisawa et al. [19] found that systemic knockout of TMEM2 increased serum HA levels by approximately 40-fold, and that TMEM2 deficiency led to substantial accumulation of high-molecular-weight HA (HMW-HA) in multiple tissues, to an extent far exceeding the phenotypes observed upon HYAL1 and HYAL2 deficiency [20,21], suggesting that TMEM2 plays an important role in systemic HA catabolism and turnover in vivo.

However, evidence questioning the direct enzymatic activity of human TMEM2 also deserves attention. A study published by Sato et al. [16] in 2023 found that human TMEM2 lacks the key catalytic residues of classical hyaluronidases, and no significant HA-degrading activity of recombinant human TMEM2 protein was detected in in vitro systems; the team subsequently reported that naked mole-rat TMEM2 (nmrTMEM2) likewise lacks physiological hyaluronidase activity [18]. Accordingly, Sato et al. proposed that TMEM2 may not be an enzyme that directly catalyzes HA degradation, but rather acts as a regulatory factor of HYBID (KIAA1199/CEMIP) and HAS2 expression, indirectly influencing HA metabolism [16].

Taken together, a more reasonable understanding at present is that the evidence for the HA-degrading function of TMEM2 is relatively robust in mouse models and in vivo studies [8,19], whereas whether human TMEM2 possesses stable and reproducible intrinsic catalytic activity still requires confirmation by more direct structural biology and biochemistry evidence [9,10]. TMEM2 may participate in HA metabolism through both direct enzymatic activity and indirect regulation (such as the regulation of HYBID/HAS2 expression), and these two pathways are not mutually exclusive; their relative contributions may differ across cellular contexts and experimental systems [9,16,17]. In summary, the current consensus is that TMEM2 plays an important role in HA metabolism in vivo; the divergence lies in the manner in which human TMEM2 functions: direct catalysis versus indirect regulation. This divergence is critical: if human TMEM2 mainly serves as a regulatory factor rather than a catalytic enzyme, drug design strategies targeting its enzymatic activity need to be re-evaluated, and the interpretation of its tumor-promoting mechanisms should incorporate the contribution of cooperating molecules such as HYBID. Clarifying this controversy will help accurately interpret the role of TMEM2 in tumor ECM remodeling and guide the selection of appropriate experimental systems for subsequent research.

2.3. Roles in cellular stress responses and development

In addition to its HA-degrading function, TMEM2 is also involved in endoplasmic reticulum (ER) stress responses and the regulation of cellular homeostasis. In 2019, Schinzel et al. [22] discovered that TMEM2 is a novel ER stress regulator that promotes the maintenance of ER homeostasis through the CD44-MAPK signaling pathway, and this function is independent of the classical unfolded protein response (UPR); in Caenorhabditis elegans, loss of the TMEM2 homolog shortened lifespan, whereas its overexpression extended lifespan, suggesting an evolutionarily conserved cytoprotective function [22].

In 2024, Zhang et al. [23] further revealed that HA degradation products generated by TMEM2 can act as signaling molecules to regulate the dynamic balance of mitochondrial fission and fusion; upon TMEM2 loss, the accumulation of high-molecular-weight HA led to aggravated mitochondrial fragmentation and oxidative

phosphorylation dysfunction, thereby triggering cellular senescence. These findings directly link ECM remodeling to the regulation of cellular metabolism and provide a theoretical basis for understanding the role of HA in tumor metabolic reprogramming [22,23].

In terms of developmental biology, Inubushi et al. [35] found that TMEM2 deficiency caused severe developmental defects in mouse neural crest-derived tissues and led to embryonic lethality, suggesting that TMEM2 can clear a path for migrating cells through local HA degradation and is an indispensable molecule for embryonic development [35].

3. TMEM2-mediated extracellular matrix remodeling

3.1. Cell-surface HA degradation and focal adhesion dynamics

Local degradation of cell-surface HA is essential for cell migration. In 2021, Irie et al. [24] found that TMEM2 localizes to focal adhesions (FAs) and directly binds integrins α5β1 and αLβ2 through its ectodomain, precisely targeting HA-degrading activity to the cell-matrix adhesion interface and promoting the dynamic reorganization of adhesion structures; loss of TMEM2 led to abnormal focal adhesion turnover and a significant decline in cell migration capacity. This finding refines the function of TMEM2 from generalized HA degradation to spatiotemporally specific ECM remodeling [24].

It is worth noting that the pericellular matrix (PCM) formed by HA on the cell surface can reach a thickness several times the cell diameter, constituting a physical barrier to cell migration [25]. Degradation of HA by TMEM2 at focal adhesions can disrupt the integrity of the PCM, creating space for the extension of cellular protrusions (such as lamellipodia and filopodia); when its activity is lost, excessive PCM accumulation hinders cell morphological changes and migration [24,25], providing a cell-level explanation for the role of TMEM2 in tumor invasion and metastasis.

3.2. ECM mechanical properties and tumor invasion

The ECM is not a passive cellular scaffold but an active microenvironment with dynamic mechanical properties. HA accumulation can increase ECM hydration and elevate interstitial fluid pressure (IFP), forming a dense matrix barrier that limits drug penetration and immune cell infiltration [5,6,31]. In pancreatic ductal adenocarcinoma (PDAC), massive HA deposition is an important contributor to tumor stromal fibrosis and vascular compression; studies by Provenzano et al. [5,6] demonstrated that degrading tumor stromal HA with the hyaluronidase PEGPH20 reduced IFP, improved vascular function and chemotherapeutic drug delivery, enhanced the efficacy of gemcitabine, and prompted several clinical trials of combination chemotherapy [2].

As an endogenous cell-surface hyaluronidase, TMEM2 plays a more refined role in the mechanical remodeling of the ECM. Unlike traditional secreted hyaluronidases (such as the systemic degradation strategy of PEGPH20), the local degrading activity of TMEM2 at the cell-matrix interface enables precise regulation of HA distribution in the microenvironment rather than global depletion of HA [24]. Such precise regulation may be of great significance for maintaining the functional architecture of the ECM microenvironment. A 2025 study by Yao et al. [26] showed that restoring TMEM2 expression in PDAC can rearrange collagen fibers by degrading stromal HA, thereby reducing tumor stromal density, improving drug permeability, and ultimately sensitizing chemotherapy. This finding reveals the potential application of TMEM2 in ECM

normalization strategies, that is, improving the tumor microenvironment and promoting therapeutic efficacy through fine-tuned regulation rather than complete eradication of the ECM [26].

In addition, the HA degradation products mediated by TMEM2, namely low-molecular-weight HA (LMW-HA) fragments, are themselves biologically active. Contrary to the anti-inflammatory and anti-angiogenic effects of high-molecular-weight HA, LMW-HA can activate Toll-like receptors (TLR2/TLR4) and the CD44 receptor, promoting inflammation, angiogenesis, and tumor progression [4,29]. Therefore, the ECM-remodeling activity of TMEM2 has dual effects: it can provide spatial conditions for tumor invasion by degrading HA, but may also exacerbate the malignant transformation of the microenvironment by generating tumor-promoting LMW-HA fragments; its net effect depends on the tumor type, the spatiotemporal distribution of HA molecular-weight spectra, and the integration of receptor signaling [4,29].

4. Mechanisms of TMEM2 in tumor development and progression

4.1. Tumor cell proliferation and survival

Available evidence suggests that TMEM2 may promote tumor cell proliferation and survival through multiple pathways. First, LMW-HA fragments generated by HA degradation can serve as ligands for CD44, activating downstream PI3K/AKT and MAPK/ERK signaling pathways and promoting cell cycle progression and the expression of anti-apoptotic genes [29]. Second, TMEM2 participates in the formation and maturation of focal adhesions through direct interaction with integrin α5β1, which may contribute to integrin-mediated cell adhesion and survival signaling [24]. In breast cancer cells, SOX4-dependent transcriptional activation of TMEM2 significantly promotes anchorage-independent growth of tumor cells by enhancing the activity of the above signaling pathways [11].

The protective effect of TMEM2 on cell survival is also reflected in the regulation of ER stress [22]: factors such as hypoxia, nutrient deprivation, and oxidative stress in the tumor microenvironment continuously trigger ER stress, and TMEM2 enhances ER folding capacity and maintains calcium homeostasis through the CD44-MAPK pathway, which may confer a survival advantage to tumor cells under stress conditions [22]; its mediation of mitochondrial homeostasis regulation may also support tumor cell proliferation under high metabolic demand [23].

4.2. Epithelial-mesenchymal transition

EMT is a key process by which epithelial-derived tumors acquire invasive and metastatic capabilities. During this process, epithelial cells lose apical-basal polarity and intercellular junctions and acquire the spindle-shaped morphology and migratory capacity of mesenchymal cells [27]. Multiple research teams have suggested that TMEM2 promotes EMT in various tumor types. Using chromatin immunoprecipitation sequencing (ChIP-seq) and luciferase reporter assays in prostate and breast cancer cells, Lee et al. [11] demonstrated that the transcription factor SOX4 directly binds to the promoter region of the TMEM2 gene to activate its transcription; TMEM2 in turn alters cell-matrix adhesion properties through HA degradation, inducing the upregulation of mesenchymal marker genes (such as Vimentin and N-cadherin) and the downregulation of the epithelial marker gene E-cadherin.

In GBM, Gao et al. [13] found that high TMEM2 expression was significantly associated with the mesenchymal subtype, which is the most invasive molecular subtype of GBM with the worst prognosis. Mechanistic studies showed that TMEM2 activates core EMT transcription factors such as Snail and ZEB1

through downstream effects of the CD44-HA signaling axis, driving the EMT-like mesenchymal program and invasive migration of GBM cells [13]. Given that GBM is not a typical epithelial-derived tumor, all references to EMT in GBM in this review refer to EMT-like mesenchymal transition. In addition, Gan et al. [14] suggested that, in triple-negative breast cancer (TNBC), miR-518a-3p suppresses TMEM2 expression by targeting the 3'-UTR of TMEM2 mRNA, thereby reversing the EMT process and weakening tumor cell migration and invasion. This study not only revealed the post-transcriptional regulatory mechanism of TMEM2 but also provided a potential therapeutic strategy of restoring miRNA expression to inhibit the TMEM2-EMT axis [14].

4.3. Tumor drug resistance

Tumor drug resistance is the main cause of treatment failure and disease progression. The physical barrier effect of the ECM is one of the important mechanisms underlying insufficient chemotherapeutic drug penetration and resistance. As mentioned above, HA accumulation leads to tumor stromal densification and elevated IFP, severely hindering the entry of macromolecular and small-molecule drugs from blood vessels into the tumor parenchyma [5,6,31]. By degrading HA to reduce IFP and improve vascular perfusion, TMEM2 may overcome this type of chemoresistance based on the ECM physical barrier [26]. The study by Yao et al. [26] directly supports this hypothesis: in a PDAC mouse model, restoration of TMEM2 expression combined with gemcitabine treatment significantly reduced tumor volume, accompanied by a marked increase in drug concentration in tumor tissue.

In addition, TMEM2 can mediate intrinsic drug resistance of tumors through EMT and signaling pathway regulation. In GBM research, Gao et al. [13] found that high TMEM2 expression conferred significant resistance to temozolomide (TMZ) in GBM cells. At the mechanistic level, TMEM2 enhanced the expression of O6-methylguanine-DNA methyltransferase (MGMT), the main determinant of TMZ resistance, through HA-CD44 signaling, while simultaneously activating the PI3K/AKT pathway to promote cell survival signals, weakening the cytotoxicity of TMZ on both fronts [13]. After TMEM2 knockdown, the sensitivity of GBM cells to TMZ was significantly restored, indicating that targeting TMEM2 may be a feasible strategy to overcome TMZ resistance in GBM [13].

4.4. Comprehensive regulation of the tumor microenvironment by ECM remodeling

The impact of TMEM2-mediated ECM remodeling on the TME goes far beyond the elimination of physical barriers. Research evidence indicates that TMEM2 activity regulates the cellular composition and functional states of the TME in multiple dimensions. First, LMW-HA fragments produced by TMEM2-mediated HA degradation can recruit and activate tumor-associated macrophages (TAMs) and cancer-associated fibroblasts (CAFs), promoting the formation of an immunosuppressive TME [4,29]. Second, the mechanical relaxation of the ECM caused by HA degradation can release various growth factors locked in the matrix, such as vascular endothelial growth factor (VEGF), transforming growth factor-β (TGF-β), and basic fibroblast growth factor (bFGF), further promoting angiogenesis and fibrosis [29,31].

Through bioinformatics analysis and functional experiments, Srivastava et al. [30] identified TMEM2 as one of the CAF markers in PDAC, suggesting that TMEM2 may exert bidirectional regulatory functions in tumor-stroma communication. Tumor cell-derived TMEM2 degrades HA to generate signaling molecules, which act on CAFs and thereby remodel the stromal environment, forming a positive feedback loop that

exacerbates tumor progression [30]. The study by Yao et al. [26] more directly demonstrated the importance of the TMEM2/HA axis in TME remodeling: restoring TMEM2 expression led to the reprogramming of CAFs in PDAC tumor tissue, shifting them from a tumor-promoting phenotype (such as myofibroblasts with high α-smooth muscle actin (α-SMA) expression) toward a relatively quiescent phenotype, while increasing the infiltration and activity of CD8+ T cells. This suggests that the ECM state regulated by TMEM2 may be a key factor determining the immune landscape of the TME [26].

Taken together, TMEM2 appears to exert important regulatory effects in the TME through a multi-level cascade of mechanisms involving HA degradation, ECM mechanical remodeling, signaling molecule release, and immune microenvironment remodeling [28]. Understanding the complexity of this regulatory network is crucial for designing precise therapeutic strategies targeting TMEM2. Simply inhibiting TMEM2 may lead to HA accumulation and further stromal densification, which is detrimental to drug delivery; whereas excessive activation of TMEM2 may generate large amounts of tumor-promoting LMW-HA fragments and aggravate invasion and metastasis. Therefore, precisely modulating TMEM2 activity or intervening in its downstream effector pathways in a spatiotemporally specific manner may be the direction of future therapeutic development [9,10].

5. Research progress of TMEM2 in various tumors

The main research evidence for TMEM2 in various tumors is summarized in **Table 1**.

Table 1. Summary of research evidence for TMEM2 in different tumors

Tumor type	Expression and prognostic association	Main mechanisms	Evidence type	References
Breast cancer	High expression associated with shortened overall survival and distant metastasis-free survival	SOX4 transcriptional activation; miR-518a-3p targeting; EMT	Clinical samples + cell-based experiments + public database analysis	[11,14]
Pancreatic ductal adenocarcinoma	High expression associated with lymph node metastasis, higher TNM stage, and shortened overall survival; concurrent high expression with KIAA1199 indicates worse prognosis	ECM normalization sensitizing chemotherapy; CAF phenotype regulation	Clinical samples + animal models + cell-based experiments	[12,26,30,32]
Glioblastoma	High expression associated with shortened overall survival; combination with IDH/1p19q improves molecular subtyping	EMT-like mesenchymal transition; TMZ resistance (MGMT upregulation, PI3K/AKT activation)	Public database analysis + cell-based experiments	[13,33]
Laryngeal cancer	High expression associated with increased postoperative recurrence risk (included in a 9-gene recurrence prediction model)	Recurrence prediction model construction	Public database analysis	[34]

5.1. Breast cancer

Breast cancer is one of the tumor types in which TMEM2 was first studied in depth. In a landmark study published in Cancer Research in 2016, Lee et al. [11] used the Cancer Genome Atlas (TCGA) database and paired clinical sample analysis to show that TMEM2 is significantly overexpressed in breast cancer tissue and positively correlated with SOX4; ChIP-seq confirmed that the transcription factor SOX4 can directly bind the TMEM2 promoter and activate its transcription, and SOX4-dependent overexpression of TMEM2 enhanced the migration, invasion, and experimental lung metastasis of breast cancer cells [11]. Clinically,

patients with high TMEM2 expression had significantly shorter overall survival and distant metastasis-free survival. This study established a signaling axis linking SOX4, TMEM2, HA degradation, and cell migration/invasion [11].

In TNBC, Gan et al. [14] further enriched the understanding of TMEM2 at the post-transcriptional regulatory level. Through bioinformatics prediction combined with luciferase reporter assays, the study suggested that miR-518a-3p can directly target the 3'-UTR region of TMEM2 mRNA and inhibit its translation. In TNBC tissues, miR-518a-3p expression was downregulated and negatively correlated with TMEM2 protein levels. Restoring miR-518a-3p expression effectively suppressed TMEM2 protein levels, reversed the expression of EMT markers, and reduced the number of lung metastatic nodules in in vivo models [14]. This finding provides a potential therapeutic approach for restoring the negative regulatory network of TMEM2 using miRNA mimics or small-molecule compounds, and also suggests that TMEM2 expression is precisely controlled by multi-level regulatory networks [14]. The above evidence mainly derives from bioinformatics analyses and in vitro cell-based experiments, and validation in in vivo studies and preclinical models remains limited.

5.2. Pancreatic cancer

Pancreatic cancer (especially PDAC), owing to its dense fibrotic stroma and extremely poor prognosis, is a key tumor type for research on HA metabolism and ECM remodeling. In 2020, Kudo et al. [12] first systematically evaluated the expression and prognostic value of TMEM2 in PDAC. Immunohistochemical analysis of 110 surgically resected PDAC specimens showed that TMEM2 protein was highly expressed in approximately 70% of PDAC tissues, and that high expression was independently associated with lymph node metastasis, higher TNM stage, and significantly shortened overall survival. Multivariate Cox regression analysis indicated that TMEM2 is an independent prognostic factor for PDAC [12]. Unexpectedly, the study also found that small interfering RNA (siRNA) knockdown of TMEM2 in human PDAC cell lines did not inhibit cell migration as expected, but instead led to a compensatory enhancement of migration capacity, accompanied by upregulation of HYBID (KIAA1199/CEMIP) mRNA levels. This finding suggests that a functional compensation mechanism between TMEM2 and HYBID may exist in PDAC [12].

In a 2022 follow-up study, Kudo et al. [32] further examined the combined prognostic value of TMEM2 and KIAA1199 in PDAC. Dual immunohistochemical analysis of 167 resected PDAC specimens showed that the median overall survival of the group with concurrent high expression of TMEM2 and KIAA1199 was only 12.5 months, significantly lower than the 30.2 months of the group with concurrent low expression; after adjustment for age, tumor size, lymph node metastasis, and margin status, concurrent high expression remained an independent adverse prognostic factor (HR = 3.2) [32]. These results provide a new molecular indicator for prognostic stratification of PDAC and highlight the synergistic pathogenic role of the two HA-degrading enzymes in PDAC.

A study published by Yao et al. [26] in Cancer Letters in 2025 provided important insights into the function of TMEM2 in PDAC from a therapeutic perspective. The study suggested that CEMIP2 (TMEM2) normalizes the ECM by degrading HA in the tumor stroma, a process that involves not only the removal of physical barriers but also the rearrangement of collagen fibers and the phenotypic remodeling of CAFs. PDAC mice with restored CEMIP2 expression showed a tumor volume reduction of more than 70% compared with the control group after receiving gemcitabine combined with nab-paclitaxel, accompanied

by a significant increase in CD8+ T cell infiltration and a decrease in regulatory T (Treg) cells. This study provides evidence in animal models for the potential of ECM normalization strategies in sensitizing PDAC treatment, and offers an experimental basis for exploring the conversion of TMEM2 from a tumor-promoting molecule into a therapeutic target [26].

In 2024, Srivastava et al. [30] reported NSC777201, a small-molecule candidate compound targeting TMEM2. Molecular docking simulations showed that NSC777201 can stably bind to TMEM2; in PDAC cell models, NSC777201 treatment reduced TMEM2 expression, inhibited the activity of cancer-associated fibroblasts (CAFs) and induced their senescence, and rescue experiments supported that its effect depends on TMEM2; in mouse models, NSC777201 inhibited tumor growth and improved the tumor microenvironment [30]. Although the selectivity and in vivo efficacy of NSC777201 remain to be systematically evaluated, this study provides preliminary proof of concept for the development of TMEM2-targeted drugs [30]. The studies by Kudo et al. provided clinical relevance evidence based on clinical sample analyses, while Yao et al. further provided in vivo functional evidence through animal models and single-cell sequencing.

5.3. Glioblastoma

GBM is the most common primary malignant brain tumor in adults, notorious for its high invasiveness and therapeutic resistance. In 2023, through analyses of the TCGA and Chinese Glioma Genome Atlas (CGGA) databases, Gao et al. [13] found that TMEM2 mRNA levels in GBM tissue were significantly higher than those in lower-grade glioma and normal brain tissue, and that high expression was associated with shorter overall survival and progression-free survival; gene set enrichment analysis (GSEA) showed significant enrichment of EMT pathways and HA metabolism pathways in the high-expression group [13]. Functional experiments suggested that overexpression of TMEM2 induced typical EMT-like morphological changes in GBM cells, including a transition toward a spindle-shaped mesenchymal morphology, accompanied by downregulation of E-cadherin, upregulation of N-cadherin and Vimentin, and enhanced cell invasion. Conversely, short hairpin RNA (shRNA) knockdown of TMEM2 reversed the above phenotypes [13].

More importantly, this study revealed the important role of TMEM2 in TMZ resistance in GBM. TMEM2 overexpression increased the half-maximal inhibitory concentration (IC50) of TMZ in GBM cells by approximately 3-fold, accompanied by a significant rise in MGMT protein levels. Use of the MGMT inhibitor O6-benzylguanine (O6-BG) partially restored the cytotoxicity of TMZ, indicating that TMEM2-mediated TMZ resistance depends at least in part on MGMT upregulation. In addition, TMEM2 enhanced pro-survival signals by activating the PI3K/AKT pathway, providing another layer of protection for drug resistance in GBM cells [13]. This study suggests that TMEM2 may be one of the important molecules linking HA metabolism, EMT-like mesenchymal transition, and chemoresistance in GBM, providing a theoretical basis for developing TMEM2-targeted strategies against GBM [13].

Regarding the molecular classification of GBM, in 2021 Jiang et al. [33] found through integrated analysis of the TCGA and CGGA datasets that TMEM2 expression levels, combined with isocitrate dehydrogenase (IDH) mutation status and 1p19q co-deletion status, can be used to construct a more refined molecular subtyping system for glioma: among IDH-wildtype gliomas, the TMEM2 high-expression subgroup had significantly worse prognosis than the low-expression subgroup, and the inclusion of TMEM2 markedly improved the accuracy of the model in predicting 3-year and 5-year overall survival [33]. The infiltration proportion of immunosuppressive cells (such as M2 macrophages) was also increased in TMEM2 high-

expression tumors [33]. The above studies are mainly based on public database analyses and in vitro cell-based experiments, and in vivo validation and prospective clinical studies still need to be strengthened.

5.4. Other tumors

In addition to the intensively studied tumor types described above, multiple studies suggest that TMEM2 may exert important functions in a broader spectrum of tumors.

In laryngeal cancer, Xiang et al. [34] constructed a recurrence prediction model using combined mRNA-lncRNA expression profiles, in which TMEM2 was identified as one of the important genes, and its high expression was significantly associated with an increased risk of postoperative recurrence of laryngeal cancer. The area under the receiver operating characteristic curve (AUC) of this model exceeded 0.8 in both the training and validation sets, demonstrating good predictive performance [34]. The widespread abnormal expression of TMEM2 across different tumor types suggests that it may be a pan-cancer tumor-promoting factor, but its expression regulation mechanisms, downstream effector pathways, and functional dependencies may differ depending on tissue origin and genetic background. Future pan-cancer multi-omics integrated analyses will help systematically map the functional and dependency landscapes of TMEM2 across different tumor types.

6. Prospects and challenges of TMEM2 as a therapeutic target

The tumor-promoting effects of TMEM2 in various tumors and its association with poor prognosis make it an attractive potential therapeutic target. However, translating TMEM2 from basic research into a clinical therapeutic target still requires overcoming multiple challenges.

6.1. Current status of small-molecule targeted drug development

In terms of drug development, NSC777201, reported by Srivastava et al. [30], is currently the first small-molecule candidate compound targeting TMEM2, providing preliminary clues for drug research and development in this field. However, its inhibitory potency, selectivity, and pharmacokinetic characteristics against TMEM2 have not been systematically evaluated, and it remains far from clinical translation. In the future, lead compounds need to be optimized through structure-based drug design (SBDD) and high-throughput screening of compound libraries to obtain more potent and highly selective TMEM2 inhibitors. Meanwhile, given the differences in the catalytic activity of TMEM2 between humans and mice [16,17,18], drug development must fully consider the impact of species differences on efficacy evaluation and select appropriate humanized models for preclinical validation.

6.2. Complexity of targeting strategies and combination therapy

In terms of therapeutic strategies, TMEM2 targeting faces complex decision-making challenges arising from its dual effects: inhibiting TMEM2 may lead to HA accumulation in tumor tissue and aggravate ECM densification, thereby impairing drug delivery [5,6]; activating TMEM2 can improve drug penetration through ECM normalization [26], but may generate tumor-promoting LMW-HA fragments and accelerate the EMT process [4,29]. Neither simple inhibition nor activation is an ideal strategy. More refined approaches may include:

(1) spatiotemporally controlled modulation of TMEM2 activity (such as transient activation before

chemotherapy to promote drug penetration);

(2) combined targeting of its downstream effector pathways (such as CD44 antagonists or PI3K/AKT inhibitors);

(3) combination with immune checkpoint inhibitors. The efficacy and safety of the above strategies still need to be systematically evaluated in preclinical models [9,10].

The functional relationship between TMEM2 and HYBID (KIAA1199/CEMIP) also provides important implications for the design of therapeutic strategies. The findings of Kudo et al. [12] indicate that inhibiting TMEM2 alone may achieve little due to compensatory upregulation of HYBID. Therefore, strategies that target TMEM2 and HYBID simultaneously, or broad-spectrum inhibitors that block both HA-degrading enzymes, may be more effective therapeutic directions. The finding of Kudo et al. [32] that the median survival of PDAC patients with concurrent high expression of both hyaluronidases was only 12.5 months provides strong clinical demand support for this combination strategy. However, the potential systemic side effects of comprehensively inhibiting the HA-degrading enzyme system, such as HA accumulation in normal tissues including joints, skin, and kidneys, must be fully considered in the evaluation of the therapeutic window [19,21].

Notably, the study by Yao et al. [26] provides a new idea for TMEM2-targeted therapy: rather than inhibiting TMEM2, its ECM normalization function can be exploited to improve the efficacy of existing treatments. This approach of using ECM remodeling to improve the efficacy of existing therapies has precedents in the field of oncology: in pancreatic cancer, clinical trials of enhancing chemotherapy by degrading HA with PEGPH20 have achieved preliminary results [2,5]. However, unlike the systemic HA degradation of PEGPH20, restoration of endogenous TMEM2 expression may achieve more physiological and spatiotemporally precise ECM remodeling, thereby reducing side effects such as the musculoskeletal toxicity observed in PEGPH20 treatment [2]. If gene therapy or mRNA delivery technologies can achieve tumor-specific transient expression regulation of TMEM2, this strategy may have significant advantages in terms of safety.

6.3. Translational application as a prognostic biomarker

Biomarker development is another key link in the translational application of TMEM2-targeted therapy. At present, TMEM2 as a prognostic biomarker has been validated in multiple retrospective studies [12,32,33], but prospective evidence is still lacking for its use as a predictive biomarker to screen patient populations who may benefit from TMEM2-targeted therapy. Future clinical translational research needs to:

(1) establish standardized detection methods for TMEM2 protein/activity to ensure the comparability of data across studies;

(2) conduct prospective cohort studies to validate the prognostic and predictive value of TMEM2 in larger independent cohorts;

(3) explore the interaction between TMEM2 and the efficacy of approved targeted drugs, for example, whether PDAC patients with high TMEM2 expression respond differently to anti-fibrotic drugs or immunotherapy [26,32];

(4) develop non-invasive TMEM2 detection methods (such as liquid biopsy) to achieve dynamic monitoring during treatment.

6.4. Limitations of current research

Although the value of TMEM2 in tumor research is increasingly prominent, several limitations remain:

(1) direct tumor research on TMEM2 is still concentrated in a few tumor types (breast cancer, pancreatic cancer, and glioblastoma); direct experimental evidence in other tumor types is insufficient, and most correlational conclusions derive from database analyses rather than functional experimental validation;

(2) whether human TMEM2 possesses stable intrinsic hyaluronidase catalytic activity remains controversial, affecting the definitive interpretation of its participation in tumor mechanisms as an HA-degrading enzyme;

(3) the functional compensation and synergistic relationship between TMEM2 and HYBID increase the complexity of single-target intervention;

(4) existing studies are dominated by retrospective clinical sample analyses and in vitro cell-based experiments, lacking prospective clinical studies and rigorously controlled animal models;

(5) the small-molecule compound NSC777201 targeting TMEM2 is still in the preclinical research stage, and its safety, selectivity, and pharmacokinetic characteristics remain to be systematically evaluated.

These limitations suggest that research on TMEM2 tumor biology is still in an early stage of development, and more direct functional validation in additional tumor types and preclinical model studies are needed in the future.

7. Conclusions and future perspectives

Since Yamamoto et al. [8] first identified TMEM2 as a cell-surface hyaluronidase in 2017, research on this molecule has made remarkable progress. Existing studies suggest that TMEM2 plays an important role in HA metabolism in vivo and, through its unique cell-surface localization and local degrading activity, exerts key biological functions at multiple levels, including ECM remodeling, cell migration, EMT, ER stress tolerance, and mitochondrial homeostasis [9,10,15]. In the field of oncology, existing studies suggest that TMEM2 is highly expressed in various solid tumors, including breast cancer [11,14], pancreatic cancer [12,26,32], and GBM [13,33], and is associated with poor patient prognosis; it may participate in tumor invasion, metastasis, and drug resistance through both HA degradation-dependent and -independent mechanisms.

However, as described in Section 6.4, TMEM2 tumor research still faces multiple challenges in terms of catalytic activity confirmation, functional context analysis, and clinical translation.

Looking ahead, TMEM2 research can be advanced in the following directions:

(1) at the functional mechanism level: using single-cell sequencing, spatial transcriptomics, and other technologies to reveal the differential functions of TMEM2 in different cell populations of the TME;

(2) at the structural pharmacology level: developing highly selective inhibitors or activity modulators through artificial intelligence-assisted drug design based on the high-resolution structure of its ectodomain [36];

(3) at the clinical translation level: conducting prospective biomarker studies to validate its value in diagnosis, prognostic assessment, and efficacy monitoring;

(4) at the interdisciplinary integration level: integrating the multiple functions of TMEM2 in ECM mechanics [6,24], mitochondrial metabolism [23], and immune regulation [26] into a unified network model of HA metabolism and TME interactions.

In summary, TMEM2, as a late-discovered but significant molecule in the field of HA metabolism, is gradually deepening our understanding of tumor ECM remodeling and TME regulation. Although the path to translating it into clinical benefit is full of challenges, based on the research evidence accumulated so far, TMEM2 has preliminarily demonstrated its potential value as an intersection of basic tumor research and clinical translation. Future systematic research across multiple disciplines is expected to fully reveal the biological complexity of TMEM2 and provide a new research foundation and translational direction for improving the prognosis of tumor patients.

Disclosure statement

The authors declare no conflict of interest.

References

[1] Toole BP, 2004, Hyaluronan: From Extracellular Glue to Pericellular Cue. Nature Reviews Cancer, 4(7): 528–539.

[2] Whatcott CJ, Han H, Posner RG, et al., 2011, Targeting the Tumor Microenvironment in Cancer: Why Hyaluronidase Deserves a Second Look. Cancer Discovery, 1(4): 291–296.

[3] Tammi RH, Kultti A, Kosma VM, et al., 2008, Hyaluronan in Human Tumors: Pathobiological and Prognostic Messages from Cell-Associated and Stromal Hyaluronan. Seminars in Cancer Biology, 18(4): 288–295.

[4] Chanmee T, Ontong P, Itano N, 2016, Hyaluronan: A Modulator of the Tumor Microenvironment. Cancer Letters, 375(1): 20–30.

[5] Provenzano PP, Cuevas C, Chang AE, et al., 2012, Enzymatic Targeting of the Stroma Ablates Physical Barriers to Treatment of Pancreatic Ductal Adenocarcinoma. Cancer Cell, 21(3): 418–429.

[6] Provenzano PP, Hingorani SR, 2013, Hyaluronan, Fluid Pressure, and Stromal Resistance in Pancreas Cancer. British Journal of Cancer, 108(1): 1–8.

[7] Stern R, 2008, Hyaluronidases in Cancer Biology. Seminars in Cancer Biology, 18(4): 275–280.

[8] Yamamoto H, Tobisawa Y, Inubushi T, et al., 2017, A Mammalian Homolog of the Zebrafish Transmembrane Protein 2 (TMEM2) Is the Long-Sought-After Cell-Surface Hyaluronidase. Journal of Biological Chemistry, 292(18): 7304–7313.

[9] Yamaguchi Y, 2025, TMEM2: A New Dimension in Hyaluronan Biology. Proteoglycan Research, 3(2): e70019.

[10] Yoshida H, Inoue S, Okada Y, 2025, New Molecules Indispensable for Hyaluronan Degradation, HYBID (CEMIP/KIAA1199) and TMEM2 (CEMIP2): Differential Roles in Physiological and Pathological Non-Neoplastic Conditions. Proceedings of the Japan Academy, Series B, 101(6): 317–338.

[11] Lee H, Goodarzi H, Tavazoie SF, et al., 2016, TMEM2 Is a SOX4-Regulated Gene That Mediates Metastatic Migration and Invasion in Breast Cancer. Cancer Research, 76(17): 4994–5005.

[12] Kudo Y, Sato N, Adachi Y, et al., 2020, Overexpression of Transmembrane Protein 2 (TMEM2), a Novel Hyaluronidase, Predicts Poor Prognosis in Pancreatic Ductal Adenocarcinoma. Pancreatology, 20(7): 1479–1485.

[13] Gao L, Tong S, Liu J, et al., 2023, TMEM2 Induces Epithelial-Mesenchymal Transition and Promotes Resistance to Temozolomide in GBM Cells. Heliyon, 9(6): e16559.

[14] Gan L, Yang H, Xiong Z, et al., 2020, miR-518a-3p Suppresses Triple-Negative Breast Cancer Invasion and Migration Through Regulation of TMEM2. Technology in Cancer Research & Treatment, 19: 1533033820977523.

[15] Yamaguchi Y, Yamamoto H, Tobisawa Y, et al., 2019, TMEM2: A Missing Link in Hyaluronan Catabolism

Identified? Matrix Biology, 78–79: 139–146.

[16] Sato S, Miyazaki M, Fukuda S, et al., 2023, Human TMEM2 Is Not a Catalytic Hyaluronidase, but a Regulator of Hyaluronan Metabolism via HYBID (KIAA1199/CEMIP) and HAS2 Expression. Journal of Biological Chemistry, 299(6): 104826.

[17] Narita T, Tobisawa Y, Bobkov A, et al., 2023, TMEM2 Is a Bona Fide Hyaluronidase Possessing Intrinsic Catalytic Activity. Journal of Biological Chemistry, 299(9): 105120.

[18] Sato S, Mizutani Y, Abe M, et al., 2024, Naked Mole-Rat TMEM2 Lacks Physiological Hyaluronan-Degrading Activity and Resembles Human TMEM2 More Closely Than Active Mouse TMEM2. Archives of Biochemistry and Biophysics, 758: 110098.

[19] Tobisawa Y, Fujita N, Yamamoto H, et al., 2021, The Cell Surface Hyaluronidase TMEM2 Is Essential for Systemic Hyaluronan Catabolism and Turnover. Journal of Biological Chemistry, 297(5): 101281.

[20] Bourguignon V, Flamion B, 2016, Respective Roles of Hyaluronidases 1 and 2 in Endogenous Hyaluronan Turnover. The FASEB Journal, 30(6): 2108–2114.

[21] Chowdhury B, Hemming R, Hombach-Klonisch S, et al., 2013, Murine Hyaluronidase 2 Deficiency Results in Extracellular Hyaluronan Accumulation and Severe Cardiopulmonary Dysfunction. Journal of Biological Chemistry, 288(1): 520–528.

[22] Schinzel RT, Higuchi-Sanabria R, Shalem O, et al., 2019, The Hyaluronidase, TMEM2, Promotes ER Homeostasis and Longevity Independent of the UPR(ER). Cell, 179(6): 1306–1318.e18.

[23] Zhang H, Tsui CK, Garcia G, et al., 2024, The Extracellular Matrix Integrates Mitochondrial Homeostasis. Cell, 187(16): 4289–4304.e26.

[24] Irie F, Tobisawa Y, Murao A, et al., 2021, The Cell Surface Hyaluronidase TMEM2 Regulates Cell Adhesion and Migration via Degradation of Hyaluronan at Focal Adhesion Sites. Journal of Biological Chemistry, 296: 100481.

[25] Evanko SP, Tammi MI, Tammi RH, et al., 2007, Hyaluronan-Dependent Pericellular Matrix. Advanced Drug Delivery Reviews, 59(13): 1351–1365.

[26] Yao N, Fu Y, Wang T, et al., 2025, CEMIP2 Sensitizes PDAC to Chemotherapy Through Extracellular Matrix Remodeling by Hyaluronan Degradation. Cancer Letters, 630: 217898.

[27] Nieto MA, Huang RY, Jackson RA, et al., 2016, EMT: 2016. Cell, 166(1): 21–45.

[28] Hanahan D, Weinberg RA, 2011, Hallmarks of Cancer: The Next Generation. Cell, 144(5): 646–674.

[29] Misra S, Hascall VC, Markwald RR, et al., 2015, Interactions Between Hyaluronan and Its Receptors (CD44, RHAMM) Regulate the Activities of Inflammation and Cancer. Frontiers in Immunology, 6: 201.

[30] Srivastava P, Yadav VK, Chang TH, et al., 2024, In-Silico Analysis of TMEM2 as a Pancreatic Adenocarcinoma and Cancer-Associated Fibroblast Biomarker, and Functional Characterization of NSC777201, for Targeted Drug Development. American Journal of Cancer Research, 14(6): 3010–3035.

[31] Jacobetz MA, Chan DS, Neesse A, et al., 2013, Hyaluronan Impairs Vascular Function and Drug Delivery in a Mouse Model of Pancreatic Cancer. Gut, 62(1): 112–120.

[32] Kudo Y, Sato N, Oba T, et al., 2022, Concurrent Overexpression of Two Hyaluronidases, KIAA1199 and TMEM2, Strongly Predicts Shorter Survival After Resection in Pancreatic Ductal Adenocarcinoma. Pancreas, 51(7): 800–807.

[33] Jiang Q, Wang X, Yang Q, et al., 2021, TMEM2 Combined with IDH and 1p19q in Refining Molecular Subtypes for Predicting Survival of Patients with Glioma. DNA and Cell Biology, 40(11): 1381–1395.

[34] Xiang Y, Li C, Liao Y, et al., 2019, An Integrated mRNA-lncRNA Signature for Relapse Prediction in Laryngeal

Cancer. Journal of Cellular Biochemistry, 120(9): 15883–15890.

[35] Inubushi T, Nakanishi Y, Abe M, et al., 2022, The Cell Surface Hyaluronidase TMEM2 Plays an Essential Role in Mouse Neural Crest Cell Development and Survival. PLoS Genetics, 18(7): e1009765.

[36] Niu M, McGrath M, Sammon D, et al., 2023, Structure of the Transmembrane Protein 2 (TMEM2) Ectodomain and Its Apparent Lack of Hyaluronidase Activity. Wellcome Open Research, 8: 76.

Publisher's note

Bio-Byword Scientific Publishing remains neutral with regard to jurisdictional claims in published maps and institutional affiliations.

Oncology Treatment Discovery, 2026, Volume 4, Issue 3
https://bbwpublisher.com/journal/OTD
Online ISSN: 2981-8079
Print ISSN: 3083-4996

Artificial Intelligence Risk Prediction Model for PICC Catheter-related Venous Thrombosis in Cancer Patients: A Systematic Review

Xi Yang†, Rui Wang†, Qinglan Fu, Lanying Qiu*, Xiaowei Fu*

Department of Medical Oncology, Zhejiang Cancer Hospital, Hangzhou 310000, Zhejiang, China
† These authors contributed equally to this work and share the first authorship

Author to whom correspondence should be addressed.

Copyright: © 2026 Author(s). This is an open-access article distributed under the terms of the Creative Commons Attribution License (CC BY 4.0), permitting distribution and reproduction in any medium, provided the original work is cited.

Abstract: *Background*: Despite the growing number of models predicting the risk of cancer-associated PICC catheter-related venous thrombosis, comprehensive evaluations of artificial intelligence (AI) and machine learning (ML) prediction models remain scarce. *Objective*: This systematic review aims to evaluate the methodological quality, predictive performance, and clinical applicability of ML models for PICC-related thrombosis in patients with cancer, with a specific focus on risk of bias and adherence to reporting guidelines. *Methods*: A systematic search was performed across PubMed, Embase, Scopus, Web of Science, the Cochrane Library, and CINAHL. The study protocol was registered with PROSPERO prior to data collection, and the review adhered to the Preferred Reporting Items for Systematic Reviews and Meta-Analyses (PRISMA) guidelines. The search sought to identify all relevant studies published from database inception to December 30, 2025. Literature screening and data extraction were performed independently by two investigators. Finally, model quality was evaluated using the PROBAST+AI framework, integrating reported model performance metrics. *Results*: A total of seven studies were included, wherein all developed models demonstrated an Area Under the Curve (AUC) exceeding 0.7. The six most frequently utilized machine learning algorithms were Random Forest (RF; 28.57%), Least Absolute Shrinkage and Selection Operator (Lasso; 17.86%), Boosting (10.71%), Support Vector Machine (SVM; 7.14%), Logistic Regression (LR; 7.14%), and Artificial Neural Network (ANN; 7.14%). Overall, the included studies exhibited a high risk of bias, although clinical applicability was deemed acceptable. *Conclusions*: Current evidence indicates that machine learning models are effective in predicting PICC-related thromboembolism in patients with cancer. However, the majority of current models are limited by suboptimal methodological quality, a lack of external validation, and restricted generalizability. Future research should prioritize external validation and focus on developing clinical decision support tools to facilitate seamless integration into clinical practice.

Keywords: Peripherally inserted central catheter-related venous thrombosis; Neoplasms; Risk prediction; Machine learning; Systematic review

Online publication: October 20, 2026

1. Introduction

Peripherally inserted central catheters (PICCs) are extensively utilized in patients with cancer to facilitate chemotherapy, significantly mitigating peripheral vascular injury and toxicity associated with vesicant or irritant agents. However, concomitant with their increasing widespread use, associated complications—particularly catheter-related thrombosis (CRT)—have garnered significant attention. Current evidence indicates that the incidence of PICC-related venous thrombosis (PICC-RVT) ranges from 1.4% to 51.4% [1-3]. PICC-RVT is not only associated with an increased risk of pulmonary embolism but is also closely linked to catheter dysfunction, delays in chemotherapy, and prolonged hospitalization [4]. Encouragingly, PICC-RVT can be effectively managed through early prevention strategies and precise risk stratification. The *Infusion Therapy Standards of Practice* published by the Infusion Nurses Society (INS) explicitly state that risk assessment is effective in preventing PICC-RVT [5]. However, the efficacy of such preventive measures relies heavily on the availability of high-precision assessment tools. Currently, established assessment tools applied to patients with cancer include the Michigan Risk Score (MRS) by Chopra et al. [6], the Seeley prediction model [7], the Autar scale [8], and the Caprini risk assessment model [9]. Nevertheless, these models often fail to adequately account for the specific characteristics of the oncological population, thereby limiting their clinical applicability.

In recent years, the increasing accessibility of advanced software and high-performance computing resources has catalyzed the development of artificial intelligence (AI) and machine learning (ML) prediction models in healthcare. Leveraging advantages in data processing and pattern recognition, ML techniques have been demonstrated in numerous studies to outperform traditional statistical methods [10,11]. Concurrently, with intensified research efforts in the field of PICC-related thrombosis, a growing number of AI-based risk prediction models for cancer-associated PICC-RVT have emerged. However, existing studies exhibit significant heterogeneity regarding the ML algorithms employed, the target oncological populations, and the predictor variables included. Furthermore, a comprehensive systematic evaluation of model quality and clinical applicability remains lacking.

The Prediction model Risk of Bias Assessment Tool (PROBAST) provides a framework to enhance the methodological quality and transparency of prediction models [12]. Given the ubiquitous adoption of artificial intelligence (AI), this framework has evolved into the PROBAST+AI extension. This adaptation is specifically tailored to address the unique challenges posed by machine learning models, including ensuring transparency in model development, evaluation, and generalizability.

Consequently, we conducted a systematic review to evaluate the performance of AI-based models developed for predicting PICC-RVT. This study aims to synthesize current evidence regarding their predictive performance, thereby providing an evidence-based reference for clinical model selection and the implementation of precision nursing care for patients with cancer.

2. Methods

2.1. Design

The study protocol was registered with the International Prospective Register of Systematic Reviews (PROSPERO) prior to data analysis (Registration No. CRD420251246431). This systematic review was conducted in accordance with the Preferred Reporting Items for Systematic Reviews and Meta-Analyses (PRISMA) 2020 statement [13]. Ethical approval was not required, as this study relied exclusively on

secondary data from published literature and did not involve direct intervention with human or animal subjects.

The research question was formulated using the PIPOST framework recommended by the Joanna Briggs Institute (JBI). The specific components were defined as follows: Population (P) comprised patients with cancer undergoing PICC catheterization; Intervention (I) involved the development and validation of machine learning (ML)-based risk prediction models for PICC-RVT; Professionals (P) referred to clinical healthcare providers; Outcomes (O) focused on model performance metrics (e.g., sensitivity, specificity); Setting (S) included inpatient healthcare settings; and Type of Evidence (T) encompassed primary studies, including cohort, case-control, and cross-sectional studies)[14]. Due to the significant heterogeneity observed in model development algorithms and analytical approaches across the included studies, a quantitative meta-analysis was not performed; instead, a narrative synthesis was conducted.

2.2. Search strategies

Databases including PubMed, Embase, Scopus, Web of Science, the Cochrane Library, and CINAHL were searched. Briefly, the search strategy employed a combination of keywords and controlled vocabulary (e.g., MeSH) related to “Cancer” OR “Malignancy” AND “PICC” AND “Deep Vein Thrombosis” AND “Artificial Intelligence” OR “Machine Learning”. The literature search was executed on December 30, 2025, covering the period from database inception to the search date. The electronic search strategy was developed and verified by the first author. Subsequently, two independent investigators performed the search across the six aforementioned databases. Reference lists of relevant publications and reviews were hand-searched to identify additional eligible studies. Corresponding authors were contacted via email to request missing data where necessary.

2.3. Inclusion and exclusion criteria

The inclusion criteria were as follows:

(1) studies focusing on the prediction of PICC-related venous thrombosis (PICC-RVT) in patients with cancer;
(2) study designs including cohort, case-control, or cross-sectional studies;
(3) risk prediction models developed using machine learning (ML) algorithms;
(4) studies published in the English language.

The exclusion criteria were:

(1) studies involving pediatric populations or animal models;
(2) studies primarily investigating risk factors for venous thromboembolism (VTE) rather than developing prediction models;
(3) reviews, letters, editorials, or conference abstracts;
(4) models derived from systematic reviews or meta-analyses;
(5) studies solely comparing existing models;
(6) studies for which full text remained unavailable despite contacting the authors.

2.4. Study selection

Literature screening and data extraction were performed independently by two investigators (Rui Wang, LanYing Qiu). Initially, retrieved records were imported into reference management software (EndNote

X9), and duplicates were removed. Subsequently, titles and abstracts were screened to exclude irrelevant articles, followed by a full-text review to determine final eligibility based on the inclusion and exclusion criteria. Reference lists of the included studies were also scrutinized to identify any potential relevant studies. Any discrepancies were resolved through discussion and consensus involving three investigators (Xi Yang, QingLan Fu, XiaoWei Fu). A standardized data extraction form was developed in accordance with the Critical Appraisal and Data Extraction for Systematic Reviews of Prediction Modelling Studies (CHARMS) checklist [15]. The extracted data items included: first author, publication year, country, study design, study population, sample size, ML algorithms utilized, model validation methods, key predictors, and performance metrics (**Table 1** and **Table 2**).

Table 1. Characteristic of the included studies

Author, year	Design	Country	Participants	Database	Sample Size	RVT cases, n (%)	Measuring tools
Feifei Zhang 2024	Retrospective cohort study	China	cancer patients	Ningbo No.2 Hospital	266	3.00%	vascular Doppler ultrasound
Guiyuan Ma 2024	Prospective cohort study	China	cancer patients	Xiangya Hospital of Central South University: Qinghai University Affiliated Hospital and Hainan Provincial People's Hospital	831	4.68%	vascular Doppler ultrasound
Hankui Hu 2024	Prospective cohort study	China	cancer patients	West China Hospital of Sichuan University	452	16.10%	vascular Doppler ultrasound
Jianqin Fu 2022	Prospective cohort study	China	breast cancer patients	Fujian Medical University Union Hospital	1844	13.90%	vascular Doppler ultrasound
Shanshan Liu 2019	Prospective cohort study	China	cancer patients	the Department of Oncology of West China Hospital	348	16.30%	vascular Doppler ultrasound
Tao An 2025	Retrospective cohort study	China	breast cancer patients	National Canter-National Clinical Research Center for the Cancer Hospital, Chinese Academy of Medical Sciences	1137	9.05%	vascular Doppler ultrasound/ color imaging
Yue Li 2025	Retrospective multi-center cohort study	China	cancer patients	27 hospitals in China	3453	15.20%	vascular Doppler ultrasound

Table 2. Information on the included prediction models

Author, year	Model development	Missing data	Continuous variable processing method	Feature selection	Validation method	Calibration method	Model performance	Features included
Feifei Zhang 2024	LASSO, SVM, GBM, RF	——	Normalization Continuous variable	multivariate LASSO logistic regression	Random split validation	——	B: 0.790	BMI, diabetic status and age

Author, year	Model development	Missing data	Continuous variable processing method	Feature selection	Validation method	Calibration method	Model performance	Features included
Guiyuan Ma 2024	LR, RF, SVM	Complete Case Analysis	Categorization	LASSO	Random split validation	H-L test	A: 0.868 B: 0.806 C: 0.708	Age, catheterisation method, catheter valve, catheter material, infection, insertion history, D-dimer concentration, operation history anaemia, diabetes and targeted drugs
Hankui Hu 2024	ML-seeley-LASSO, ML-LASSO	——	Mixed Processing	LASSO	——	——	B: 0.856	BMI, smoking, family history of DVT, NRS2002
Jianqin Fu 2022	ANN	——	Normalization Continuous variable	Stepwise logistic regression	Bootstrap	——	B: 0.742	Age, Laterality, Education status, comorbidities, CVC history, Chemotherapy status, insertion attempts, upper extremity activity
Shanshan Liu 2019	RF, Lasso-RF, Seeley-RF, Seeley-LASSO-RF	——	Normalization	LASSO	cross-validation	Kaplan-Meier curves	A: 0.935 B: 0.809	Drinking, NRS2002, Family History of DVT, Diabetes, Tip Location, Chemotherapy Cycle, Radiotherapy, Anticoagulation
Tao An 2025	RFEntr, RFGini, CatBoost, XGBoost, NeuralNet FastAI, ExtraTrees Entr, LR,Weighted Ensemble, Bayesian	Complete Case Analysis	Categorization	The Weighted Ensemble feature importance scores from Auto Gluon	Internal verification: Random split validation External verification: Independent queue	Kaplan-Meier curves	A: 0.888 B: 0.688	Hemoglobin, APTT, total cholesterol, catheterization approach

Author, year	Model development	Missing data	Continuous variable processing method	Feature selection	Validation method	Calibration method	Model performance	Features included
Yue Li 2025	network-based algorithms, RSF, MP-LogitR, MP-AdaBoost, ThresReg	Complete Case Analysis	Feature Scaling	Shap	five-fold cross-validation, Random split validation	Brier	A: 0.950 B: 0.950	Albumin, Pre-filled tube sealing fluid, APTT, Main diagnosis of admission, Targeted drugs, PICC catheter opening, Platinum drugs, Tube placement method

A, development model; B, internal validation of model; C, external validation of model; SVM, Support Vector Machine; GBM, Gradient Boosting Machine; LR, Logistic Regression; RF, Random Forest; ANN, Artificial Neural Network; RSF, Random Survival Forest; H-L test, HosmerLemeshow

2.5. Data extraction and quality assessment

The risk of bias and clinical applicability of the included studies were assessed independently by two investigators using the PROBAST+AI tool [12]. Each domain was graded as "low risk," "high risk," or "unclear." An overall judgment of "low risk" was made only if all domains were rated as low risk. Conversely, if at least one domain was adjudicated as "high risk," the overall assessment was classified as "high risk." Finally, if one or more domains were rated as "unclear" in the absence of any "high risk" domains, the overall assessment was deemed "unclear."

The risk of bias was assessed across four domains—participants, predictors, outcome, and analysis—comprising a total of 20 signaling questions. Each signaling question was answered as "Yes," "Probably Yes," "Probably No," "No," or "No Information." Specifically, "Yes" and "Probably Yes" indicate a low risk of bias, whereas "No" and "Probably No" imply a high risk. "No Information" was selected when the original study failed to report sufficient data. Regarding domain-level judgment, a domain was deemed "low risk" only if all signaling questions were answered as "Yes" or "Probably Yes." Conversely, if any signaling question was answered as "No" or "Probably No," the domain was categorized as "high risk." A domain was labeled as "unclear risk" if one or more questions were answered as "No Information" in the absence of any "No" or "Probably No" responses. Two investigators (LanYing Qiu, QingLan Fu) independently conducted the assessment and data extraction. Any discrepancies were resolved through consensus involving a third investigator (Rui Wang).

3. Results

3.1. Study selection

The initial database search yielded a total of 1,299 records. After removing 495 duplicates, the remaining records were screened by title and abstract. Subsequently, 38 full-text articles were assessed for eligibility. Ultimately, seven studies met the inclusion criteria and were included in this systematic review [16-22]. The detailed study selection process is illustrated in **Figure 1**.

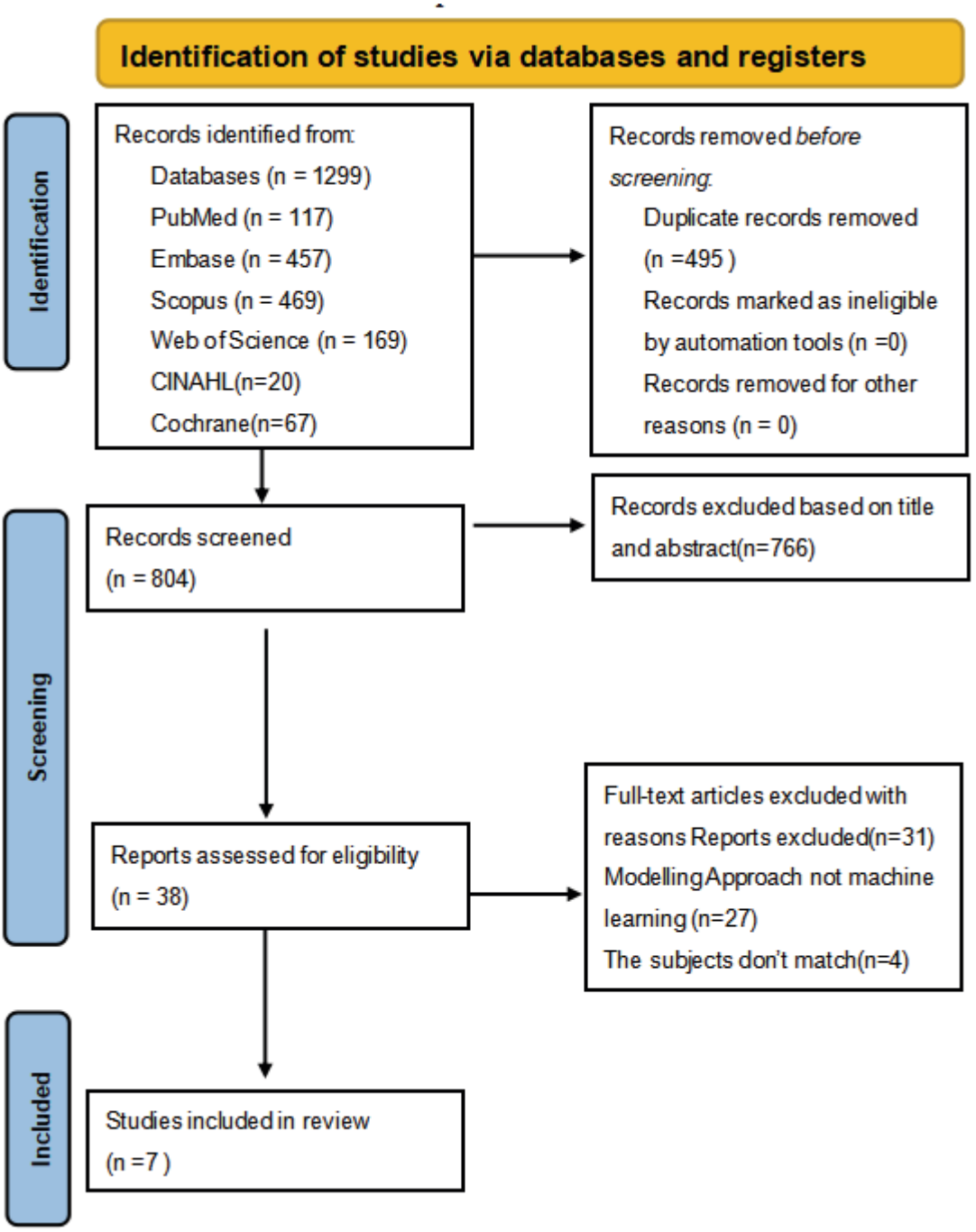

Figure 1. PRISMA diagram.

3.2. Study characteristics

Table 1 summarizes the study designs and participant characteristics of the included studies. The systematic review comprised five single-center studies [16-19, 21], and two multicenter studies [20, 22]. Geographically, all seven studies originated from China. In terms of study design, three were retrospective [16, 21, 22], while four were prospective [17-20]. Sample sizes ranged from 266 to 3,453 participants. Studies utilizing machine learning approaches to predict cancer-associated PICC-RVT have emerged since 2019. Regarding outcome

assessment, the majority of studies employed vascular Doppler ultrasound to confirm thrombosis. Notably, one study broadened its inclusion criteria to encompass all venous access devices, involving Central Venous Catheters (CVCs) and Implantable Venous Access Ports (IVAPs) in addition to PICCs [20]. Another study assessed outcomes extending beyond PICC-RVT to include other PICC-related complications [21].

Table 2 summarizes the characteristics of the prediction models within the included studies. Generally, the studies employed multiple machine learning algorithms to develop risk prediction models, aiming to identify the optimal model for subsequent validation. The six most frequently utilized algorithms were Random Forest (RF; 28.57%), Lasso (17.86%), Boosting (10.71%), Support Vector Machine (SVM; 7.14%), Logistic Regression (LR; 7.14%), and Artificial Neural Network (ANN; 7.14%).

The primary predictor variables integrated into the final machine learning models encompassed participant demographics, comorbidities, catheter- and treatment-related factors, laboratory indices, and medication usage. Age emerged as the most frequently identified demographic characteristic, followed by Body Mass Index (BMI). Regarding comorbidities, diabetes mellitus was the most prevalent predictor, followed by a family history of Deep Vein Thrombosis (DVT). A detailed overview of these predictor variables is presented in **Table 2**.

3.3. Models' validation

All included studies implemented internal validation procedures [16,19,20], while three studies additionally performed independent external validation. The reported Area Under the Curve (AUC) or C-statistics ranged from 0.688 to 0.984. Regarding calibration, reporting was limited; only a single study [20] assessed goodness-of-fit using the Hosmer-Lemeshow (H-L) test.

3.4. Bias risk and suitability assessment

3.4.1. Bias risk

The results of the risk of bias assessment are summarized in **Figure 2**. All included studies were adjudicated as having a high risk of bias, primarily stemming from deficiencies within the "Analysis" and "Participants" domains. Specifically, two studies [20,21] exhibited a high risk in the participants domain; this was attributed to sampling strategies that distorted the original distribution of predictors within the target population, and inappropriate exclusion criteria that compromised dataset representativeness. Regarding the "Analysis" domain, all studies were rated as high risk. This was predominantly driven by insufficient sample sizes leading to potential overfitting, the dichotomization of continuous predictors, and the application of the Synthetic Minority Over-sampling Technique (SMOTE) to address class imbalance without subsequent model recalibration. Conversely, the risk of bias was deemed low across all studies within the "Predictors" and "Outcome" domains.

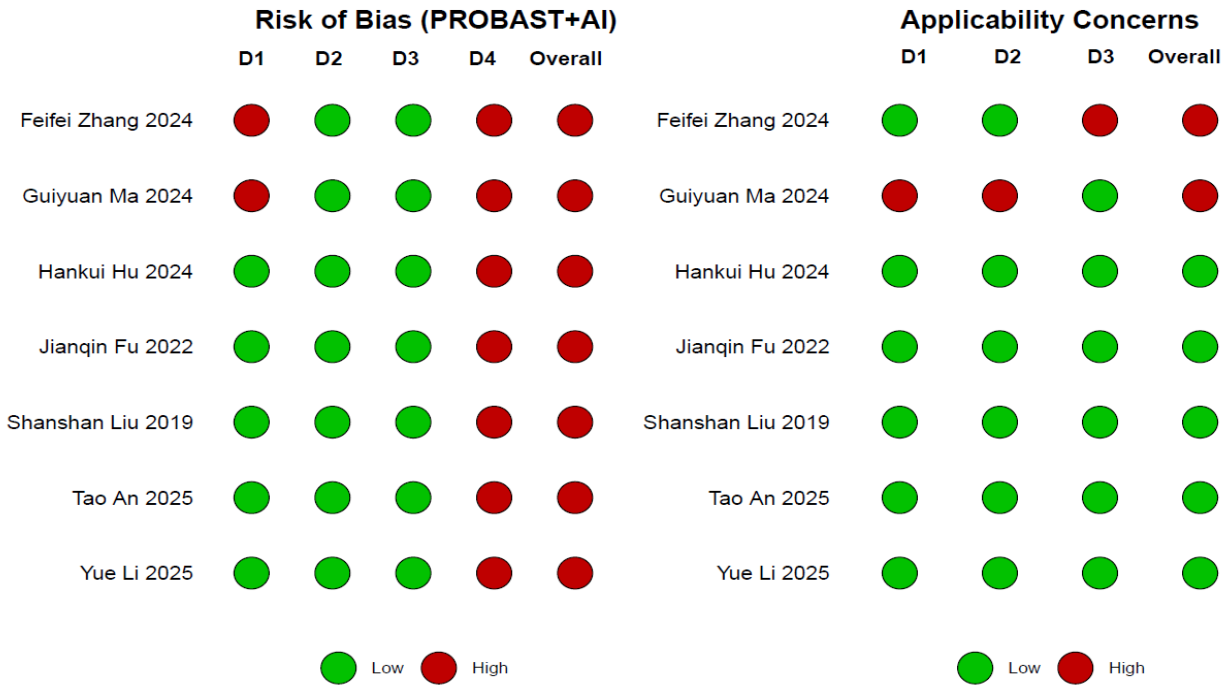

Figure 2. Risk of bias and applicability concerns of the included studies.

3.4.2. Suitability assessment

The results of the clinical applicability assessment are summarized in **Figure 2**. Specifically, two studies [20,21] were rated as having great concern regarding applicability. This was attributed to the use of composite outcome measures and the inclusion of broad Central Venous Access Devices (CVADs) rather than exclusively PICCs, respectively. The remaining studies demonstrated low concern regarding applicability.

Our findings indicate that compared to existing clinical risk scales, machine learning models generally exhibit superior predictive performance, characterized by higher sensitivity and specificity in screening for PICC-RVT in patients with cancer, suggesting their potential to guide prophylactic strategies. However, several limitations persist within the current literature, including the absence of external validation, inadequate handling of missing data, and insufficient sample sizes.

4. Discussion

This systematic review synthesized evidence from seven studies retrieved from English-language databases, focusing on machine learning models developed to predict PICC-RVT in patients with cancer. We comprehensively summarized the characteristics and predictive performance of these models, while concurrently assessing their risk of bias and clinical applicability. The majority of the included models demonstrated low concern regarding applicability and excellent discriminative performance. However, notable methodological shortcomings were identified, resulting in a high risk of bias, particularly within the statistical "analysis" domain.

Regarding data sources, the majority of included studies relied on single-center designs, with only two studies [20,22] utilizing multicenter data. Specifically, Ma et al. [20] conducted external validation using

multicenter data, while Li et al. [22] leveraged retrospective data from multiple institutions, employing a random partitioning strategy for performance validation. The remaining studies were dependent on single-center datasets derived from hospital admission registries. Given the inherent variability in data registration protocols across institutions, such heterogeneity poses a potential threat to the generalizability of these models. Consequently, large-scale multicenter studies utilizing standardized data collection protocols are warranted. Notably, it was observed that Ma et al. [20] employed a 1:2 case-control sampling strategy to construct their training set. This implies that the training dataset did not reflect the natural prevalence of the disease within the target population. While such sampling strategies are often adopted for efficiency, they necessitate subsequent correction, such as recalibration or weighting adjustments based on the sampling fraction, to ensure accurate probability estimates.

In terms of predictor selection, compared to traditional modeling approaches, machine learning (ML) facilitates the incorporation of a more diverse array of variables, including tumor-specific and genomic characteristics. Furthermore, given the multifactorial etiology of catheter-related thrombosis, the predictors identified vary significantly across different cancer types, and the predictive weight assigned to identical features differs among models. This observed heterogeneity suggests that future PICC-RVT prediction models may need to account for the specificity inherent to different cancer types. Consequently, future research should prioritize robust feature selection and aim to elucidate the complex interplay between tumor-specific predictors and PICC-RVT risk.

In terms of statistical analysis, developing prediction models based on machine learning algorithms typically necessitates substantial sample sizes to mitigate the risk of overfitting. We observed that although Liu et al. [17] and Zhang et al. [21] employed shrinkage methods to reduce the number of included features, such techniques cannot compensate for an insufficient sample size. Even applying conventional rules of thumb, the Events Per Variable (EPV) in these studies remained below 10. Training machine learning models with such limited sample sizes poses a substantial risk of overfitting and model instability [23,24]. Furthermore, An et al. and Fu et al. utilized the Synthetic Minority Over-sampling Technique (SMOTE) to address class imbalance [16,19]. However, in the context of risk prediction, this approach may cause more harm than good. Evidence suggests that without subsequent recalibration, such methods for handling class imbalance are often detrimental to model performance [25,26].

4.1. Comparative performance: AI-based versus traditional prediction models

Our comparative analysis of traditional scoring systems versus machine learning (ML)-based models for predicting PICC-RVT yielded several key insights:

(1) Performance Disparity: ML-based prediction models consistently demonstrated superior discrimination compared to traditional methods.

(2) Clinical Trade-offs: ML models exhibited significant performance variability across different institutions, suggesting that simpler, more parsimonious models may offer greater robustness. Research indicates that despite the superior accuracy of ML models, clinicians often prioritize interpretability, favoring established risk stratification tools [27]. For instance, Deng et al. [28] reported that despite the availability of precise ML predictions, 78% of clinicians preferred using the Caprini risk classification, highlighting the barrier posed by the “black box” nature of complex algorithms.

(3) Implementation Challenges: Studies note that ML models often require time-intensive data preprocessing

[29]. This underscores the critical necessity of developing integrated PICC-RVT informatics systems to streamline data management and enhance thrombosis control measures in clinical practice. Collectively, these findings suggest that while AI-based models offer quantifiable performance advantages, their successful clinical translation requires addressing stringent prerequisites. These include demonstrating clear evidence of clinical impact, developing specialized intelligent systems to improve efficiency, and ensuring model interpretability to facilitate user acceptance.

4.2. The nascent stage of machine learning models for predicting PICC-RVT risk in patients with cancer

This systematic review identified a diverse array of over 20 machine learning algorithms employed to predict PICC-related thrombosis in patients with cancer, with the literature predominantly concentrated within the last five years. While research in this specific domain emerged relatively recently, it is experiencing rapid expansion, characterized by the active exploration of various algorithms for clinical application. Regarding predictive performance, all included models yielded an Area Under the Curve (AUC) exceeding 0.7, demonstrating generally acceptable discriminative ability. However, the total volume of literature remains limited. Furthermore, the studies exhibited a high risk of bias, particularly regarding data analysis, and frequently lacked rigorous external validation in their study designs. Consequently, the landscape of risk prediction modeling for PICC-RVT in patients with cancer remains in a developmental phase.

4.3. Limitations and future research directions

Several critical limitations exist regarding the evaluation and development of machine learning models for predicting PICC-related thromboembolism. First, while the PROBAST+AI tool facilitated a rigorous quality assessment, it does not offer a quantitative evaluation of predictive performance. Given that a quantitative meta-analysis was deemed unreliable due to substantial heterogeneity in model development, analysis, and validation, we relied on this qualitative assessment framework to characterize these methodological variations. The absence of established “gold standards” for ML development in this domain (e.g., protocols for handling missing data) [30] further exacerbates this methodological ambiguity. Additionally, variability in patient populations across studies—and even between hospitals within the same region—contributes to heterogeneity, potentially leading to substantial fluctuations in model performance [31,32]. Notably, the majority of included studies originated from China, which may restrict the generalizability of findings to Western populations. Consequently, recalibration or local validation is essential prior to applying these models in diverse settings. Therefore, this review does not endorse a single specific model as the optimal tool for predicting PICC-RVT in patients with cancer. Furthermore, all studies shared AI-specific limitations, specifically the lack of assessment regarding algorithmic fairness and the absence of analyses concerning deployment feasibility. While this field demonstrates promise for future clinical application, current evidence does not support replacing established risk assessment tools with AI-based methods. Substantial methodological improvements and extensive clinical validation are required prior to routine implementation.

Consequently, future research is advised to leverage machine learning technologies to develop and rigorously validate robust risk prediction models for PICC-RVT. Emphasizing the mitigation of bias is essential to facilitate the effective translation of these models into clinical practice, ultimately enhancing patient safety and quality of life.

5. Conclusion

This systematic review included seven studies and comprehensively evaluated the characteristics of AI-based risk prediction models for PICC-RVT in patients with cancer across four dimensions: participants, predictors, outcome, and analysis. Our findings indicate a generally high risk of bias across the included literature, despite the clinical applicability of the models being deemed acceptable. The majority of models lacked multicenter validation, thereby compromising their stability and generalizability. Furthermore, research utilizing unstructured data remains underexplored, and few prediction models have been effectively implemented in clinical settings to date. Future research should integrate multimodal data using rigorous machine learning methodologies to elucidate the complex interactions among risk factors across different tumor types. Such efforts are essential to facilitate the clinical translation of these models, ultimately enhancing the efficacy of prophylactic strategies for PICC-RVT.

Funding

Zhejiang Provincial Medical and Health Research Program, "Establishment of a database on PICC catheter-related thrombosis in the "real world" based on tumors and research on evidence-based nursing practice" (Project No.: 2022KY672)

Disclosure statement

The authors declare no conflict of interest.

References

[1] Chen P, Zhu B, Wan G, et al., 2021, The Incidence of Asymptomatic Thrombosis Related to Peripherally Inserted Central Catheter in Adults: A Systematic Review and Meta-Analysis. Nurs Open, 8: 2249–2261.

[2] Luo L, Jing XM, Wang GR, et al., 2016, Peripherally Inserted Central Catheter-Related Upper Extremity Venous Thrombosis in Oncology Patients: A Prospective Study Based on Doppler Sonography. J Ultrasound Med, 35: 1759–1763.

[3] Fallouh N, McGuirk HM, Flanders SA, et al., 2015, Peripherally Inserted Central Catheter-Associated Deep Vein Thrombosis: A Narrative Review. Am J Med, 128: 722–738.

[4] Chen P, Wan G, Zhu B, 2021, Incidence and Risk Factors of Symptomatic Thrombosis Related to Peripherally Inserted Central Catheter in Patients with Lung Cancer. J Adv Nurs, 77: 1284–1292.

[5] Lopez-Rubio M, Lago-Rodriguez MO, Ordieres-Ortega L, et al., 2024, A Comprehensive Review of Catheter-Related Thrombosis. J Clin Med, 13: 7818.

[6] Chopra V, Kaatz S, Conlon A, et al., 2017, The Michigan Risk Score to Predict Peripherally Inserted Central Catheter-Associated Thrombosis. J Thromb Haemost, 15: 1951–1962.

[7] Seeley MA, Santiago M, Shott S, 2007, Prediction Tool for Thrombi Associated with Peripherally Inserted Central Catheters. J Infus Nurs, 30: 280–286.

[8] Autar R, 1996, Nursing Assessment of Clients at Risk of Deep Vein Thrombosis (DVT): The Autar DVT Scale. J Adv Nurs, 23: 763–770.

[9] Caprini JA, 2005, Thrombosis Risk Assessment as a Guide to Quality Patient Care. Dis Mon, 51: 70–78.

[10] Dhillon SK, Ganggayah MD, Sinnadurai S, et al., 2022, Theory and Practice of Integrating Machine Learning and Conventional Statistics in Medical Data Analysis. Diagnostics (Basel), 12: 2526.

[11] Yu MY, Yoo HY, Han GI, et al., 2025, Comparing the Performance of Machine Learning Models and Conventional Risk Scores for Predicting Major Adverse Cardiovascular Cerebrovascular Events After Percutaneous Coronary Intervention in Patients with Acute Myocardial Infarction: Systematic Review and Meta-Analysis. J Med Internet Res, 27: e76215.

[12] Moons KGM, Damen JAA, Kaul T, et al., 2025, PROBAST+AI: An Updated Quality, Risk of Bias, and Applicability Assessment Tool for Prediction Models Using Regression or Artificial Intelligence Methods. BMJ, 388: e082505.

[13] Page MJ, McKenzie JE, Bossuyt PM, et al., 2021, The PRISMA 2020 Statement: An Updated Guideline for Reporting Systematic Reviews. BMJ, 372: n71.

[14] Aromataris E, Lockwood C, Porritt K, et al., JBI Manual for Evidence Synthesis. JBI Manual for Evidence Synthesis, visited on January 20. 2026, https://jbi-global-wiki.refined.site/space/MANUAL/4685837/jbi-global-wiki.refined.site.

[15] Moons KG, de Groot JA, Bouwmeester W, et al., 2014, Critical Appraisal and Data Extraction for Systematic Reviews of Prediction Modelling Studies: The CHARMS Checklist. PLoS Med, 11: e1001744.

[16] An T, Han H, Xie J, et al., 2025, Enhancing Prediction and Stratifying Risk: Machine Learning and Bayesian-Learning Models for Catheter-Related Thrombosis in Chemotherapy Patients. BMC Cancer, 25: 552.

[17] Liu S, Zhang F, Xie L, et al., 2019, Machine Learning Approaches for Risk Assessment of Peripherally Inserted Central Catheter-Related Vein Thrombosis in Hospitalized Patients with Cancer. Int J Med Inform, 129: 175–183.

[18] Hu H, Wu Z, Zhao J, 2024, Peripherally Inserted Central-Related Upper Extremity Deep Vein Thrombosis and Machine Learning. Vascular, 32: 1346–1351.

[19] Fu J, Cai W, Zeng B, et al., 2022, Development and Validation of a Predictive Model for Peripherally Inserted Central Catheter-Related Thrombosis in Breast Cancer Patients Based on Artificial Neural Network: A Prospective Cohort Study. Int J Nurs Stud, 135: 104341.

[20] Ma G, Chen S, Peng S, et al., 2025, Construction and Validation of a Nomogram Prediction Model for the Catheter-Related Thrombosis Risk of Central Venous Access Devices in Patients with Cancer: A Prospective Machine Learning Study. J Thromb Thrombolysis, 58: 220–231.

[21] Zhang F, Ye G, Chen P, et al., 2024, Comparative Predictive Modeling for PICC Line Complications in Oncology: A Retrospective Study. Br J Hosp Med (Lond), 85: 1–15.

[22] Li Y, Nie S, Wang L, et al., 2024, Integrating Deep Learning in Public Health: A Novel Approach to PICC-RVT Risk Assessment. Front Public Health, 12: 1445425.

[23] Van Calster B, van Smeden M, De Cock B, et al., 2020, Regression Shrinkage Methods for Clinical Prediction Models Do Not Guarantee Improved Performance: Simulation Study. Stat Methods Med Res, 29: 3166–3178.

[24] Riley RD, Snell KIE, Martin GP, et al., 2021, Penalization and Shrinkage Methods Produced Unreliable Clinical Prediction Models Especially When Sample Size Was Small. J Clin Epidemiol, 132: 88–96.

[25] van den Goorbergh R, van Smeden M, Timmerman D, et al., 2022, The Harm of Class Imbalance Corrections for Risk Prediction Models: Illustration and Simulation Using Logistic Regression. J Am Med Inform Assoc, 29: 1525–1534.

[26] Carriero A, Luijken K, de Hond A, et al., 2025, The Harms of Class Imbalance Corrections for Machine Learning Based Prediction Models: A Simulation Study. Stat Med, 44: e10320.

[27] Adlung L, Cohen Y, Mor U, et al., 2021, Machine Learning in Clinical Decision Making. Med, 2: 642–665.

[28] Deng RX, Zhu XL, Zhang AB, et al., 2023, Machine Learning Algorithm as a Prognostic Tool for Venous Thromboembolism in Allogeneic Transplant Patients. Transplant Cell Ther, 29: 57.e1–57.e10.

[29] Maharana K, Mondal S, Nemade B, 2022, A Review: Data Pre-Processing and Data Augmentation Techniques. Glob Transit Proc, 3: 91–99.

[30] Nijman S, Leeuwenberg AM, Beekers I, et al., 2022, Missing Data Is Poorly Handled and Reported in Prediction Model Studies Using Machine Learning: A Literature Review. J Clin Epidemiol, 142: 218–229.

[31] Rockenschaub P, Hilbert A, Kossen T, et al., 2024, The Impact of Multi-Institution Datasets on the Generalizability of Machine Learning Prediction Models in the ICU. Crit Care Med, 52: 1710–1721.

[32] de Jong VMT, Moons KGM, Eijkemans MJC, et al., 2021, Developing More Generalizable Prediction Models from Pooled Studies and Large Clustered Data Sets. Stat Med, 40: 3533–3559.

Publisher's note

Bio-Byword Scientific Publishing remains neutral with regard to jurisdictional claims in published maps and institutional affiliations.

Oncology Treatment Discovery, 2026, Volume 4, Issue 3
https://bbwpublisher.com/journal/OTD
Online ISSN: 2981-8079
Print ISSN: 3083-4996

Mechanisms of Lactate and Targeted Therapeutic Strategies in the Colorectal Cancer Microenvironment

Zijie Yang, Chao Chen, Yinhua Zhang*

Department of Colorectal and Anal Surgery, Gansu Provincial Central Hospital, Lanzhou 730050, Gansu, China

***Corresponding author*:** Yinhua Zhang, 1097089469@qq.com

Copyright: © 2026 Author(s). This is an open-access article distributed under the terms of the Creative Commons Attribution License (CC BY 4.0), permitting distribution and reproduction in any medium, provided the original work is cited.

Abstract: Colorectal cancer (CRC) ranks among the most prevalent and lethal malignancies worldwide. Metabolic reprogramming is a hallmark of CRC, in which the Warburg effect drives massive lactate accumulation in the tumor microenvironment (TME) at concentrations far exceeding those in normal tissues. Traditionally recognized as a glycolytic waste product, lactate is now defined as a pleiotropic signaling molecule that profoundly remodels TME homeostasis and tumor progression. This review focuses on how lactate modulates CRC immunosuppressive networks via metabolic reprogramming, signal transduction and epigenetic regulation, and summarizes current advances in lactate-targeted therapeutic strategies for CRC.

Keywords: Colorectal cancer; Lactate; Tumor microenvironment; Metabolic reprogramming; Immunosuppression; Histone lactylation; Monocarboxylate transporter; Targeted therapy

Online publication: October 20, 2026

1. Introduction

CRC is the third most common human cancer and the second leading cause of cancer-related mortality globally [1]. Current therapeutic regimens, including surgery, chemotherapy, targeted therapy, and immunotherapy, have improved clinical outcomes for patients with partial CRC. However, the prognosis of advanced CRC remains poor, with low five-year survival rates. Accumulating evidence indicates that TME metabolic reprogramming is a central driver of CRC progression and immune evasion [2].

Aerobic glycolysis (the Warburg effect) constitutes a core metabolic signature of CRC. Regardless of oxygen availability, CRC cells preferentially utilize glycolysis rather than oxidative phosphorylation, leading to robust lactate production and secretion into the TME [3]. Lactate dehydrogenase A (LDHA), a rate-limiting enzyme converting pyruvate to lactate, is frequently upregulated in CRC and correlates with unfavorable clinical prognosis [4]. Physiologically, normal tissues contain 1.5–3 mM lactate, whereas the lactate

concentration in CRC TME reaches 10–40 mM. Such high lactate levels create an acidic TME that broadly regulates tumor malignant behaviors [5]. Lactate was previously considered a terminal glycolytic byproduct. Recent studies have revised this concept, identifying lactate as a vital signaling mediator in the TME [6]. Lactate shuttles between tumor and stromal cells via monocarboxylate transporters (MCTs) to sustain metabolic symbiosis within tumors [7]. Lactate metabolic signatures are tightly associated with immune infiltration and clinical prognosis in CRC [8,9]. In 2019, histone lactylation was identified as a novel epigenetic modification that links metabolic lactate to transcriptional regulation, establishing a new metabolism – epigenetics crosstalk paradigm [10]. Subsequent studies have validated the critical roles of lactylation in tumor immunosuppression, metabolic rewiring and therapeutic resistance [11]. This review systematically elucidates lactate-driven immunosuppressive mechanisms and discusses translational lactate-targeted strategies for CRC intervention.

2. Metabolic basis of lactate production and shuttling in CRC TME

2.1. Warburg effect and glycolytic reprogramming in CRC

The Warburg effect dominates metabolic reprogramming in CRC. Oncogenic alterations drive CRC cells to prioritize glycolysis over aerobic oxidation even under normoxic conditions [1]. KRAS mutations upregulate GLUT1 and glycolytic enzymes to enhance glucose uptake and glycolytic flux, while c-MYC activation transcriptionally induces LDHA expression. MicroRNAs negatively modulate LDHA overexpression in CRC and facilitate aerobic glycolysis and tumor proliferation [4]. Clinical cohort analyses have further verified the prognostic value of lactate metabolic signatures in CRC [12].

2.2. MCT1/MCT4-mediated lactate shuttling and metabolic symbiosis

MCT family members govern intercellular lactate transport in the TME. MCT4 (encoded by SLC16A3) possesses low lactate affinity and primarily exports lactate from glycolytic tumor cells. In contrast, high-affinity MCT1 (encoded by SLC16A1) mediates lactate uptake in oxidative tumor cells and stromal cells to support energy metabolism [7]. In CRC, NRF2 differentially regulates MCT1 and MCT4 expression to shape tumor–stroma metabolic coupling. CRC cells discharge lactate via MCT4, whereas cancer-associated fibroblasts (CAFs) uptake lactate through MCT1, forming a reverse Warburg effect that sustains tumor metabolic fitness [13,14].

2.3. Prognostic significance of lactate metabolic signatures

Lactate-related gene expression profiles reliably predict CRC prognosis and immune landscape. Lactate regulatory gene patterns correlate with immune cell infiltration, immune checkpoint expression and overall survival of CRC patients [8]. Integrated omics analyses further confirm lactate as a central hub bridging metabolic reprogramming and TME immunosuppression in CRC [9].

3. Lactate-mediated remodeling of CRC immune microenvironment

3.1. Lactate suppresses anti-tumor effector immune cells

CD8+ cytotoxic T lymphocytes (CTLs) are the primary anti-tumor immune effectors. TME lactate accumulation impairs CTL function by reducing intracellular pH and inhibiting NFAT transcriptional activity,

thereby suppressing IL-2 and IFN-γ production [15]. Lactate also blocks mTOR signaling, restraining CTL proliferation and effector differentiation. Moreover, lactate disrupts T cell metabolic flexibility and prohibits the glycolytic switch required for effector T cell activation [16].

Natural killer (NK) cell anti-tumor activity is also lactate-dependent. TME lactate downregulates NK cell activating receptors NKG2D and NKp46, reduces granzyme B and perforin release, and ultimately impairs NK-mediated tumor cytotoxicity, representing a major barrier for NK-based immunotherapy [17].

3.2. Lactate promotes immunosuppressive cell polarization and activation

Lactate actively recruits and activates immunosuppressive cell populations. It enhances latent TGF-β1 activity to facilitate FoxP3+ regulatory T cell (Treg) differentiation, strengthening TME immune suppression [18]. For tumor-associated macrophages (TAMs), lactate activates HIF-1α and STAT3 signaling to induce M2 polarization, upregulating M2 markers (ARG1, IL-10) and inhibiting pro-inflammatory cytokine secretion [19]. M2-TAMs further secrete IL-10 and TGF-β to amplify immunosuppression.

Myeloid-derived suppressor cells (MDSCs) are also lactate-responsive. LDHA-dependent lactate production promotes MDSC expansion and activation via STAT3 signaling in solid tumors, suggesting a conserved immunosuppressive axis applicable to CRC [20].

3.3. Lactate impairs antigen presentation

Lactate-induced histone lactylation in dendritic cells (DCs) disrupts antigen processing and presentation. This epigenetic impairment blocks adaptive immune priming and weakens systemic anti-tumor immune responses [21].

3.4. Positive feedback between immunosuppression and tumor glycolysis

Immunosuppressive TME sustains tumor glycolysis via a positive feedback loop. Tregs, M2-TAMs and MDSCs secrete IL-10 and TGF-β to upregulate HIF-1α in CRC cells. HIF-1α further transcriptionally activates glycolytic genes including GLUT1, HK2, LDHA and MCT4, which in turn increases lactate accumulation and exacerbates immunosuppression [22]. This self-reinforcing loop stabilizes the glycolytic and immunosuppressive TME phenotype.

3.5. Single-cell and spatial transcriptomic evidence for lactate–immune crosstalk

Single-cell RNA sequencing and spatial transcriptomics reveal distinct cell–cell interactions in CRC. Lactate-hyperactive CRC epithelial subpopulations are closely associated with T cell exhaustion and M2-TAM infiltration, confirming lactate as a core regulator of TME immune remodeling at high spatial and cellular resolution [23].

4. Lactate functions as a multifunctional signaling molecule

4.1. GPR81/HCAR1-dependent pro-tumor signaling

GPR81 (HCAR1) is a specific cell-surface lactate receptor. Lactate–GPR81 signaling drives tumor angiogenesis, immune escape and metabolic adaptation across multiple cancers [24]. In CRC, GPR81 activation enhances tumor cell proliferation and anti-apoptotic capacity [25]. GPR81 signaling also modulates antigen-presenting cell function and reshapes the immunosuppressive TME [26].

4.2. Lactate induces angiogenesis via NF-κB/IL-8 signaling

Endothelial MCT1-mediated lactate uptake activates NF-κB signaling, upregulates IL-8 expression and promotes tumor angiogenesis [27]. Targeting endothelial MCT1 abrogates lactate-induced HIF-1α activation and neovascularization, providing a novel anti-angiogenic strategy [28].

4.3. Lactate directly inhibits STING-mediated innate immunity

A recent 2026 study demonstrated that lactate directly binds and inhibits the STING sensor, thereby suppressing cGAS-STING-dependent type I interferon responses and facilitating tumor innate immune evasion.This receptor-independent mechanism defines lactate as a critical immune checkpoint modulator [29].

5. Histone lactylation: Metabolite-driven epigenetic reprogramming

5.1. Regulatory roles of histone lactylation in CRC

Histone lactylation bridges lactate metabolism and epigenetic regulation in CRC. Lactylation rewires tumor metabolic programs and sustains malignant progression [30]. Targeting lactylation improves immunotherapeutic efficacy in gastrointestinal cancers, indicating broad translational potential for CRC treatment [31]. Lactylation-associated positive feedback loops further stabilize tumor metabolic and epigenetic dysregulation [32].

5.2. Lactylation sustains immunosuppression and therapeutic resistance

Lactylation epigenetically locks immunosuppressive transcriptional programs, endowing the TME with epigenetic immune memory [33]. Additionally, lactylation contributes to CRC therapeutic resistance by modulating drug efflux, DNA damage repair and apoptotic escape, severely limiting clinical treatment efficacy [34].

6. Lactate-targeted therapeutic strategies for CRC

6.1. MCT1 inhibition

MCT1 is essential for stromal and oxidative tumor cell lactate utilization. High-resolution MCT1 structural analysis supports rational targeted drug design [35]. The clinical-stage MCT1 inhibitor AZD3965 exhibits favorable safety and anti-tumor activity in preclinical models [36]. In drug-resistant CRC, MCT1 dependency creates a metabolic vulnerability; MCT1 blockade suppresses resistant tumor growth and synergizes with chemotherapy and immunotherapy [37–39].

6.2. MCT4 inhibition and immunotherapy combination

MCT4 is overexpressed in metastatic CRC and drives tumor migration and invasion [40]. Pharmacological MCT4 inhibition reduces lactate efflux, reverses TME acidification, restores CD8+ T cell anti-tumor activity, and enhances immune checkpoint blockade efficacy [41]. Selective MCT4 chemical probes have been developed to support further drug development [42].

6.3. LDHA-targeted metabolic intervention

As a key lactate-producing enzyme, LDHA is an upstream therapeutic node. Although LDHA inhibitors

exert anti-tumor effects in preclinical models, clinical translation is hindered by poor selectivity and systemic toxicity [43]. Alternatively, EGCG disrupts CAF glycolysis and tumor–stroma metabolic coupling, providing an indirect lactate-targeting strategy for CRC [44].

6.4. Lactate-depleting nanotherapeutics

Nanoplatforms enable precise TME lactate depletion and acid neutralization, effectively reversing tumor immunosuppression [45,46]. Although CRC-specific lactate-targeted nanomedicines remain under development, emerging nanotechnologies provide robust proof-of-concept for future clinical translation.

6.5. Targeting histone lactylation

Pharmacological inhibition of histone lactylation enhances gastrointestinal tumor immunotherapy responses, representing an innovative epigenetic strategy for CRC treatment [47]. Nevertheless, the regulatory mechanisms and translational applications of lactylation require further investigation.

7. Discussion and conclusions

Lactate orchestrates a self-amplifying "metabolism–immunity–epigenetics" tripartite network in CRC TME. Warburg effect-derived lactate inhibits anti-tumor immune cells, recruits immunosuppressive populations and impairs antigen presentation. It also promotes immune evasion via GPR81 signaling and STING suppression. Furthermore, lactate-induced histone lactylation transforms transient metabolic stress into stable epigenetic memory, sustaining TME immunosuppression and tumor malignancy.

Future CRC therapeutic strategies will shift from single-target inhibition to multi-modal combinatorial interventions targeting lactate-centered networks, combined with molecular subtype-based precise stratification. Current limitations include insufficient clinical data on MCT inhibitors in CRC and incomplete understanding of lactylation regulatory mechanisms. Systematic preclinical evaluation of multi-node combination regimens is urgently needed to advance lactate-targeted therapy for clinical CRC.

Disclosure statement

The authors declare no conflict of interest.

References

[1] Zhong X, He X, Wang Y, et al., 2022, Warburg Effect in Colorectal Cancer: The Emerging Roles in Tumor Microenvironment and Therapeutic Implications. J Hematol Oncol, 15(1): 160.

[2] García-Cañaveras JC, Chen L, Rabinowitz JD, 2019, The Tumor Metabolic Microenvironment: Lessons from Lactate. Cancer Res, 79(13): 3155–3162.

[3] Kocianova E, Piatrikova V, Golias T, 2022, Revisiting the Warburg Effect with Focus on Lactate. Cancers (Basel), 14(24): 6028.

[4] Wang J, Wang H, Liu A, et al., 2015, Lactate Dehydrogenase A Negatively Regulated by miRNAs Promotes Aerobic Glycolysis and Is Increased in Colorectal Cancer. Oncotarget, 6(23): 19456–19468.

[5] Jiang B, 2017, Aerobic Glycolysis and High Level of Lactate in Cancer Metabolism and Microenvironment. Genes

Dis, 4(1): 25–27.

[6] Long Y, Xu J, Xu Z, et al., 2026, The Warburg Effect and Beyond: Glycolytic Reprogramming in Cancer Progression and Emerging Therapeutic Strategies. Biomed Pharmacother, 201: 119692.

[7] Payen VL, Mina E, Van Hée VF, et al., 2020, Monocarboxylate Transporters in Cancer. Mol Metab, 33: 48–66.

[8] Zhu D, Jiang Y, Cao H, et al., 2022, Lactate: A Regulator of Immune Microenvironment and a Clinical Prognosis Indicator in Colorectal Cancer. Front Immunol, 13: 876195.

[9] Sun Q, Wu J, Zhu G, et al., 2022, Lactate-Related Metabolic Reprogramming and Immune Regulation in Colorectal Cancer. Front Endocrinol (Lausanne), 13: 1089918.

[10] Zhang D, Tang Z, Huang H, et al., 2019, Metabolic Regulation of Gene Expression by Histone Lactylation. Nature, 574(7779): 575–580.

[11] Fang C, Zhou S, Yu K, et al., 2026, Lactate Metabolism and Lactylation in Cancer: From Pathogenesis to Therapeutic Advances. Signal Transduct Target Ther, 11(1): 190.

[12] Wang K, Lou Y, Tao Z, 2024, A New Genetic Signature of Lactate Metabolism-Associated Genes Predicting Clinically Distinctive Features and Tumor Microenvironment in Colorectal Cancer. Cancer Control, 31: 10732748241272721.

[13] Diehl K, Dinges LA, Helm O, et al., 2018, Nuclear Factor E2-Related Factor-2 Has a Differential Impact on MCT1 and MCT4 Lactate Carrier Expression in Colonic Epithelial Cells: A Condition Favoring Metabolic Symbiosis Between Colorectal Cancer and Stromal Cells. Oncogene, 37(1): 39–51.

[14] Xiao L, Na J, Dang F, et al., 2026, Current Research Status of the Reverse Warburg Effect in Cancer-Associated Fibroblasts of Solid Tumors. Int Immunopharmacol, 179: 116586.

[15] Dai X, Chang J, Wang S, et al., 2026, Beyond a Waste Product: Lactate as a Master Metabolite Dictating Anti-Tumor T-Cell Fate. Cell Death Dis, 17(1): 715.

[16] Gu XY, Yang JL, Lai R, et al., 2025, Impact of Lactate on Immune Cell Function in the Tumor Microenvironment: Mechanisms and Therapeutic Perspectives. Front Immunol, 16: 1563303.

[17] Jedlička M, Feglarová T, Janstová L, et al., 2022, Lactate from the Tumor Microenvironment – A Key Obstacle in NK Cell-Based Immunotherapies. Front Immunol, 13: 932055.

[18] Wang Y, Zhang X, Hu C, et al., 2026, Lactic Acid Facilitates the Generation of Regulatory T Cells and Promotes Cancer Progression by Activating Latent TGF-β1. Int Immunopharmacol, 186: 117066.

[19] Tao H, Zhong X, Zeng A, et al., 2023, Unveiling the Veil of Lactate in Tumor-Associated Macrophages: A Successful Strategy for Immunometabolic Therapy. Front Immunol, 14: 1208870.

[20] Wei X, Li X, Pan Y, et al., 2026, LDHA-Driven Lactate Metabolism Promotes MDSC Activation and Immunosuppressive Microenvironment in Prostate Cancer. Oncogene, 45(17): 1544–1556.

[21] Zhang B, Xu A, Wang H, et al., 2025, MPC-Mediated Lactate Production Drives Histone Lactylation in Dendritic Cells to Affect Tumor Progression and Immunotherapy. Cell Mol Life Sci, 82(1): 371.

[22] Nicolini A, Ferrari P, 2024, Involvement of Tumor Immune Microenvironment Metabolic Reprogramming in Colorectal Cancer Progression, Immune Escape, and Response to Immunotherapy. Front Immunol, 15: 1353787.

[23] Lan H, Li Y, Li H, et al., 2026, Single-Cell and Spatial Transcriptomics Reveal Lactate-Active Epithelial-Immune Cell Crosstalk That Reprograms the Immune Microenvironment in Colorectal Cancer. Transl Oncol, 71: 102864.

[24] Brown TP, Ganapathy V, 2020, Lactate/GPR81 Signaling and Proton Motive Force in Cancer: Role in Angiogenesis, Immune Escape, Nutrition, and Warburg Phenomenon. Pharmacol Ther, 206: 107451.

[25] Roland CL, Arumugam T, Deng D, et al., 2014, Cell Surface Lactate Receptor GPR81 Is Crucial for Cancer Cell

Survival. Cancer Res, 74(18): 5301–5310.

[26] Brown TP, Bhattacharjee P, Ramachandran S, et al., 2020, The Lactate Receptor GPR81 Promotes Breast Cancer Growth via a Paracrine Mechanism Involving Antigen-Presenting Cells in the Tumor Microenvironment. Oncogene, 39(16): 3292–3304.

[27] Végran F, Boidot R, Michiels C, et al., 2011, Lactate Influx Through the Endothelial Cell Monocarboxylate Transporter MCT1 Supports an NF-κB/IL-8 Pathway That Drives Tumor Angiogenesis. Cancer Res, 71(7): 2550–2560.

[28] Sonveaux P, Copetti T, De Saedeleer CJ, et al., 2012, Targeting the Lactate Transporter MCT1 in Endothelial Cells Inhibits Lactate-Induced HIF-1 Activation and Tumor Angiogenesis. PLoS One, 7(3): e33418.

[29] Guo D, Meng Y, Yang Q, et al., 2026, Lactate Binds and Inhibits the Innate Immune Sensor STING to Promote Tumor Immune Evasion. Immunity, 59(7): 1811–1824.e7.

[30] Song Y, Zou M, Wu S, et al., 2026, Lactate Metabolism and Protein Lactylation in Colorectal Cancer: From Metabolic Reprogramming to Epigenetic Regulation. Front Oncol, 16: 1741782.

[31] Huang M, 2025, Histone Lactylation in Gastrointestinal Cancers: Developing Immunotherapeutic Drugs Targeting Epigenetics. Arch Pharm Res, 48(9–10): 831–842.

[32] Lin S, Yan Y, Zhou J, et al., 2026, Positive Feedback Loop via HIF-1α Lactylation Driven by Kynurenine Promotes Glycolysis. Oncogene, 45(34): 3604–3619.

[33] Gong J, Xie Y, Weng Z, et al., 2026, Targeting Lactate and Lactylation in Cancer Metabolism and Immunotherapy. Adv Sci (Weinh), 13(35): e15403.

[34] Sun Y, Wang H, Cui Z, et al., 2025, Lactylation in Cancer Progression and Drug Resistance. Drug Resist Updat, 81: 101248.

[35] Wang N, Jiang X, Zhang S, et al., 2021, Structural Basis of Human Monocarboxylate Transporter 1 Inhibition by Anti-Cancer Drug Candidates. Cell, 184(2): 370–383.e13.

[36] Benyahia Z, Blackman MCNM, Hamelin L, et al., 2021, In Vitro and In Vivo Characterization of MCT1 Inhibitor AZD3965 Confirms Preclinical Safety Compatible with Breast Cancer Treatment. Cancers (Basel), 13(3): 569.

[37] Richiardone E, Al Roumi R, Lardinois F, et al., 2024, MCT1-Dependent Lactate Recycling Is a Metabolic Vulnerability in Colorectal Cancer Cells Upon Acquired Resistance to Anti-EGFR Targeted Therapy. Cancer Lett, 598: 217091.

[38] Amorim R, Pinheiro C, Miranda-Gonçalves V, et al., 2015, Monocarboxylate Transport Inhibition Potentiates the Cytotoxic Effect of 5-Fluorouracil in Colorectal Cancer Cells. Cancer Lett, 365(1): 68–78.

[39] Zhang Y, Liu C, Han F, et al., 2025, MCT1 Inhibition Remodels the Tumor Immune Microenvironment for Enhanced Cancer Immunotherapy. Mol Cancer Ther, 25(8): 1330–1341.

[40] Kim HK, Lee I, Bang H, et al., 2018, MCT4 Expression Is a Potential Therapeutic Target in Colorectal Cancer with Peritoneal Carcinomatosis. Mol Cancer Ther, 17(4): 838–848.

[41] Babl N, Decking SM, Voll F, et al., 2023, MCT4 Blockade Increases the Efficacy of Immune Checkpoint Blockade. J Immunother Cancer, 11(10).

[42] Heinrich T, Sala-Hojman A, Ferretti R, et al., 2021, Discovery of 5-{2-[5-Chloro-2-(5-Ethoxyquinoline-8-Sulfonamido)Phenyl]Ethynyl}-4-Methoxypyridine-2-Carboxylic Acid, a Highly Selective In Vivo Useable Chemical Probe to Dissect MCT4 Biology. J Med Chem, 64(16): 11904–11933.

[43] Alobaidi B, Hashimi SM, Alqosaibi AI, et al., 2023, Targeting the Monocarboxylate Transporter MCT2 and Lactate Dehydrogenase A LDHA in Cancer Cells with FX-11 and AR-C155858 Inhibitors. Eur Rev Med

Pharmacol Sci, 27(14): 6605–6617.

[44] Chen S, Nishi M, Morine Y, et al., 2022, Epigallocatechin-3-Gallate Hinders Metabolic Coupling to Suppress Colorectal Cancer Malignancy Through Targeting Aerobic Glycolysis in Cancer-Associated Fibroblasts. Int J Oncol, 60(2): 19.

[45] Fang C, Peng Q, Li X, et al., 2026, Multichannel Immune Nanoregulators Suppress Lactic Acid Metabolism and Lactic Acid-Shaped Acidic Microenvironment to Uproot Anti-Tumor Immunosuppression. Adv Mater, 38(3): e12230.

[46] Du J, Han S, Song R, et al., 2026, Nano-Enabled Spatially Selective Protein Degradation Modulates Lactate Metabolism to Potentiate Antitumor Immunity in Liver Cancer. Nat Nanotechnol, 21(7): 1036–1047.

[47] Li B, Jiao L, Zhang Y, 2026, Pharmacological Inhibition of Histone Lactylation Enhances Immunotherapy Efficacy in Gastrointestinal Cancers. Bioorg Chem, 170: 109536.

Publisher's note

Bio-Byword Scientific Publishing remains neutral with regard to jurisdictional claims in published maps and institutional affiliations.

Oncology Treatment Discovery, 2026, Volume 4, Issue 3
https://bbwpublisher.com/journal/OTD
Online ISSN: 2981-8079
Print ISSN: 3083-4996

A Study on the Diagnostic Value of Multimodal MRI in Assessing Early Radiation-Induced Brain Injury Following Intensity-Modulated Radiation Therapy for Nasopharyngeal Carcinoma

Jingyin Ma, Xueping Zheng, Ning Zhai, Chengtong Zhu, Ying Wang, Yun Ren, Feifei Lu

Lu'an Municipal Hospital of Traditional Chinese Medicine, Lu'an 237006, Anhui, China

Copyright: © 2026 Author(s). This is an open-access article distributed under the terms of the Creative Commons Attribution License (CC BY 4.0), permitting distribution and reproduction in any medium, provided the original work is cited.

Abstract: *Objectives*: Intensity-modulated radiation therapy is the cornerstone of curative treatment for nasopharyngeal carcinoma; however, radiation-induced brain injury has an insidious onset, with no obvious morphological abnormalities in brain tissue in the early stages. It is difficult to detect through routine imaging examinations, making it easy to miss the optimal window for intervention. To investigate the dynamic progression of early radiation-induced brain injury following radiation therapy for nasopharyngeal carcinoma, identify the optimal evaluation window, and determine the correlation between tumor staging and brain injury, this study conducted a dynamic follow-up study using multimodal MRI technology. *Methods*: Thirty patients with newly diagnosed nasopharyngeal carcinoma were enrolled and divided into three groups based on TNM staging: T1/T2, T3, and T4, with 10 patients in each group. All patients underwent radical intensity-modulated radiation therapy. Multimodal MRI scans were performed 1 day before radiotherapy and 1, 3, and 7 weeks after radiotherapy. Changes in the microstructure of the temporal lobe and hippocampal white matter, as well as brain functional network parameters, were quantitatively compared across groups. *Results*: One week after radiotherapy, only physiological fluctuations in brain tissue parameters were observed, with no pathological damage; three weeks after radiotherapy, subclinical white matter structural disorganization and abnormalities in brain functional networks could be consistently detected, representing the optimal time window for assessing early damage; seven weeks after radiotherapy, brain damage showed cumulative worsening in proportion to radiation dose. The overall detection rate of early brain injury in this group was 46.67%. The incidence and severity of brain injury in stage T4 patients were significantly higher than those in patients with early- to mid-stage disease ($P < 0.05$). The FA, ReHo, and ALFF parameters measured in the temporal lobe 3 weeks after radiotherapy demonstrated good diagnostic performance for early brain injury. *Conclusion*: Multimodal MRI can accurately detect occult early-stage radiation-induced brain injury following radiotherapy for nasopharyngeal carcinoma. Abnormal changes in brain function occur earlier than morphological damage to brain tissue, and TNM staging is positively correlated with the severity of brain injury. This technique provides reliable imaging evidence to support the early implementation of neuroprotective interventions and the optimization of individualized radiotherapy regimens.

Keywords: Nasopharyngeal carcinoma; Intensity-modulated radiation therapy; Radiation-induced brain injury; Multimodal magnetic resonance imaging; Early diagnosis

Online publication: October 20, 2026

1. Introduction

Nasopharyngeal carcinoma is a head and neck malignancy with a high incidence in southern China, exhibiting a distinct regional clustering pattern. Intensity-modulated radiation therapy, with its advantages of precise dose delivery to the target area and protection of normal tissues, has become the treatment of choice for curative therapy in newly diagnosed nasopharyngeal carcinoma. Due to the deep anatomical location of the nasopharynx and its proximity to important brain structures such as the bilateral temporal lobes and the hippocampus, scattered radiation and cumulative doses generated during radiation therapy can cause sustained damage to normal brain tissue, leading to radiation-induced brain injury—one of the most common long-term complications following radiation therapy for nasopharyngeal carcinoma, which severely impacts patients' quality of life after surgery [1].

Radiation-induced brain injury progresses insidiously and gradually. In the early stages of the disease, there are no specific clinical symptoms, and no macroscopic morphological lesions are visible in the brain tissue; it manifests only as microstructural disruption in the white matter and reduced functional coordination between brain regions, making it difficult to detect effectively with conventional CT and standard MRI. As radiation damage continues to accumulate, patients may gradually develop symptoms such as memory impairment, inattention, and cognitive decline. In severe cases, irreversible pathological changes—such as cerebral softening and brain tissue necrosis—may occur, constituting major risk factors for poor long-term prognosis. Therefore, achieving early and accurate screening and assessment of radiation-induced brain injury holds significant clinical value for improving the long-term prognosis of nasopharyngeal carcinoma patients [1,2].

Multimodal MRI, which integrates diffusion tensor imaging and resting-state functional MRI, can quantitatively assess subclinical brain tissue damage at both the microstructural and functional levels, thereby addressing the technical limitations of conventional imaging, which can only observe macroscopic morphological lesions. Currently, most domestic studies focus on retrospective analyses of long-term organic brain damage following radiation therapy; however, there remains a lack of systematic dynamic follow-up studies regarding the dynamic evolution patterns of subclinical damage in the very early stages of radiation therapy, the optimal screening time window, and the impact of different TNM stages on the severity of brain damage. Through dynamic monitoring at multiple time points, this study compares and analyzes the evolutionary characteristics of brain tissue MRI parameters before and after radiotherapy in nasopharyngeal carcinoma patients at different stages to identify specific indicators for early brain injury assessment. The aim is to provide objective radiological data support for the early clinical prevention and control of radiation-induced brain injury and the optimization of radiotherapy protection strategies [2,3,4].

2. Materials and methods

2.1. General materials

This study included 30 treatment-naive nasopharyngeal carcinoma patients diagnosed and treated in the Oncology Department of our hospital between June 2024 and June 2026.

2.1.1. Inclusion criteria

(1) Diagnosis of primary nasopharyngeal carcinoma confirmed by pathological biopsy of the nasopharynx;

(2) First-time diagnosis, with no history of cranial surgery or cranial radiation therapy; ③ No underlying

cranial or brain diseases such as cerebral infarction, intracranial tumors, or encephalitis;

(3) No contraindications for MRI;

(4) Complete clinical and imaging records, with the ability to cooperate in completing the full course of follow-up scans.

2.1.2. Exclusion criteria

(1) Severe imaging artifacts or missing data rendering the case ineligible for analysis; (2) Patients who dropped out during follow-up or were unable to complete the entire follow-up process.

Patients were grouped according to the TNM staging criteria for nasopharyngeal carcinoma, with 10 cases each in stages T1/T2, T3, and T4. The study included 21 male and 9 female patients, ranging in age from 40 to 75 years, with a median age of 58 years. All patients and their families were informed of the study details and voluntarily signed informed consent forms. This study was approved by our hospital's Medical Ethics Committee. There were no statistically significant differences in baseline characteristics, such as age and gender, among the three groups ($P > 0.05$), indicating that the groups were well-balanced and comparable [5].

2.2. Testing methods

All subjects underwent whole-brain scans using our hospital's Siemens Skyra 3.0T medical MRI scanner. Parameters such as slice thickness, field of view, and patient positioning were standardized across all scans to minimize equipment and operational errors. The scanning sequences included 3D-T1 structural imaging, DTI, and rs-fMRI. Scans were scheduled at fixed time points: 1 day before radiotherapy and 1 week, 3 weeks, and 7 weeks after radiotherapy. The same experienced radiologic technologist performed all scans. Prior to scanning, patients were instructed to keep their heads still, remain calm, and rest with their eyes closed to minimize motion artifacts and ensure image quality met the requirements for data analysis.

2.3. Data processing and metric extraction

Import the raw image data into the SPM12 image analysis software and perform image registration, smoothing, denoising, and standardization as part of the preprocessing. The bilateral temporal lobes and hippocampus—areas with a high incidence of radiation-induced brain injury—were selected as regions of interest. Quantitative metrics such as the anisotropy fraction (FA), apparent diffusion coefficient (ADC), regional homogeneity (ReHo), low-frequency amplitude (ALFF), and default mode network (DMN) functional connectivity strength were extracted at each time point. Two senior radiologists with over 10 years of experience independently reviewed the images and compiled the statistics using a double-blind method. In cases of data discrepancies, they jointly reviewed and corrected the results, and invalid samples were excluded to ensure the authenticity and reliability of the data.

2.4. Statistical methods

Data were analyzed using SPSS 26.0 statistical software. Continuous variables are expressed as "mean ± standard deviation (SD)"; repeated-measures analysis of variance was used to compare measures at different time points within groups, and one-way analysis of variance was used to compare measures at the same time point across groups. Categorical variables are expressed as counts and percentages, and the chi-square (χ^2) test was used for between-group comparisons. Pearson's correlation analysis was used to assess the

correlation among variables. The significance level was set at $\alpha = 0.05$, and a P-value < 0.05 was considered statistically significant.

3. Results

3.1. Comparison of baseline characteristics among the three groups of patients

There were no statistically significant differences in age or gender distribution among the three patient groups ($P > 0.05$). Furthermore, baseline levels of temporal lobe and hippocampal brain structure and brain function indicators were essentially consistent across all groups prior to radiotherapy; baseline characteristics were well balanced between groups, and there were no confounding factors. All patients completed four imaging follow-up sessions, with no dropouts or missing data, as shown in **Table 1**.

Table 1. Comparison of general baseline characteristics among the three groups of patients

Indicators	Stage T1/T2 group (n=10)	Stage T3 group (n=10)	Stage T4 group (n=10)	χ^2/F value	*P* value
Gender (Male/Female, Number)	7/3	7/3	7/3	0.000	1.000
Age (mean ± SD, years)	57.2 ± 8.1	58.1 ± 7.9	58.5 ± 8.3	0.089	0.915

3.2. Detection rates and temporal patterns of early radiological brain lesions

One week after radiation therapy, the imaging parameters of brain tissue in all three patient groups showed only physiological fluctuations, with no pathological changes such as nerve fiber damage or cerebral dysfunction. Three weeks after radiation therapy, pathological abnormalities in the microstructure of white matter and cerebral function in the temporal lobe and hippocampus regions could be reliably detected, representing the optimal time window for detecting early, latent brain injury. Seven weeks after radiotherapy, the extent of brain tissue damage further expanded and the severity of damage continued to worsen, demonstrating a significant time-dose cumulative effect [1,2,6].

In this study, abnormal radiological findings 3 weeks after radiotherapy were used as the criterion for a positive diagnosis of early brain injury. Among the 30 patients, 14 tested positive, resulting in an overall detection rate of 46.67% for early brain injury. Specifically, there were 3 cases (30.00%) in the T1/T2 stage group, 4 cases (40.00%) in the T3 stage group, and 7 cases (70.00%) in the T4 stage group. A comparison of the incidence of early brain injury among the three groups revealed statistically significant differences ($P < 0.05$); patients in the T4 stage had a significantly higher risk of developing early brain injury after radiation therapy than those in the T1/T2 and T3 stages [5,7].

3.3. Dynamic changes in brain tissue microstructure and brain function following radiation therapy

Conventional structural MRI results showed that, 3 weeks after radiation therapy, the thickness of the patient's bilateral temporal and frontal cortices and the volume of white matter had decreased significantly compared to pre-treatment levels, and the extent of damage continued to worsen as the follow-up period extended. DTI findings suggest that radiation therapy can cause neurofibrillary edema and disorganization in the temporal lobe and hippocampus, primarily manifested by decreased FA values and increased ADC values. As the injury progresses, this can gradually develop into irreversible organic damage, such as white matter

demyelination and axonal degeneration [3, 8, 9].

rs-fMRI results indicate that following radiation therapy, patients exhibit a progressive decline in ReHo, ALFF, and DMN functional connectivity in the temporal lobe, with continued impairment in neural synchrony and functional integration across brain regions. Overall, radiation therapy-induced abnormal changes in brain functional networks occur earlier than macroscopic morphological lesions in brain tissue, enabling the effective identification of subclinical, occult brain injury that is difficult to detect with conventional MRI [3,8].

3.4. Correlation between TNM staging and the severity of brain injury

At the same follow-up time point, the severity of brain damage in patients showed a clear gradient correlation with tumor TNM staging: patients with stage T4 exhibited the greatest degree of abnormal imaging parameters and the most severe brain damage, while those with stages T1 and T2 had the mildest damage, and those with stage T3 fell between the two. Results of Pearson correlation analysis showed that TNM staging was significantly negatively correlated with FA values in the temporal lobe and hippocampus, and significantly positively correlated with the degree of ADC elevation and the severity of brain dysfunction (all $P < 0.05$), suggesting that TNM staging is an independent risk factor influencing the severity of radiation-induced brain injury following radiotherapy for nasopharyngeal carcinoma [5,7].

3.5. Screening for early-stage specific imaging markers

Based on an analysis of the trends in parameter changes at various follow-up time points, intergroup differences, and data stability, the detection rates of abnormalities in the three temporal lobe parameters—FA, ReHo, and ALFF—were high 3 weeks after radiotherapy; significant intergroup differences were observed; and data stability was good. These parameters demonstrated high sensitivity and specificity for the diagnosis of early, subclinical radiation-induced brain injury and can serve as specific imaging biomarkers for early radiation-induced brain injury following radiotherapy for nasopharyngeal carcinoma.

3.6. Comparison of DTI parameters among patient groups at different time points

Prior to radiation therapy, there were no statistically significant differences in baseline FA and ADC parameters in the temporal lobe and hippocampus among the three patient groups; baseline levels were balanced and comparable. After radiation therapy, FA values continued to decrease and ADC values continued to increase in all groups, demonstrating a clear cumulative effect over time. Specifically, changes in these parameters 1 week after radiotherapy were not statistically significant ($P > 0.05$); however, both pre- and post-treatment comparisons within each group and intergroup comparisons at the same time points 3 and 7 weeks after radiotherapy were statistically significant ($P < 0.05$). Furthermore, the magnitude of abnormalities in imaging parameters was significantly higher in Stage T4 patients than in Stage T1/T2 and Stage T3 patients, as detailed in **Table 2**.

Table 2. Comparison of DTI parameters in the white matter of patients in each group at different radiotherapy time points (mean ± SD)

Testing Time	Grouping	FA in the temporal lobe	Temporal lobe ADC ($\times10^{-3}$ mm²/s)	Hippocampus FA	Hippocampus ADC ($\times10^{-3}$ mm²/s)
Before radiotherapy	Stages T1/T2	0.482 ± 0.021	0.786 ± 0.032	0.451 ± 0.018	0.812 ± 0.029

Before radiotherapy	Stage T3	0.479 ± 0.019	0.789 ± 0.028	0.448 ± 0.020	0.809 ± 0.031
Before radiotherapy	StageT4	0.480 ± 0.022	0.785 ± 0.030	0.449 ± 0.019	0.811 ± 0.028
1 week of radiotherapy	Stages T1/T2	0.475 ± 0.020	0.792 ± 0.031	0.445 ± 0.017	0.818 ± 0.030
1 week of radiotherapy	Stage T3	0.471 ± 0.018	0.798 ± 0.029	0.442 ± 0.019	0.822 ± 0.027
1 week of radiotherapy	StageT4	0.468 ± 0.021	0.803 ± 0.032	0.439 ± 0.018	0.826 ± 0.029
3 weeks of radiotherapy	Stages T1/T2	$0.441 \pm 0.017^{*\#}$	$0.835 \pm 0.028^{*\#}$	$0.412 \pm 0.016^{*\#}$	$0.859 \pm 0.026^{*\#}$
3 weeks of radiotherapy	Stage T3	$0.425 \pm 0.015^{*\#}$	$0.858 \pm 0.025^{*\#}$	$0.398 \pm 0.014^{*\#}$	$0.878 \pm 0.024^{*\#}$
3 weeks of radiotherapy	StageT4	$0.402 \pm 0.016^{*\#}$	$0.889 \pm 0.027^{*\#}$	$0.375 \pm 0.015^{*\#}$	$0.905 \pm 0.025^{*\#}$
7 weeks of radiotherapy	Stages T1/T2	$0.410 \pm 0.014^{*\#\triangle}$	$0.868 \pm 0.025^{*\#\triangle}$	$0.385 \pm 0.013^{*\#\triangle}$	$0.886 \pm 0.023^{*\#\triangle}$
7 weeks of radiotherapy	Stage T3	$0.386 \pm 0.013^{*\#\triangle}$	$0.895 \pm 0.022^{*\#\triangle}$	$0.362 \pm 0.012^{*\#\triangle}$	$0.912 \pm 0.021^{*\#\triangle}$
7 weeks of radiotherapy	StageT4	$0.358 \pm 0.012^{*\#\triangle}$	$0.932 \pm 0.024^{*\#\triangle}$	$0.335 \pm 0.011^{*\#\triangle}$	$0.948 \pm 0.022^{*\#\triangle}$

Note: Compared with pre-radiotherapy, $^{*}P < 0.05$; compared with 1 week after radiotherapy, $^{\#}P < 0.05$; compared with 3 weeks after radiotherapy, $^{\triangle}P < 0.05$.

3.7. Comparison of changes in brain functional network indicators

Prior to radiotherapy, baseline levels of ReHo, ALFF and DMN functional connectivity in the temporal lobe were balanced across the three patient groups, with no significant differences observed between groups ($P > 0.05$). One week after radiotherapy, only minor fluctuations were observed in the brain functional indicators across all groups, with no statistically significant pathological abnormalities detected ($P > 0.05$); Three weeks after radiotherapy, the ReHo, ALFF and DMN functional connectivity strengths in the temporal lobe of patients in all three groups had decreased significantly compared with pre-treatment levels. Among these, the extent of decline in patients with advanced stage T4 was significantly greater than that in patients with stages T1/T2 and T3, with significant differences between groups ($P < 0.05$). Seven weeks following radiotherapy, the degree of disruption to the brain's functional networks had further increased, with functional synchrony and integrative capacity continuing to deteriorate. Overall, the temporal patterns of brain functional impairment were highly consistent with the progression of microstructural damage in the white matter, confirming the pathological characteristic of radiation-induced brain injury as 'functional abnormalities first, followed by structural damage'. For detailed data, see **Table 3**.

Table 3. Comparison of temporal lobe functional parameters among patient groups at different time points (mean ± SD)

Testing time	Grouping	Temporal lobe ReHo	ALFF in the temporal lobe	DMN functional connectivity strength
Before radiotherapy	Stages T1/T2	0.892 ± 0.035	1.025 ± 0.042	0.915 ± 0.038
Before radiotherapy	Stage T3	0.889 ± 0.032	1.021 ± 0.040	0.912 ± 0.035
Before radiotherapy	StageT4	0.890 ± 0.034	1.023 ± 0.041	0.913 ± 0.036
3 weeks of radiotherapy	Stages T1/T2	$0.815 \pm 0.030^{*}$	$0.936 \pm 0.038^{*}$	$0.842 \pm 0.032^{*}$

Testing time	Grouping	Temporal lobe ReHo	ALFF in the temporal lobe	DMN functional connectivity strength
3 weeks of radiotherapy	Stage T3	$0.772 \pm 0.028^{*}$	$0.885 \pm 0.035^{*}$	$0.796 \pm 0.030^{*}$
3 weeks of radiotherapy	StageT4	$0.721 \pm 0.025^{*}$	$0.824 \pm 0.032^{*}$	$0.735 \pm 0.028^{*}$
7 weeks of radiotherapy	Stages T1/T2	$0.753 \pm 0.027^{*\#}$	$0.872 \pm 0.034^{*\#}$	$0.781 \pm 0.029^{*\#}$
7 weeks of radiotherapy	Stage T3	$0.701 \pm 0.024^{*\#}$	$0.813 \pm 0.031^{*\#}$	$0.725 \pm 0.026^{*\#}$
7 weeks of radiotherapy	StageT4	$0.642 \pm 0.022^{*\#}$	$0.745 \pm 0.028^{*\#}$	$0.658 \pm 0.024^{*\#}$

Note: Compared with pre-radiotherapy, $^{*}P < 0.05$; compared with 3 weeks after radiotherapy, $^{\#}P < 0.05$.

4. Discussion

Intensity-modulated radiotherapy is the standard treatment for the radical treatment of nasopharyngeal carcinoma, enabling precise coverage of the tumour target area and effective control of local lesions. However, due to the anatomical proximity of the nasopharynx to brain structures such as the temporal lobe and hippocampus, the scattered and cumulative doses resulting from radiotherapy can cause persistent damage to normal brain tissue, leading to radiation-induced brain injury. Early-stage manifestations of this complication are extremely subtle, with no obvious morphological or clinical abnormalities, making them difficult to detect through routine imaging examinations. By the time organic lesions such as cognitive decline or cerebral softening become apparent, the damage is already irreversible, severely compromising patients' long-term quality of life. Therefore, establishing a precise early assessment system and clarifying the temporal patterns of damage onset are of significant practical importance for guiding early clinical intervention and reducing the incidence of long-term brain damage [1,7].

This study established multiple standardised follow-up time points to dynamically track the occurrence and progression of brain damage in nasopharyngeal carcinoma patients following radiotherapy. The results showed that one week after radiotherapy, brain tissue exhibited only temporary fluctuations in physiological parameters, with no pathological or organic damage observed; three weeks after radiotherapy, microstructural disturbances in the white matter of the temporal lobe and hippocampus, as well as imbalances in brain functional networks, could be reliably detected, representing the optimal time point for the assessment and clinical intervention of early, latent brain injury; seven weeks after radiotherapy, functional damage gradually progressed to structural damage such as demyelination and axonal degeneration, with the extent and severity of the damage continuing to worsen, confirming the existence of a clear time-dose cumulative effect in radiation-induced brain injury. The temporal patterns of early damage identified in this study provide data support for the development of personalised follow-up protocols and early neuroprotective strategies in clinical practice [1,2.10].

The findings of this study suggest that tumour TNM staging is closely associated with the risk of and severity of radiation-induced brain injury. Patients with advanced T4 nasopharyngeal carcinoma have a wider extent of tumour infiltration and a larger radiotherapy treatment field; consequently, the surrounding normal brain tissue is exposed to higher doses of scattered radiation. Compared with patients with T1/T2 or T3 disease, they exhibit a higher incidence of early brain injury and more pronounced abnormalities in imaging parameters. In clinical practice, for patients with advanced nasopharyngeal carcinoma, it is necessary to optimise further radiotherapy planning to minimise the extent of radiation exposure to normal brain tissue, strengthen early postoperative imaging follow-up, and promptly implement neuroprotective interventions to

mitigate the adverse effects of radiation-induced brain injury on patients' long-term prognosis [5,7].

Multimodal MRI enables the simultaneous quantitative assessment of white matter microstructure and functional brain networks, effectively overcoming the limitations of conventional imaging examinations. In particular, DTI parameters objectively reflect the integrity of white matter fibre tracts and the extent of microscopic damage, whilst rs-fMRI parameters accurately assess the synchrony of neural activity and the state of functional integration between brain regions. The results of this study confirm that, three weeks following radiotherapy, the FA, ReHo and ALFF parameters in the temporal lobe demonstrate good stability, significant intergroup differences and high diagnostic performance. They can effectively detect subclinical brain damage that cannot be identified by conventional imaging and may serve as specific assessment indicators for early radiation-induced brain damage following radiotherapy for nasopharyngeal carcinoma, providing an objective basis for clinical risk prediction and the individualised adjustment of radiotherapy regimens [3,8].

This study has certain limitations: as a single-centre study with a small sample size, there may be a slight selection bias; the follow-up period covered only the early stages following radiotherapy, and did not further track changes in patients' long-term cognitive function or long-term prognostic outcomes. Furthermore, the analysis in this study was based solely on radiological indicators; it did not incorporate neurocognitive scales or serum damage markers for multidimensional validation, and therefore could not establish a precise correlation between radiological abnormalities and clinical cognitive impairment. Future research could involve multicentre, large-sample prospective studies with extended follow-up periods, integrating radiological, neuropsychological and serological indicators to construct multidimensional early prediction models, thereby further refining the system for the early screening and prevention of radiation-induced brain injury.

5. Conclusion

Multimodal MRI enables dynamic, quantitative monitoring of early, subtle changes in the microstructure and function of brain tissue following intensity-modulated radiotherapy for nasopharyngeal carcinoma, and can effectively detect subclinical, occult radiation-induced brain injury that is difficult to identify using conventional imaging. Three weeks after radiotherapy represents the optimal window for the assessment and intervention of early brain injury; furthermore, changes in brain function precede morphological damage to brain tissue, thereby allowing sufficient time for early clinical intervention. There is a positive correlation between the TNM staging of nasopharyngeal carcinoma and the severity of post-radiotherapy brain injury, with patients at an advanced stage being at higher risk of brain injury. The diagnostic performance of FA, ReHo and ALFF parameters in the temporal lobe at three weeks post-radiotherapy is excellent; these can serve as specific imaging biomarkers for early radiation-induced brain injury. They hold significant clinical value for optimising individualised radiotherapy protection strategies for nasopharyngeal carcinoma, guiding early neuroprotective treatment and improving patients' long-term prognosis.

Funding

Anhui University of Chinese Medicine University-level Research Project (Project No.: 2024LC013)

Disclosure statement

The authors declare no conflict of interest.

References

[1] Tang Y, Chen L, 2022, Recent Advances in the Mechanisms and Early Intervention of Radiation-Induced Brain Injury in Head and Neck Tumours. Chinese Journal of Radiation Oncology, 31(04): 361–366.

[2] Wang C, Liu M, Zhou F, 2023, Diagnostic Value of Multimodal MRI in Early Radiation-Induced Brain Injury Following Intensity-Modulated Radiotherapy for Nasopharyngeal Carcinoma. Journal of Clinical Radiology, 42(08): 1245–1249.

[3] Zhang Y, Li J, Chen J, 2022, An Applied Study on the Assessment of White Matter and Cerebral Functional Network Damage Following Radiotherapy for Nasopharyngeal Carcinoma Using DTI Combined with Resting-State fMRI. Radiology Practice, 37(11): 1432–1437.

[4] Qiu Q, Chen H, Cui Y, et al., 2023, Advances in Imaging Studies of Radiation-Induced Damage to the Skull Base Tissues Following Radiotherapy for Nasopharyngeal Carcinoma. Chinese Journal of Clinical Medicine, 16(1): 1–7.

[5] Chen Q, Lin X, Han L, 2022, Imaging Analysis of Differences in Brain Damage Following Radiotherapy in Nasopharyngeal Carcinoma Patients with Different TNM Stages. Tumour Imaging, 31(03): 278–283.

[6] Lv X, Guo Z, Tang L, 2021, A One-Year Follow-Up Study on Dynamic Morphological Changes in the Cerebral Cortex Following Radiotherapy for Nasopharyngeal Carcinoma Based on Structural MRI. Quant Imaging Med Surg, 11(6): 2307–2320.

[7] Ouyang P, Ma J, Sun Y, 2023, A Study on the Correlation Between the Three-Dimensional Distribution of Radiation Dose in the Temporal Lobe and Radiation-Induced Brain Injury in Nasopharyngeal Carcinoma. Int J Radiat Oncol Biol Phys, 115(5): 1291–1300.

[8] Lv X, Mai H, Qiu Y, 2022, Early Microstructural and Functional Brain Alterations After Intensity-Modulated Radiotherapy in Nasopharyngeal Carcinoma Patients. J Neuroimaging, 32(5): 689–696.

[9] Tang Y, Zhang Y, 2023, Pericyte Dysfunction Mediates Radiation-Induced Brain Injury After Radiotherapy for Head and Neck Cancer. Sci Transl Med, 15(698): eabm6543.

[10] Liu Y, Wang X, 2021, Dynamic Changes of Default Mode Network in Nasopharyngeal Carcinoma Patients with Radiation-Induced Brain Injury. Radiol Oncol, 55(3): 312–319.

Publisher's note

Bio-Byword Scientific Publishing remains neutral with regard to jurisdictional claims in published maps and institutional affiliations.

Oncology Treatment Discovery, 2026, Volume 4, Issue 3
https://bbwpublisher.com/journal/OTD
Online ISSN: 2981-8079
Print ISSN: 3083-4996

A Study on the Patterns of Recurrence of Liver Metastases after Curative Surgery for Gastric Cancer, Based on the SEER Database

Wei Xu[1], Yue Qiu[1]†, Shiqi Zhang[1,2]†, Caiyue Gao[4], Xiaoyan Wang[2], Changfeng Man[3]*, Yu Fan[1,4]*

[1]Cancer Institute, the Suqian Clinical College of Xuzhou Medical University, Suqian 223800, Jiangsu, China
[2]Department of Gastroenterology, the Suqian Clinical College of Xuzhou Medical University, Suqian 223800, Jiangsu, China
[3]Cancer Institute, Zhenjiang Clinical Medical College of Nanjing Medical University, Zhenjiang 212002, Jiangsu, China
[4]Clinical Medical Research Center, the Suqian Clinical College of Xuzhou Medical University, Suqian 223800, Jiangsu, P.R.China.
† These authors contributed equally to this work and share the first authorship.

***Corresponding authors*: Yu Fan, yuf9987@njmu.edu.cn; Changfeng Man, changfengman@*njmu.edu.cn*

Copyright: © 2026 Author(s). This is an open-access article distributed under the terms of the Creative Commons Attribution License (CC BY 4.0), permitting distribution and reproduction in any medium, provided the original work is cited.

Abstract: Gastric cancer is a prevalent malignancy of the digestive system worldwide. Even after curative surgical intervention, distant metastasis remains the primary cause of treatment failure, with hepatic metastasis being the most common type of hematogenous spread. The Surveillance, Epidemiology, and End Results (SEER) database, a large-scale population-based cancer registry in North America, provides extensive data on gastric cancer, including demographics, clinical pathology, treatment modalities, and long-term follow-up. This data is invaluable for understanding the real-world patterns of hepatic metastasis, risk factors, prognostic features, and the development of predictive models. This paper systematically reviews research based on the SEER database related to gastric cancer hepatic metastasis, summarizing findings regarding epidemiological characteristics, clinical risk factors, prognostic factors, benefits of surgical treatment, various predictive models, and features in specific patient subgroups. The aim is to provide evidence-based guidance for clinical risk stratification, follow-up strategies, and personalized treatment decisions following gastric cancer surgery.

Keywords: Gastric cancer; SEER database; Hepatic metastasis; Risk factors; Prognosis; Scatter plot; Machine learning

Online publication: October 20, 2026

1. Introduction

Gastric cancer is highly invasive, and the majority of gastric cancer cases in China are at an advanced stage. Despite curative surgery, a considerable number still develop distant metastasis, which markedly shortens long-term survival. Metastasis from gastric cancer shows organ preference, mainly involving the peritoneum,

liver, lung, and bone. The liver is the most common site of hematogenous dissemination, and hepatic involvement can be synchronous or postoperative. Synchronous liver metastasis is found at initial diagnosis, whereas postoperative liver metastasis appears during follow-up after surgery. The two forms differ in mechanism, clinical presentation, and outcome.

In the conventional AJCC TNM system, all distant metastases are grouped as stage IV, without distinguishing the organ involved, such as the liver. As a result, prognosis within the gastric cancer liver metastasis population is not well reflected, and individualized assessment remains difficult. Because single-center samples are often small, domestic institutions have found it hard to collect enough cases for large retrospective studies of gastric cancer with liver metastasis. The SEER database covers several regions of the United States and records demographic data, tumor site, differentiation, T and N stage, treatment, and survival. It has therefore been widely used to study the epidemiology, risk factors, and predictive models of gastric cancer liver metastasis. In recent years, researchers in China and abroad have published many SEER-based studies using cohort analysis, propensity score matching (PSM), competing risk models, scatter plots, and machine learning. However, there is currently a lack of a comprehensive review article summarizing these types of studies.

This article reviews and summarizes the literature on gastric cancer metastasis to the liver, as found in the SEER database. It examines the epidemiological characteristics, risk factors, prognosis, surgical treatment outcomes, predictive models, and specific patient subgroups within the included studies. The aim is to provide a reference for clinical practice and future domestic research in this area.

2. Basic epidemiological characteristics of liver metastasis in gastric cancer

Utilizing the extensive SEER registration data, it is possible to determine the prevalence and characteristics of liver metastasis in gastric cancer at the population level. Studies by Horn et al. [1] on the epidemiology of liver metastasis in various cancers have shown that the risk of liver metastasis varies significantly depending on the type of malignancy, with gastric cancer being a high-risk type. Qiu et al. [2] used the SEER database to analyze the distribution of distant organ metastases in gastric cancer, finding that liver metastasis is the most common type, often manifesting as a solitary liver metastasis, but frequently occurring alongside metastasis to the peritoneum, bone, or lungs. In most cases, patients with liver metastasis do not exhibit a single, isolated lesion.

Based on the timing of metastasis, gastric cancer liver metastasis is classified as synchronous liver metastasis and metachronous liver metastasis. Synchronous liver metastasis refers to the presence of liver metastasis at the initial diagnosis; metachronous liver metastasis refers to the development of liver metastasis during follow-up after curative surgery. Due to the lack of detailed records of post-operative recurrence time in some cases, some studies combine all cases of liver metastasis in gastric cancer for analysis. Other studies focus on synchronous liver metastasis. Zhang et al. [3] studied incidence trends of synchronous liver metastasis in gastric cancer and found that its proportion remained relatively stable over the past decade, without a clear downward trend. Overall, patients with synchronous liver metastasis have a markedly worse prognosis than those without liver metastasis.

Patient distribution also differs by age. Zhang et al. [4] used PSM with SEER to analyze metastasis patterns in young gastric cancer patients and found a higher liver metastasis risk than in older patients. Young patients with liver metastasis also more often had multi-organ involvement, indicating a heavier disease

burden. Wang et al. [5] compared early- and late-stage gastric cancer and found that early-stage disease had a higher rate of liver metastasis and more frequent multi-organ metastasis. This suggests that age influences the preferred metastatic organs in gastric cancer. Wu et al. [6] likewise confirmed that early-stage gastric cancer is more likely to spread to the liver, while advanced disease mainly involves the peritoneum. Differences in pathological subtype distribution by age are important: young patients have more diffuse and signet-ring cell carcinoma, which is biologically aggressive and prone to hematogenous spread to the liver.

Pathological subtype also matters. Gastric neuroendocrine tumors can metastasize to the liver, not only the peritoneum. Huang et al. [7] constructed survival curves for gastric neuroendocrine tumors with liver metastasis using SEER and confirmed that these tumors can spread to the liver. Survival was significantly worse in patients with liver metastasis than in those without. Huang et al. [8] developed a personalized prediction tool for metastatic gastric neuroendocrine tumors, noting that peritoneal metastasis is most common while liver metastasis is relatively rare. Prognosis among neuroendocrine tumor patients with liver metastasis is highly heterogeneous, so individualized risk assessment is needed rather than a uniform judgment.

3. Clinical and pathological risk factors for gastric cancer metastasis to the liver

Identifying independent risk factors for liver metastasis is important for screening high-risk individuals and guiding close postoperative follow-up. Several multivariate regression analyses based on SEER have been performed.

An W et al. [9] conducted a SEER collaborative external validation study and confirmed that age, tumor stage, and tumor differentiation are independent risk factors for liver metastasis. Later stage, greater lymph node involvement, and poorer differentiation were associated with a significantly higher risk. Lymph node involvement was a notable predisposing factor: patients with positive nodes had a much higher risk than those with negative nodes, highlighting the link between lymphatic and hematogenous spread in gastric cancer.

At the TNM level, liver metastasis risk rises with tumor invasion depth. Song et al. [10] developed a machine learning model to identify liver metastasis in gastric cancer, and their study showed that patients with T2-T4 stage gastric cancer have a significantly higher risk of liver metastasis compared to those with T1 stage gastric cancer. However, even in T1-stage gastric cancer, there is a small probability of liver metastasis, and early-stage blood metastasis cannot be completely ruled out. Tumor invasion depth and lymph node status are among the most important predictors of liver metastasis. Li et al. [11] developed a decision tree model specifically for predicting liver metastasis in gastric cancer, which also confirmed that TN and N staging are independent and key predictors of liver metastasis. Lymph node metastasis had the highest weight, and the number of positive nodes was positively correlated with liver metastasis probability.

Tumor location can also affect risk. Wang et al. [12] used SEER and domestic single-center registries to study tumor subtypes associated with liver metastasis and found that gastroesophageal junction cancer has a higher risk than distal gastric cancer. Distal tumors are more prone to peritoneal metastasis, whereas proximal tumors more often spread to the liver through the bloodstream. Tumor origin may therefore serve as a reference for assessing liver metastasis risk and for planning clinical staging and examinations. Ming et al. [13] compared tubular and diffuse gastric cancer and found that tubular cancer has a higher liver metastasis risk than diffuse cancer, while diffuse cancer more often involves the peritoneum. Histological type is thus an

important pathological factor influencing liver metastasis risk.

4. Prognostic features in patients with gastric cancer and liver metastasis

SEER contains two core survival endpoints: overall survival (OS) and cancer-specific survival (CSS), which are essential for prognosis prediction in gastric cancer liver metastasis. Overall, the prognosis for patients with gastric cancer liver metastasis is poor, but there is significant heterogeneity in survival within the population. Factors such as the presence of other organ metastases, demographics, clinical pathology, and treatment options can all influence survival outcomes.

Lin Z et al. [14] conducted a comparative study on the prognosis of liver, lung, bone, and brain metastasis in gastric cancer, using the SEER database. Their findings showed that isolated liver metastasis had a better prognosis than liver metastasis combined with multiple distant metastases, but a worse prognosis than isolated peritoneal metastasis. They also found that once liver metastasis was combined with metastasis to other organs such as bone, lung, and brain, the patient's survival time was significantly reduced, and the number of metastatic organs was an important prognostic indicator. Zhao QW et al. [15] specifically investigated the heterogeneity of single-organ metastasis in gastric cancer. Their research confirmed that isolated liver metastasis had a significantly better prognosis than liver metastasis combined with multiple distant metastases. Both studies highlighted that IV-stage gastric cancer requires further stratification, rather than being treated as a homogeneous group. Meng et al. [16] developed decision curve diagrams to predict the prognosis of liver metastasis in gastric cancer, using OS and CSS as outcome measures. Age, tumor grade, N stage, and whether the patient underwent surgery were identified as independent prognostic factors. Older age, higher tumor grade, and a greater number of lymph node metastases were associated with poorer prognosis, while patients who received tumor-related treatment had better survival outcomes compared to those receiving conservative care. Dong et al. [17] developed two independent decision curve diagrams to predict OS and CSS in patients with liver metastasis from gastric cancer. Their study confirmed that T stage, N stage, age, tumor differentiation, and treatment method jointly determined the prognosis of liver metastasis from gastric cancer. Traditional TNM staging systems had limited predictive value for this subgroup, while the decision curve models provided individualized survival probability estimates and demonstrated superior risk stratification compared to traditional staging systems.

Wu et al. [18] analyzed the causes of death in patients with liver metastasis from gastric cancer using the SEER database. Their research found that the primary cause of death for patients with liver metastasis from gastric cancer was the gastric cancer itself, with a low proportion of deaths due to non-tumor causes. They also found that advanced stages of the disease (high age and late T/N stages) significantly increased the risk of overall and tumor-specific mortality, highlighting the importance of controlling tumor progression for improving the prognosis of this group. Liu et al. [19] conducted a retrospective study on the prognosis of organ-specific metastasis in late-stage gastric cancer, which also confirmed that the prognosis for patients with liver metastasis was significantly worse than that of those without distant metastasis. Furthermore, the risk of death increased when liver metastasis occurred in combination with metastasis to other organs, and the type of organ affected by metastasis was an independent prognostic factor, separate from T/N staging.

5. The impact of surgical treatment on the survival of patients with gastric cancer metastasis to the liver

The benefit of surgery for gastric cancer with liver metastases, specifically involving resection of the primary tumor and liver lesions, has always been a subject of debate. However, using a large SEER (Cancer Registries) cohort and propensity score matching, it is possible to assess the benefits of surgical treatment in real-world settings.

Studies using multiple SEER sources confirmed significant heterogeneity in the surgical treatment of gastric cancer with liver metastases. Wu et al. [20] found that patients with surgically resectable primary tumors had improved survival, whereas those with extensive or large tumor burdens did not benefit and sometimes had increased perioperative risk. Ren et al. [21] also used SEER propensity score matching to examine the value of palliative gastrectomy in liver metastasis. Only a small subgroup with low tumor burden and single-organ liver metastasis appeared to benefit. For patients with multiple organ metastases, surgery did not significantly improve survival. Clinicians should therefore carefully consider whether palliative gastrectomy is appropriate.

Su et al. [22] developed a specialized decision-making model to predict survival after primary tumor resection in gastric cancer liver metastasis and to quantify potential surgical benefit. The model incorporates demographic, pathological, and staging variables and can distinguish patients likely to benefit from surgery from those unlikely to benefit, providing a quantitative tool to reduce experience-based bias. Ji et al. [23] analyzed the impact of surgery on the prognosis of gastric cancer liver metastasis and emphasized that benefit depends heavily on baseline characteristics. Surgery should not be decided solely by the presence of liver metastasis, but by comprehensive assessment of individual clinical and pathological features.

Wang et al. [24] developed a machine learning dynamic prediction model based on SEER to assess the prognosis of liver metastasis in gastric cancer and support treatment decisions. The model indicated that tumor burden and lymph node involvement are key prognostic factors. It can output expected survival rates under different treatment plans, helping clinicians weigh surgery and systemic therapy for personalized decisions. Li et al. [25] investigated the prognostic value of distant metastasis sites and surgical intervention in metastatic gastric cancer using SEER. They confirmed that surgical benefit in liver metastasis gastric cancer is significantly biased: patients with single-organ metastasis and generally good condition are more likely to benefit, while systemic treatment is recommended for widespread multi-organ metastasis.

6. A prediction model for the risk and prognosis of liver metastasis in gastric cancer, based on the SEER database

Traditional TNM staging is often inadequate for assessing individualized risk and prognosis in gastric cancer patients with liver metastasis. In recent years, many studies have used SEER to develop nomograms, web-based calculators, and machine learning models. These fall into two groups: models predicting liver metastasis risk and models predicting survival after liver metastasis diagnosis.

6.1. Predictive model for risk of liver metastasis

Song et al. [10] developed a machine learning model to identify liver metastasis risk in gastric cancer. It included demographics, T/N staging, tumor differentiation, and tumor location. Internal validation showed good discriminatory power, allowing quantification of liver metastasis probability for individual patients. The

model can help identify high-risk individuals and guide imaging surveillance and early detection. Li et al. [11] constructed a decision tree to predict liver metastasis risk. T staging, N staging, and tumor differentiation were the most important input variables. A web-based tool was developed for clinical use to help identify high-risk individuals.

6.2. Predictive model for survival prognosis in patients with liver metastatic gastric cancer

Meng N et al. [16] developed a prognostic nomogram based on SEER to predict liver metastasis in gastric cancer, incorporating age, sex, TNM stage, tumor grade, and treatment. The nomogram can predict 13-year survival probability and is used for risk stratification, physician-patient communication, and treatment selection. Dong Z et al. [17] developed two independent nomograms for OS and CSS. They were internally validated and confirmed the limitations of traditional TNM staging in stratifying liver metastasis patients. Su R et al. [22] developed a nomogram specifically for patients with liver metastasis after primary tumor resection. It incorporates survival prediction and assessment of surgical benefit, facilitating treatment decisions and showing high clinical utility. Wang Z et al. [24] developed a machine learning-based dynamic prediction model. In addition to survival prediction, it can compare expected outcomes of different treatment strategies, expanding the use of prediction models in treatment decision-making.

7. Distinct features of gastric cancer metastasis to the liver in specific subgroups

7.1. Early-stage gastric cancer with liver metastasis

Early-onset gastric cancer is generally defined as occurring at age 50 or younger. Zhang et al. [4] used SEER data and showed that early-onset patients had a higher risk of liver metastasis and multiple organ involvement than older patients. Wang et al. [5] conducted a large-scale, multi-population retrospective study that also confirmed a higher incidence of liver metastasis in early-onset gastric cancer. Furthermore, early-onset gastric cancer patients with liver metastasis had a poorer prognosis compared to those with late-onset disease. This highlights the importance of regular screening and follow-up for liver metastasis in young gastric cancer patients. Wu et al. [6] also found similar results, indicating that the distribution of pathological subtypes differs in early-onset gastric cancer, with a higher proportion of disseminated and infiltrative subtypes, which are more prone to hematogenous spread to the liver.

7.2. Metastatic liver cancer originating from gastric carcinoid tumors

Previous clinical observations suggested that gastric neuroendocrine tumors (NETs) primarily metastasize to the peritoneum. However, SEER data analysis confirmed that gastric NETs also carry a risk of liver metastasis. Huang et al. [7] developed a survival prognostic index for gastric NETs with liver metastasis, demonstrating significantly poorer survival outcomes for patients with gastric NETs and liver metastasis compared to those without. Huang et al. [8] established a personalized prediction tool for metastatic gastric NETs, highlighting significant differences in prognosis among different metastatic sites. Even in patients with liver metastasis, there was considerable heterogeneity in survival outcomes, necessitating individualized treatment decisions. Ji et al. [26] analyzed the impact of surgical resection combined with chemotherapy on survival in different metastatic sites for gastric NETs. They found that only a small subset of patients with gastric NETs and liver metastasis benefited from the combined approach, with most patients opting for

systemic therapy.

7.3. Primary tumor site – Gastric cancer, metastasis to the liver

Wang et al. [12] found in a nationwide, single-center study that gastric cancer with metastasis to the liver at the pylorus and gastroesophageal junction has a higher risk compared to gastric cancer at the distal end of the stomach. Tumors at the distal end tend to metastasize via the peritoneum, while those at the proximal end are more likely to spread through the bloodstream. This anatomical characteristic is significant for pre-operative and post-operative imaging selection. Proximal gastric cancers require more attention to liver imaging screening and vigilance regarding metastasis. In a study by Ming et al. [13], patients with diffuse gastric cancer are more likely to experience metastasis to the peritoneum, while those with diffuse tumors are more prone to metastasis via the bloodstream. The histological type and tumor location jointly determine the preferred site of metastasis in gastric cancer.

8. Limitations of research on SEER databases

The SEER database is a cancer registry for the US population, providing a valuable large-sample resource for research on gastric cancer metastasis to the liver. However, the database itself has several inherent limitations, and conclusions drawn from research based on SEER data on gastric cancer metastasis to the liver should be interpreted with careful consideration of its potential biases.

Firstly, differences in population and ethnicity. The SEER data primarily reflects the epidemiology of gastric cancer in North America. There are significant differences in the causes of gastric cancer, the subtypes of tumors, screening strategies, clinical treatment patterns, and follow-up systems in North America compared to the Chinese population. Therefore, regression and machine learning models trained on SEER data cannot be directly applied to Chinese patients and must undergo multicenter external validation before implementation.

Second, key clinical and pathological information is lacking. SEER does not include biomarkers such as HER2 and MSI, so the impact of molecular subtypes on the development and prognosis of gastric cancer liver metastasis cannot be analyzed. It also lacks important pathological indicators such as vascular and nerve involvement, as well as tumor recurrence data. Specific drug regimens and durations for chemotherapy, targeted therapy, and immunotherapy are not fully documented, making it difficult to assess how different systemic treatments affect prognosis. This can bias risk factor identification.

Third, recurrence timing information is incomplete. Some studies cannot distinguish synchronous liver metastasis from postoperative delayed liver metastasis, and recurrence times are not recorded. Many studies pooled all liver metastases from gastric cancer, making it difficult to separate initial liver metastasis from postoperative recurrence. In addition, the database lacks a standardized coding system for retroperitoneal metastasis, leading to registration errors in some cases involving both liver and retroperitoneal metastasis and interfering with statistical results for multi-organ metastasis.

Fourth, the database is retrospective so that it can reveal associations but not causality. Although SEER studies use methods such as propensity score matching and multivariate regression to adjust for confounders, selection bias cannot be completely eliminated. For example, patients who undergo surgery may have better overall health and lower tumor burden, which cannot be fully ruled out and introduces baseline differences. Therefore, conclusions about surgical benefits from SEER data are real-world observational findings and

cannot replace randomized controlled trials.

Fifth, the study lacks key clinical information such as performance status scores and comorbidities, which are important for treatment and survival. Moreover, some confounding variables could not be included.

9. Conclusion

A large retrospective study of SEER data showed that liver metastasis is the most common form of distant metastasis in gastric cancer, with substantial population heterogeneity. Age, TNM staging, tumor differentiation, tumor size, primary tumor location, and histological subtype were important independent risk factors for gastric cancer liver metastasis.

Patients with gastric cancer that has metastasized to the liver generally have a poor prognosis. However, there is significant variation in survival rates depending on the specific circumstances. Patients with liver metastasis alone have a better prognosis than those with liver metastasis combined with multiple organ involvement. Age, lymph node status, tumor differentiation, presence of other metastases, and treatment approach all contribute to survival. Surgical intervention for liver metastasis in gastric cancer is highly dependent on patient selection and is only recommended for patients with low tumor burden and single-organ liver metastasis. Blind palliative surgery is not recommended for patients with widespread multi-organ metastasis. Currently, several decision diagrams and machine learning models based on SEER have been developed to predict liver metastasis risk and assess survival prognosis. These tools address the limitations of traditional TNM staging in stratifying liver metastasis patients.

It is also important to acknowledge the inherent limitations of SEER, including racial disparities, missing key pathology and treatment information, and potential biases in retrospective observations. All predictive models based on SEER data require validation in multiple geographically diverse centers in China. Future work should integrate multicenter Chinese cohorts and molecular data to improve model transferability and clinical utility.

Funding

Suqian Sci & Tech Program (Project No.: KY202203); Key Program Fund of Jiangsu Provincial Health Commission (Project No.: ZD2022052); Zhenjiang Social Development Fund (Project No.: SH2024002)

Disclosure statement

The authors declare no conflict of interest.

References

[1] Horn SR, Stoltzfus KC, Lehrer EJ, et al., 2020, Epidemiology of Liver Metastases. Cancer Epidemiol, 67: 101760.

[2] Qiu MZ, Shi SM, Chen ZH, et al., 2018, Frequency and Clinicopathological Features of Metastasis to Liver, Lung, Bone, and Brain from Gastric Cancer: A SEER-Based Study. Cancer Med, 7(8): 3662–3672.

[3] Zhang X, Lei K, Zhang T, et al., 2026, Incidence Trends and Surgical Outcomes of Synchronous Liver Metastasis Across Cancer Types: A Population-Based Cohort Study. Int J Surg, 112(1): 1308–1317.

[4] Zhang H, Cheng X, Guo W, et al., 2024, Metastasis Patterns and Prognosis in Young Gastric Cancer Patients: A Propensity Score-Matched SEER Database Analysis. PLoS One, 19(4): e0301834.

[5] Wang Y, Yin K, Liu D, et al., 2025, Prognosis and Distant Metastasis Patterns of Early-Onset Gastric Cancer Compared with Late-Onset: A Large-Scale, Cross-Population Retrospective Study. J Gastrointest Surg, 29(9): 102148.

[6] Wu F, Wu S, Shuai S, 2024, Distinct Characteristics of Distant Metastasis in Early-Onset Gastric Cancer Patients Compared to Late-Onset Patients: An Observational Study. Medicine (Baltimore), 103(20): e38098.

[7] Huang T, Zhuang H, Dai S, et al., 2024, Nomogram Predicting Survival of Patients with Liver Metastasis from Gastric Signet Ring-Cell Carcinoma: A SEER-Based Population Study. Asian J Surg, 47(3): 1669–1672.

[8] Huang D, Li X, Huang Y, et al., 2025, Individualized Prediction Tool for Patients with Metastatic Gastric Signet Cell Carcinoma. Sci Rep, 15(1): 33163.

[9] An W, Bao L, Wang C, et al., 2023, Analysis of Related Risk Factors and Prognostic Factors of Gastric Cancer with Liver Metastasis: A SEER and External Validation Based Study. Int J Gen Med, 16: 5969–5978.

[10] Song P, Chen Z, Tian W, et al., 2026, Developing and Interpreting a Machine Learning Model for Identifying Liver Metastasis in Gastric Cancer. Cancer Control, 33: 10732748261454462.

[11] Li B, Yu J, Zhang Y, et al., 2026, Development and Validation of a Nomogram to Predict Liver Metastases in Patients with Gastric Cancer. Indian J Surg Oncol, 17(6): 1446–1457.

[12] Wang L, Liang B, Jiang Y, et al., 2022, Subsite-Specific Metastatic Organotropism and Risk in Gastric Cancer: A Population-Based Cohort Study of the US SEER Database and a Chinese Single-Institutional Registry. Cancer Med, 12(19): 19595–19606.

[13] Ming Y, Shang A, Zhou Y, et al., 2026, Distinct Metastatic Patterns and Survival Outcomes in Intestinal- versus Diffuse-Type Gastric Cancer: A SEER-Based Propensity Score-Matched Analysis. J Gastrointest Oncol, 17(4): 222.

[14] Lin Z, Wang R, Zhou Y, et al., 2022, Prediction of Distant Metastasis and Survival Prediction of Gastric Cancer Patients with Metastasis to the Liver, Lung, Bone, and Brain: Research Based on the SEER Database. Ann Transl Med, 10(1): 16.

[15] Zhao QW, Quan Z, Liu SS, et al., 2024, Heterogeneity and Prognosis of Single Organ Metastases in Gastric Cancer. Transl Gastroenterol Hepatol, 9: 61.

[16] Meng N, Niu X, Wu J, et al., 2024, Development and Validation of Nomogram Models for Predicting Overall Survival and Cancer-Specific Survival in Gastric Cancer Patients with Liver Metastases: A Cohort Study Based on the SEER Database. Am J Cancer Res, 14(5): 2272–2286.

[17] Dong Z, Zhang Y, Geng H, et al., 2022, Development and Validation of Two Nomograms for Predicting Overall Survival and Cancer-Specific Survival in Gastric Cancer Patients with Liver Metastases: A Retrospective Cohort Study from SEER Database. Transl Oncol, 24: 101480.

[18] Wu Y, Guo Y, Luo W, 2024, Prediction of All-Cause Death and Specific Causes of Death in Patients with Gastric Cancer with Liver Metastasis: A Surveillance, Epidemiology, and End Results-Based Study. J Gastrointest Surg, 28(6): 880–888.

[19] Liu G, Gu J, Wang J, et al., 2025, Prognostic Implications of Organ-Specific Metastases in Advanced Gastric Cancer: A Retrospective Observational Analysis of the SEER Database. Medicine (Baltimore), 104(44): e45570.

[20] Wu J, Yu J, Chen Z, et al., 2022, Survival Benefit of Primary Tumor Resection for Gastric Cancer with Liver Metastasis: A Propensity Score-Matched, Population-Based Study. Front Oncol, 12: 1039086.

[21] Ren B, Yang Y, Lv Y, et al., 2023, Survival Benefits of Palliative Gastrectomy for Gastric Cancer Patients with Liver Metastasis: A Population-Based Propensity Score-Matched Cohort Analysis. Front Oncol, 13: 1309699.

[22] Su R, Sun X, Chen S, et al., 2024, Development and Validation of a Nomogram to Predict the Survival and Estimate Surgical Benefits for Gastric Cancer with Liver Metastasis Receiving Primary Tumor Resection. Front Oncol, 14: 1418548.

[23] Ji NN, Wu XW, Cao Q, et al., 2024, Influence of Cancer-Directed Surgery on the Prognosis of Liver Metastases from Gastric Cancer. Clin Transl Oncol, 26(3): 756–764.

[24] Wang Z, Jia X, Yang Y, et al., 2024, Machine Learning-Based Dynamic Predictive Models for Prognosis and Treatment Decisions in Patients with Liver Metastases from Gastric Cancer. Am J Cancer Res, 14(11): 5521–5538.

[25] Li Y, Xie D, Chen X, et al., 2020, Prognostic Value of the Site of Distant Metastasis and Surgical Interventions in Metastatic Gastric Cancer: A Population-Based Study. Technol Cancer Res Treat, 19: 1533033820964131.

[26] Ji J, Zhang X, Yuan S, et al., 2024, Survival Impact of Gastrectomy and Chemotherapy on Gastric Signet Ring-Cell Carcinoma with Different Metastatic Lesions: A Population-Based Study. Asian J Surg, 47(4): 1769–1775.

Publisher's note

Bio-Byword Scientific Publishing remains neutral with regard to jurisdictional claims in published maps and institutional affiliations.

Oncology Treatment Discovery, 2026, Volume 4, Issue 3
https://bbwpublisher.com/journal/OTD
Online ISSN: 2981-8079
Print ISSN: 3083-4996

Study on the Application Value of Teleradiology in Primary-Level Imaging Services Under the Medical Alliance Model

Chungeng Tang[1], Xingxiong Zou[1], Jie Zhang[1], Menghong Zou[1], Ruohan Feng[1], Tao Li[2], Kang Zhou[3], Hui Li[3], Chunlei Jia[3], Hongwei Li[1*]

[1]Department of Radiology, Mianyang Third People's Hospital, Sichuan Mental Health Center, Mianyang 621000, Sichuan, China

[2]Department of Radiology, Mianyang Youxian District People's Hospital, Mianyang 621000, Sichuan, China
[3]Internet Hospital, Mianyang Third People's Hospital, Sichuan Mental Health Center, Mianyang 621000, Sichuan, China

***Corresponding author*:** Hongwei Li, lhw6321@163.com

Copyright: © 2026 Author(s). This is an open-access article distributed under the terms of the Creative Commons Attribution License (CC BY 4.0), permitting distribution and reproduction in any medium, provided the original work is cited.

Abstract: *Background*: Primary health care (PHC) is a fundamental component of achieving universal health coverage (UHC). However, in many resource-limited settings, primary health care institutions still face problems such as underutilization of medical imaging equipment, a shortage of professional imaging personnel, and insufficient patient recognition of the diagnostic and therapeutic capacity of primary care. As a result, there is a clear mismatch between the diagnostic service capacity of primary care and residents' medical needs. The uneven allocation of imaging resources further limits the functioning of the primary health system. Therefore, it is of great significance to explore sustainable models that rely on digital technology to enhance primary-level imaging service capacity, optimize the allocation of medical resources, and strengthen trust in primary care. *Methods*: This study conducted a cross-sectional empirical study based on a multi-stakeholder survey in southwestern China from January 2025 to January 2026. The study covered 59 primary health care institutions and obtained 118 valid questionnaires, including primary health care institution administrators (n=55) and primary care clinicians (n=63). Imaging quality control indicators were also incorporated for comprehensive evaluation. Guided by health service supply-demand theory and medical trust theory, the study constructed an analytical framework of "improving service supply—enhancing diagnostic and therapeutic quality—reshaping trust relationships" to systematically evaluate the impact of teleradiology implementation on primary-level imaging service capacity and medical quality. *Results*: The survey showed that the shortage of imaging professionals in primary health care institutions was prominent. Among primary health care institution administrators, 85.5% (47/55) reported a shortage of radiology professionals. Primary care physicians were highly dependent on imaging examinations to assist diagnosis and treatment. The proportion of imaging examination needs for common diseases reached 84.1%–98.4% (acute abdomen 93.7%, pneumonia and pneumothorax 96.8%, fracture 98.4%, stroke 98.4%, myocardial infarction 84.1%). However, only 4.8% (3/63) of primary care physicians believed that primary care institutions had strong independent imaging diagnostic capacity. After the application of teleradiology, the imaging

diagnostic concordance rate increased from 58.3% to 91.7%, and the missed diagnosis rate decreased from 12.4% to 2.1%. In addition, 96.4% (53/55) of primary care administrators reported that teleradiology promoted an increase in the number of patient visits, and 92.9% (59/63) of primary care physicians recognized the quality of remote imaging reports. *Conclusion*: Teleradiology helps alleviate the shortage of primary-level imaging resources and promotes the improvement of primary-level imaging service capacity by enhancing diagnostic support capacity, optimizing service supply, and strengthening medical trust. Based on empirical data from southwestern China, this study provides a reference for digital technology empowering the development of the primary health system and optimizing the allocation of imaging resources.

Keywords: Teleradiology; Primary care; Health system; Medical trust; Health equity; Universal health coverage

Online publication: October 20, 2026

1. Introduction

Primary health care (PHC) is an important foundation for achieving universal health coverage (UHC), but primary health care systems have long faced challenges such as a shortage of professionals, limited service capacity, and insufficient trust among residents [1-3]. China's primary health care also has an obvious imbalance between supply and demand. With population aging and the increasing burden of chronic diseases, the demand for primary health care services continues to grow, while the allocation of high-level professional and technical personnel is insufficient. In 2024, only 39.9% of practicing (assistant) physicians in township health centers had a bachelor's degree or above, lower than the 64.0% in urban community health service centers [4]. At the same time, medical imaging data are growing rapidly, while the growth rate of radiology professionals has lagged relatively behind, making the insufficient imaging diagnostic capacity at the primary level increasingly prominent [5,6]. Although China has continued to promote primary-level talent training and policies to channel medical resources to the primary level in recent years, the insufficient supply of high-level imaging services at the primary level has not been fundamentally improved.

Medical imaging is an important support for disease screening, diagnosis, and treatment decisions, and is also an important component of achieving universal health coverage. In 2025, the 78th World Health Assembly adopted resolution WHA78.13, incorporating medical imaging services into areas related to universal health coverage. Studies have shown that low- and middle-income countries generally face insufficient imaging equipment, professionals, and service accessibility, which limits the improvement of disease diagnosis and treatment capacity at the primary level [7-8]. For primary health care institutions, the quality of imaging reports not only affects clinical decisions but also affects patients' recognition of primary health care services.

From the perspective of health service supply-demand theory, medical imaging services are highly professionally dependent and resource-constrained, and primary-level areas are prone to forming a structural contradiction of "increased medical demand—insufficient professional supply." International studies have found that India, Germany, Australia, and other countries all have problems with uneven urban-rural distribution of radiologists, and insufficient spatial allocation of imaging resources has become a common challenge for the development of primary health systems [9-11]. At the same time, medical trust theory holds that the trust of patients and medical personnel in medical service capacity is an important factor affecting the utilization of medical resources. Insufficient primary-level imaging diagnostic capacity may reduce the

trust of primary care physicians and patients in primary health care services, further concentrating medical demand in higher-level hospitals and exacerbating regional imbalances in medical resources [12-13].

Teleradiology, relying on digital image transmission and remote diagnostic technology, provides a new service model for alleviating the shortage of primary-level imaging resources. Previous studies have shown that teleradiology can improve the accessibility of imaging services, improve diagnostic efficiency, and promote the extension of high-quality imaging resources to the primary level [10,14-16]. However, current related research mainly focuses on remote diagnostic accuracy and technical application effects, and research on how it improves the supply-demand relationship of primary-level imaging services and promotes the construction of medical trust is still relatively insufficient.

Therefore, based on health service supply-demand theory and medical trust theory, and relying on survey data from 59 primary health care institutions in southwestern China, this study systematically analyzes the current application status of teleradiology in primary care and its impact on imaging service capacity, diagnostic and therapeutic quality, and trust relationships, providing empirical evidence for optimizing the allocation of primary-level imaging resources and improving remote medical service models.

2. Materials and methods

2.1. Study subjects

This study used a cross-sectional survey design and was conducted in southwestern China from January 2025 to January 2026. A total of 59 primary health care institutions that had established medical alliance cooperation relationships with our hospital were selected as the study subjects, including 46 township health centers and village clinics, and 13 district/county-level medical institutions and community health service centers. All included institutions had basic imaging examination conditions, but due to limitations in imaging professionals and diagnostic capacity, some examinations required remote support from higher-level medical institutions.

The survey respondents included primary health care institution administrators and primary care clinicians. This study was approved by the medical ethics committee (approval number 2024-MSY-EC-2024013), and all survey respondents provided informed consent.

2.2. Teleradiology service model

A teleradiology collaboration platform was established relying on the medical imaging center of our hospital, and the PACS system was used to enable the upload of primary-level imaging data, remote diagnosis, and report feedback. After receiving standardized training, primary-level imaging staff completed image acquisition. Radiologists in our hospital's Department of Radiology made remote diagnoses based on imaging data and clinical information, and conducted remote consultations for difficult cases.

2.3. Survey content and data collection

A questionnaire was designed based on health service supply-demand theory and medical trust theory. Primary health care institution administrators were mainly surveyed regarding imaging resource allocation, shortage of radiology professionals, and the impact of teleradiology on medical quality, number of patient visits, and medical alliance collaboration. Primary care physicians mainly evaluated the degree of dependence on imaging examinations for common diseases, primary-level imaging diagnostic capacity, and the supportive role of remote imaging in clinical diagnosis and treatment.

2.4. Statistical analysis

Descriptive statistical methods were used to analyze the survey results, and categorical variables were expressed as frequencies and percentages. Based on the theoretical framework of supply-demand matching and trust construction, a comprehensive analysis was conducted on the status of primary-level imaging resources, clinical imaging demand, and the application value of teleradiology.

3. Results

3.1. Current status of primary-level imaging resource allocation and supply capacity

A total of 55 primary health care institution administrators and 63 primary care physicians were ultimately included in the analysis. The shortage of imaging professionals in primary health care institutions was prominent. The survey of primary health care institution administrators showed that among 55 administrators, 47 (85.5%) believed that their institution had a shortage of radiology diagnostic personnel, while only 8 (14.5%) believed that this problem did not exist. Regarding the evaluation of the application value of teleradiology, 41 (74.5%) administrators believed that teleradiology could alleviate the shortage of primary-level imaging personnel, 44 (80.0%) believed that it helped improve medical quality, 53 (96.4%) believed that teleradiology could promote an increase in the number of patient visits, and 50 (90.9%) believed that it could strengthen clinical collaboration among medical alliance member institutions (see **Table 1**, **Figure 1**).

Table 1. Current status of imaging service supply in primary health care institutions and administrators' evaluation of the value of teleradiology

Imaging resource/attitude	Yes	Neutral	No
Whether there is a shortage of radiology diagnostic personnel	47	0	8
Whether remote imaging solves personnel shortage	41	13	1
Whether remote imaging improves medical quality	44	10	1
Whether remote imaging increases the number of patient visits	53	0	2
Whether remote imaging strengthens clinical cooperation among medical alliance member institutions	50	3	2

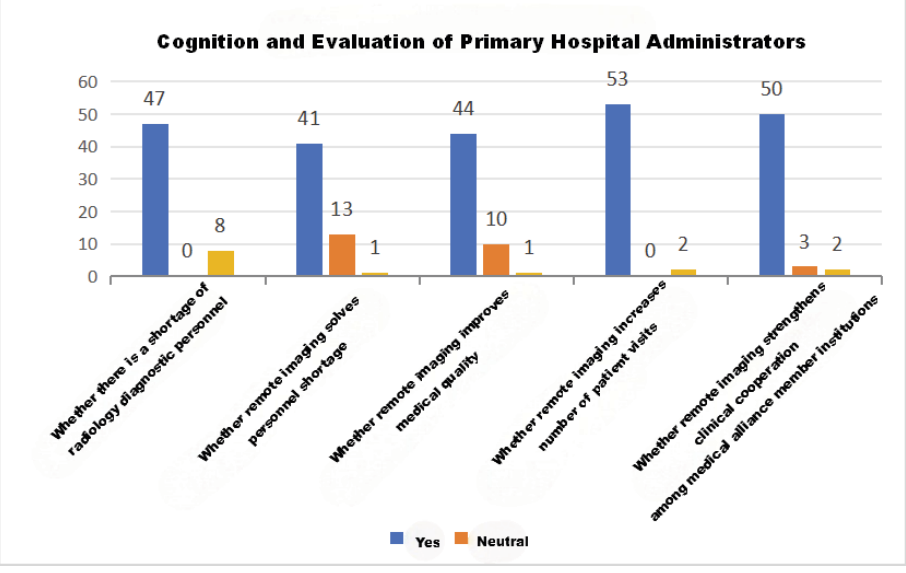

Figure 1. Primary health care institution administrators' cognitive evaluation of the current status of imaging services and the value of teleradiology.

3.2. Degree of dependence of primary-level clinical diagnosis and treatment on imaging services

The survey of primary care physicians showed that imaging examinations had become an important auxiliary tool for the diagnosis and treatment of common diseases at the primary level. For common diseases such as acute abdomen, pneumonia and pneumothorax, fracture, stroke, and myocardial infarction, primary care physicians had a high degree of dependence on imaging examinations.

Among them, the degree of imaging dependence was highest for fracture and stroke, both 62/63 (98.4%); pneumonia and pneumothorax were 61/63 (96.8%); acute abdomen was 59/63 (93.7%); and myocardial infarction was 53/63 (84.1%). The results suggest a clear mismatch between primary-level clinical diagnostic and treatment needs and imaging service capacity (see **Table 2**, **Figure 2**).

Table 2. Characteristics of primary-level clinical imaging demand and physicians' evaluation of the diagnostic and therapeutic support role of teleradiology

Common disease/degree of imaging dependence	High dependence	Moderate dependence	Low dependence
Acute abdomen	59	4	0
Pneumonia and pneumothorax	61	2	0
Fracture	62	1	0
Stroke	62	1	0
Myocardial infarction	53	6	4
Ability of primary hospital radiology department to solve problems	3	42	18
Ability of remote imaging to solve problems	56	6	1
Degree of help of remote imaging to patients	60	3	0

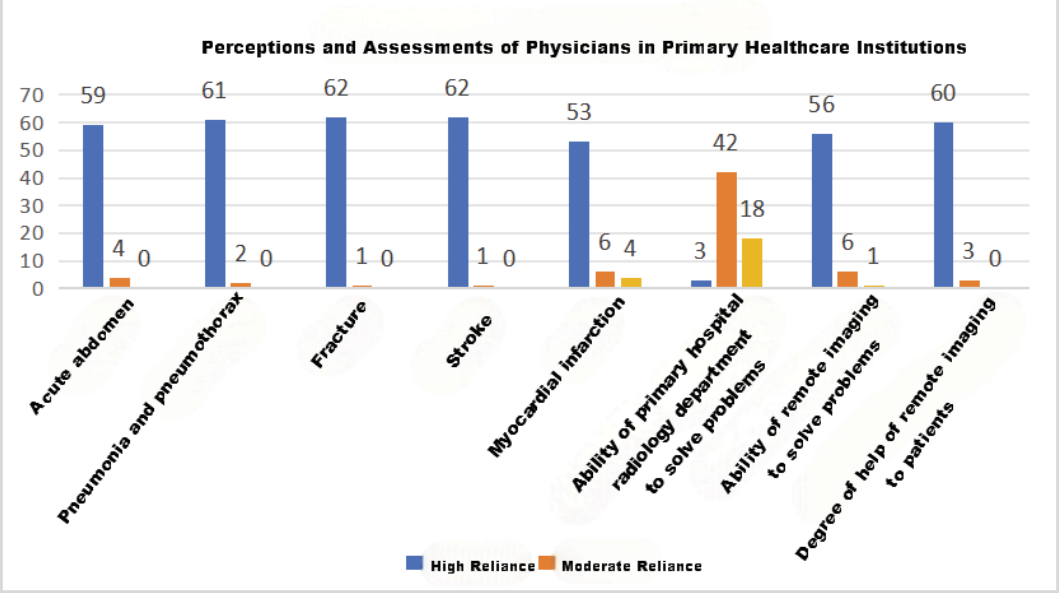

Figure 2. Primary care physicians' dependence on imaging service needs and evaluation of the diagnostic and therapeutic support role of teleradiology.

3.3. Impact of teleradiology on primary-level diagnostic and therapeutic support capacity

The evaluation of primary-level imaging diagnostic capacity by primary care physicians showed that only 3 physicians (4.8%) believed that primary health care institutions had strong independent problem-solving capacity for imaging diagnosis, 42 (66.7%) considered it to be at a moderate level, and 18 (28.6%) considered it to be low. In contrast, 56 primary care physicians (88.9%) believed that teleradiology could improve the problem-solving capacity for disease diagnosis at the primary level, and only 1 (1.6%) believed that the degree of help was low. At the same time, 60 physicians (95.2%) believed that remote imaging services could provide considerable help for patient diagnosis and treatment, suggesting that teleradiology plays a positive role in improving the accessibility of primary-level imaging services and clinical support capacity (**Table 2**).

3.4. Teleradiology promotes supply-demand matching of primary-level imaging services

Combining the survey results of primary care administrators and physicians, it was found that primary health care institutions generally had a mismatch between insufficient imaging professional resources and relatively high clinical diagnostic and treatment demand. On the one hand, the shortage of primary-level imaging professionals limited independent diagnostic capacity; on the other hand, primary care physicians had a high dependence on imaging examinations.

By connecting primary-level examination resources with the imaging diagnostic capacity of higher-level medical institutions, teleradiology compensated to a certain extent for the insufficient supply of primary-level imaging, improved the diagnostic and therapeutic support capacity of primary health care institutions for common and complex diseases, and realized the transformation of imaging resources from centralized allocation to regional collaborative utilization.

3.5. Impact of teleradiology on imaging diagnostic quality

After the implementation of teleradiology, the imaging diagnostic concordance rate increased from 58.3% to 91.7%, and the missed diagnosis rate decreased from 12.4% to 2.1%, suggesting that the remote imaging support model can improve the quality of primary-level imaging diagnosis and enhance diagnostic and therapeutic safety.

4. Discussion

4.1. Teleradiology alleviates the shortage of primary-level imaging resources and optimizes supply-demand matching of imaging services

This study found that the shortage of imaging professionals in primary health care institutions was prominent; 85.5% of primary care administrators believed that their institution had a shortage of radiology professionals. At the same time, primary care physicians had a high demand for imaging examinations, with the dependence rate on imaging examinations for common diseases reaching 84.1%–98.4%, suggesting an obvious supply-demand imbalance in primary-level imaging services. On the one hand, with population aging and the increasing burden of chronic diseases, the demand of primary health care institutions for imaging examinations and diagnostic support continues to grow; on the other hand, the long training cycle and uneven regional distribution of imaging professionals make it difficult for primary-level institutions to meet the growing demand for imaging diagnosis independently.

From the perspective of health service supply-demand theory, medical imaging services are highly

specialized and resource-dependent, and their supply capacity is limited by factors such as the number of imaging physicians, professional experience, and equipment conditions. Under the traditional model, high-quality imaging resources are mainly concentrated in large medical institutions. Although primary-level institutions have imaging examination conditions, their diagnostic capacity is insufficient, forming a structural contradiction of "examinations at the primary level, diagnosis at a higher level."

Teleradiology connects primary-level imaging acquisition sites with the diagnostic resources of higher-level hospitals through information technology, enabling imaging professional capacity to break through geographical limitations and realize a transformation from "centralized allocation of experts" to "sharing of diagnostic capacity." This study shows that most primary care administrators believed that teleradiology could alleviate the shortage of professionals and promote the improvement of medical quality, suggesting that this model has positive value in improving the allocation of primary-level imaging resources and enhancing supply-demand matching efficiency [17,18].

4.2. Teleradiology enhances primary-level imaging diagnostic and therapeutic capacity and promotes improvement of medical quality

Imaging diagnostic capacity is an important foundation for primary health care institutions to carry out standardized diagnosis and treatment. This study found that only 4.8% of primary care physicians believed that primary-level institutions had strong independent imaging diagnostic capacity, while 88.9% of physicians believed that remote imaging could improve the problem-solving capacity for disease diagnosis and treatment at the primary level, and 95.2% of physicians believed that remote imaging could provide help for patient diagnosis and treatment, indicating that teleradiology effectively compensated for the insufficient imaging diagnostic capacity at the primary level.

Previous studies have shown that teleradiology can improve the accessibility and diagnostic efficiency of primary-level imaging services through standardized image transmission, remote expert diagnosis, and quality control systems. In recent years, studies in resource-limited areas such as India have also shown that teleradiology combined with digital imaging technology can improve imaging service coverage in rural areas and alleviate the shortage of radiology professionals [19].

This study further found that after the application of teleradiology, the imaging diagnostic concordance rate increased from 58.3% to 91.7%, and the missed diagnosis rate decreased from 12.4% to 2.1%, suggesting that the remote imaging support model not only improves service coverage but may also improve the quality of primary-level imaging diagnosis. Its core value is not to replace primary care medical personnel, but to improve disease identification and clinical decision-making capacity at the primary level through a collaborative model of "primary-level examination capacity + remote diagnostic support."

4.3. Teleradiology promotes the construction of trust in primary care through capacity empowerment

The utilization of primary health care services depends not only on resource accessibility but is also affected by the degree of trust of patients and medical personnel in primary-level diagnostic and therapeutic capacity. From the perspective of medical trust theory, this study found that insufficient primary-level imaging diagnostic capacity may weaken primary care physicians' recognition of imaging results and affect patients' choice of primary health care services.

By introducing professional imaging support from higher-level hospitals, teleradiology improves primary care physicians' recognition of diagnostic results. This study shows that 92.9% of primary care physicians recognized the quality of remote imaging reports, suggesting that teleradiology can enhance the professional trust of primary care physicians. At the same time, 96.4% of primary care administrators believed that teleradiology could increase the number of patient visits, indicating that improved service capacity may further enhance patients' trust in primary health care institutions.

Therefore, the mechanism of teleradiology is not only reflected in image transmission and diagnostic support at the technical level, but more importantly, by improving the professional capacity of primary care, it promotes a virtuous cycle of "capacity improvement—trust enhancement—increased service utilization."

4.4. Teleradiology promotes the coordinated development of the primary health system and has value for promotion

This study shows that 90.9% of primary care administrators believed that teleradiology could strengthen medical alliance collaboration, suggesting that teleradiology is not only an imaging technology service but has also become an important tool for promoting the coordination of regional medical resources.

Insufficient medical imaging resources are a common challenge faced by primary health systems worldwide, especially in resource-limited areas, where insufficient imaging equipment and professionals limit primary-level disease diagnostic capacity. Related studies have pointed out that establishing regional imaging centers, strengthening the application of information technology, and developing remote imaging services are important strategies for improving imaging accessibility [20-23].

For China, teleradiology can serve as an important path to promote the channeling of high-quality medical resources to the primary level. Combined with medical alliance construction, regional imaging center construction, and artificial intelligence-assisted diagnosis, it can form a collaborative service model of "primary-level examination, regional diagnosis, and unified quality management." However, its long-term development still requires further improvement of supporting policies such as quality control, data security, responsibility determination, and payment mechanisms.

4.5. Study limitations and prospects

This study still has certain limitations. First, this study used a cross-sectional survey design, mainly evaluating the current application status of teleradiology and related influencing factors, and cannot fully infer causality. Second, the study subjects came from primary health care institutions in southwestern China, and the generalizability of the results to other regions still needs further verification in combination with local medical resource conditions. Third, this study was mainly based on evaluations by primary care administrators and physicians. Future research can further incorporate indicators such as patients' long-term medical-seeking behavior, medical costs, and health outcomes, and conduct multicenter, longitudinal follow-up studies. In the future, artificial intelligence-assisted diagnosis, regional imaging center construction, and health economics evaluation can be combined to further explore the long-term value of teleradiology in the primary health system.

5. Conclusion

Teleradiology serves as a means to address the scarcity of imaging resources at the primary care level. It

contributes to strengthening primary-level imaging service capacity through several channels: boosting diagnostic support capabilities, improving service delivery, and fostering greater medical trust. Drawing on empirical evidence from southwestern China, this study offers insights into how digital technologies can empower the development of the primary health system and improve the distribution of imaging resources.

Funding

Project of Sichuan Provincial Primary Health Care Development Research Center (Project No.: SWFZ22-C-64)

Disclosure statement

The authors declare no conflict of interest.

References

[1] de Claro V, Lava JB, Bondoc C, et al., 2024, The Role of Local Health Officers in Advancing Public Health and Primary Care Integration: Lessons From the Ongoing Universal Health Coverage Reforms in the Philippines. BMJ Global Health, 9(1): e014118.

[2] Li X, Krumholz HM, Yip W, et al., 2020, Quality of Primary Health Care in China: Challenges and Recommendations. The Lancet, 395(10239): 1802–1812.

[3] Edelman A, Marten R, Dhillon I, et al., 2025, Primary Health Care in the Context of the COVID-19 Pandemic in 10 South-East Asian Countries: A Cross-Case Synthesis With Lessons for Future Health Systems Strengthening. BMJ Global Health, 10(Suppl 2): e018076.

[4] Department of Primary Health Care, National Health Commission of the People's Republic of China, 2025, Transcript of the Press Conference on the Development of National Primary Health Care Services, visited on April 6, 2026, http://www.nhc.gov.cn/xcs/c100122/202511/a6e2048c977a41969c695f058bfc1286.shtml.

[5] Yan W, Gao X, Wang W, et al., 2025, What Changes Does Rural Medical Education Need? A Qualitative Study Exploring the Experiences of Rural Grassroots Doctors. BMC Medical Education, 25(1): 1025.

[6] Meng F, Zhan L, Liu S, et al., 2023, The Growing Problem of Radiologist Shortage: China's Perspective. Korean Journal of Radiology, 24(11): 1046–1048.

[7] World Health Organization, 2025, Strengthening Medical Imaging Capacity: WHA78.13. Geneva: World Health Organization, visited on April 6, 2026, https://apps.who.int/gb/ebwha/pdf_files/WHA78/A78_R13-en.pdf.

[8] Hricak H, Abdel-Wahab M, Atun R, et al., 2021, Medical Imaging and Nuclear Medicine: A Lancet Oncology Commission. The Lancet Oncology, 22(4): e136–e172.

[9] Chandramohan A, Krothapalli V, Augustin A, et al., 2023, Teleradiology and Technology Innovations in Radiology: Status in India and Its Role in Increasing Access to Primary Health Care. The Lancet Regional Health – Southeast Asia, 23: 100195.

[10] Reschke P, Gruenewald LD, Koch V, et al., 2025, Radiology Access in Rural Germany: A Nationwide Survey on Outpatient Imaging and Teleradiology. Diagnostics, 15(8): 962.

[11] Jeganathan S, 2023, The Growing Problem of Radiologist Shortages: Australia and New Zealand's Perspective. Korean Journal of Radiology, 24(11): 1043–1045.

[12] Phankitiya S, Luvira V, 2021, Self-Referral to the University Hospital Resulting in Unnecessary Patient Expenses: A Prospective Descriptive Study in a Super-Tertiary Hospital. Indian Journal of Community Medicine, 46(2): 295–299.

[13] Frija G, Salama DH, Kawooya MG, et al., 2023, A Paradigm Shift in Point-of-Care Imaging in Low-Income and Middle-Income Countries. EClinicalMedicine, 62: 102114.

[14] Nigatu AM, Yilma TM, Gezie LD, et al., 2025, Effect of Teleradiology on Patient Waiting Time and Service Satisfaction in Public Hospitals, Northwest Ethiopia: A Quasi-Experimental Study. BMC Health Services Research, 25(1): 603.

[15] Nopour R, 2026, Obstacles and Facilitators of Teleradiology Adoption in Healthcare: A Scoping Review. Digital Health, 12: 20552076261419231.

[16] Chikarmane SA, Thimm E, Plaxco JS, et al., 2026, Remote Diagnostic Breast Imaging: An Implementation Guide. American Journal of Roentgenology, 226(1): e2533537.

[17] Madej M, Sąsiadek MJ, 2023, The Growing Role of Telemedicine: Possibilities and Regulations Concerning Teleradiology in Poland. Polish Journal of Radiology, 88: e535–e545.

[18] Verma N, Buch B, Taralekar R, et al., 2023, Diagnostic Concordance of Telemedicine as Compared With Face-to-Face Care in Primary Health Care Clinics in Rural India: Randomized Crossover Trial. JMIR Formative Research, 7: e42775.

[19] Barry R, Green E, Robson K, et al., 2024, Factors Critical for the Successful Delivery of Telehealth to Rural Populations: A Descriptive Qualitative Study. BMC Health Services Research, 24(1): 908.

[20] Frija G, Blažić I, Frush DP, et al., 2021, How to Improve Access to Medical Imaging in Low- and Middle-Income Countries? eClinicalMedicine, 38: 101034.

[21] Fox MN, Dickson JM, Burch P, et al., 2024, Delivering Relational Continuity of Care in UK General Practice: A Scoping Review. BJGP Open, 8(2): BJGPO.2024.0041.

[22] Sheffel A, Andrews KG, Conner R, et al., 2024, Human Resource Challenges in Health Systems: Evidence From 10 African Countries. Health Policy and Planning, 39(7): 693–709.

[23] Kyei KA, Onajah GN, Daniels J, 2024, The Emergence of Telemedicine in a Low-Middle-Income Country: Challenges and Opportunities. ecancermedicalscience, 18: 1679.

Publisher's note

Bio-Byword Scientific Publishing remains neutral with regard to jurisdictional claims in published maps and institutional affiliations.

Oncology Treatment Discovery, 2026, Volume 4, Issue 3
https://bbwpublisher.com/journal/OTD
Online ISSN: 2981-8079
Print ISSN: 3083-4996

Application of an MMHEM-Based Postoperative Transitional Care Program in Patients After Laryngeal Cancer Surgery

Qingsi Chen, Liqin Lin*

Department of Otolaryngology, The First Affiliated Hospital of Wenzhou Medical University, Wenzhou 325000, Zhejiang, China

Author to whom correspondence should be addressed.

Copyright: © 2026 Author(s). This is an open-access article distributed under the terms of the Creative Commons Attribution License (CC BY 4.0), permitting distribution and reproduction in any medium, provided the original work is cited.

Abstract: *Objective*: To observe the application effect of a postoperative transitional care program based on the Multisensory Multilevel Health Education Model (MMHEM) in patients after laryngeal cancer surgery. *Methods*: A total of 110 patients who underwent laryngeal cancer surgery in our hospital between January 2023 and December 2025 were selected. They were randomly divided into a control group and an observation group by the envelope method, with 55 patients in each group. The control group received a conventional nursing program, while the observation group received an MMHEM-based postoperative transitional care program in addition to the conventional program. Self-care ability (Exercise of Self-Care Agency Scale), swallowing function (M.D. Anderson Dysphagia Inventory, MDADI), and psychological status (Self-Rating Depression Scale and Self-Rating Anxiety Scale) were compared between the two groups. The incidence of home-based adverse events was followed up for 2 months. *Results*: At baseline, there were no statistically significant differences in the indicators between the two groups. After intervention, the total score and all dimension scores of the Exercise of Self-Care Agency Scale in the observation group were higher than those in the control group ($P < 0.05$). The MDADI score in the observation group was higher than that in the control group, while the Self-Rating Depression Scale and Self-Rating Anxiety Scale scores were lower than those in the control group ($P < 0.05$). The total incidence of home-based adverse events in the observation group was lower than that in the control group ($P < 0.05$). *Conclusion*: The MMHEM-based postoperative transitional care program can effectively improve self-care ability and quality of life, relieve negative emotions, and reduce the incidence of home-based adverse events in patients after laryngeal cancer surgery, with positive significance for promoting postoperative rehabilitation.

Keywords: Postoperative laryngeal cancer; Multisensory Multilevel Health Education Model; Transitional care; Postoperative rehabilitation

Online publication: October 20, 2026

1. Introduction

Laryngeal cancer is a relatively common malignant tumor in otorhinolaryngology–head and neck surgery, and surgical resection remains one of the preferred treatments for laryngeal cancer [1]. The postoperative transitional period after laryngeal cancer surgery refers to the stage from hospitalization to home-based rehabilitation. This is a period with a high incidence of complications and profound psychological changes. However, conventional care mostly focuses on airway management and incision care during hospitalization, with insufficient continuity of care after discharge. After discharge, lacking professional guidance, patients are inadequately prepared to cope with delayed complications such as granuloma formation and swallowing aspiration [2]. In addition, negative emotions such as anxiety and depression are highly prevalent in patients after laryngeal cancer surgery, mainly related to social avoidance caused by the inability to communicate verbally after discharge [3]. Conventional care lacks individualized psychological intervention mechanisms and is difficult to help patients rebuild social confidence. Moreover, traditional health education mostly uses oral instruction or written manuals; however, because patients with laryngeal cancer are voiceless after surgery, their communication channels are already limited, and the absorption rate of one-way written education is extremely low. In response to the limitations of conventional care, the Multisensory Multilevel Health Education Model (MMHEM) emphasizes breaking through the limitations of traditional single-text or oral education. It integrates art, culture, and science in the development of health education resources. Through coordinated stimulation of multiple sensory channels, it enhances audience participation, acceptance, and information retention, and is suitable for populations with low health literacy or limited resources. This provides a new approach for improving health education and transitional management in patients after laryngeal cancer surgery [4-5]. At present, systematic evidence for the application of MMHEM in postoperative transitional care after laryngeal cancer surgery is still lacking. Therefore, this study aimed to construct an MMHEM-based postoperative transitional care program and apply it to patients after laryngeal cancer surgery, exploring its impact on postoperative rehabilitation.

2. Materials and methods

2.1. General information

A total of 110 patients who underwent laryngeal cancer surgery in our hospital between January 2023 and December 2025 were selected. They were randomly divided into a control group and an observation group by the envelope method, with 55 patients in each group. In the control group, there were 45 men and 10 women; age range 45–76 years, mean (58.97 ± 6.44) years; surgical procedures: total laryngectomy in 30 cases and subtotal laryngectomy in 25 cases; education level: junior middle school or below in 17 cases, senior high school in 27 cases, and college or above in 11 cases. In the observation group, there were 46 men and 9 women; age range 46–73 years, mean (57.91 ± 5.51) years; surgical procedures: total laryngectomy in 32 cases and subtotal laryngectomy in 23 cases; education level: junior middle school or below in 18 cases, senior high school in 25 cases, and college or above in 12 cases. Comparison of basic data between the two groups showed $P > 0.05$. Patients and their family members were informed of this study and signed informed consent. This study was approved by the hospital ethics committee.

2.1.1. Inclusion criteria

(1) Patients met the surgical indications for laryngeal cancer in the Expert Consensus on Surgical and

Comprehensive Treatment of Laryngeal Cancer [6] and were pathologically diagnosed with laryngeal cancer;

(2) Patients were conscious after surgery and able to cooperate with questionnaire surveys and follow-up;

(3) Expected survival ≥ 6 months.

2.1.2. Exclusion criteria

(1) Patients with other malignant tumors or distant metastasis;

(2) Patients with severe cardiac, hepatic, or renal dysfunction or coagulation disorders;

(3) Patients with a history of mental illness or cognitive impairment who could not cooperate with the study;

(4) Patients with severe postoperative complications requiring prolonged hospitalization.

2.2. Methods

The control group received conventional postoperative nursing for laryngeal cancer: airway humidification, incision and cannula maintenance, oral care, pain and nutrition management, and swallowing and voice training; at discharge, oral and written guidance was provided, patients and family members were taught cannula insertion and removal, disinfection, cannula instillation, and simple disinfection and isolation techniques, and follow-up arrangements were explained; after discharge, the primary nurse conducted telephone follow-up according to departmental regulations, answered questions, and reminded patients to return for review.

The observation group received an MMHEM-based transitional care program in addition to conventional care:

(1) Visual intervention: illustrated health readers were prepared for patients, covering stoma cleaning and cannula management, dietary matching, and functional exercise; concise operation reminder cards were posted at the bedside; a rehabilitation progress display area was arranged in the corridor; postoperative recovery videos were shown continuously; and centralized learning was organized using projected courseware and animations; discharge materials included a checkable daily rehabilitation list.

(2) Auditory intervention: a designated primary nurse provided continuous education from before surgery to after surgery; during ward rounds, audio devices were used to remind patients about humidification, drinking water, and other key points; relatives were asked to read positive messages aloud every day; patients were allowed and encouraged to record their rehabilitation experiences; an audio corner was set up to play rehabilitation experiences of fellow patients; after discharge, voice messages were used for remote tracking and guidance.

(3) Tactile intervention: the swallowing process was demonstrated at the bedside, and patients were asked to imitate it in front of a mirror; neck and shoulder functional exercises were arranged according to tolerance, with daily activities completed step by step; patients were involved in the stoma care process; during inspiratory training, patients held an air bag to increase proprioceptive input; foods requiring chewing were provided for practice; touchable three-dimensional picture books were used to aid cognition; auxiliary tools such as swallowing training sticks and oral motor devices were distributed to enhance operational participation.

(4) Patients were guided to inhale peppermint solution or neroli essential oil to relieve discomfort and activate the olfactory pathway; bland and easily accepted foods were provided; patients were encouraged

to choose previously favored tastes to evoke taste memory and eating pleasure; scent patches or olfactory training cards were used for olfactory stimulation; foods with different temperatures and textures were used to stimulate the tongue surface and enhance taste discrimination.

(5) Psychological status screening was completed simultaneously when the patient sat up for the first time after surgery, providing a reference for subsequent psychological support; peer mutual aid exchanges were carried out; a mood expression box was placed for patients to write or draw to vent emotions; the nurse in charge left an encouraging sentence on the bedside card every day; patients were guided to make wish cards and write down rehabilitation goals and feelings; diaphragmatic breathing and progressive muscle relaxation were trained; and targeted psychological counseling plans were designed jointly with the psychology department for high-risk patients.

(6) Continued follow-up: at discharge, a home care kit was distributed, containing illustrated materials, video courses, and rehabilitation equipment; a patient peer group chat was established, and texts, images, audio, and short videos were sent according to plan; weekly video follow-ups were arranged, with relatives invited to participate; a task checklist was developed, and personalized reminders were pushed according to recovery progress; full-time nurses provided individualized coaching; regular online consultation and mini rehabilitation classes were carried out to enhance patients' sense of active participation.

2.3. Outcome measures

(1) Self-care ability: assessed using the Exercise of Self-Care Agency Scale, which has 4 dimensions and 43 items. Each item is scored on a 5-point Likert scale, with a total score of 0–172; higher scores indicate stronger self-care ability.

(2) Swallowing function: assessed using the M.D. Anderson Dysphagia Inventory (MDADI), which contains 30 items; higher scores indicate better swallowing function.

(3) Psychological status: assessed using the Self-Rating Depression Scale and Self-Rating Anxiety Scale; higher scores indicate more severe anxiety and depression.

(4) Incidence of home-based adverse events: patients were followed up for 2 months, and the occurrence of home-based adverse events was recorded in both groups, including skin infection at the tracheostomy site, airway obstruction, unplanned extubation, and pulmonary infection.

2.4. Statistical methods

SPSS 25.0 software was used. Normally distributed continuous data were expressed as mean ± standard deviation (SD), and independent-samples *t*-tests were used for between-group comparisons. Categorical data were expressed as relative numbers, and the χ^2 test was used for between-group comparisons. $P < 0.05$ was considered statistically significant.

3. Results

3.1. Comparison of self-care ability between the two groups

The Exercise of Self-Care Agency Scale score in the observation group was higher than that in the control group ($P < 0.05$). See **Table 1**.

Table 1. Comparison of self-care ability between the two groups (mean ± SD, scores)

Group	n	Before intervention	After intervention
Observation group	55	91.85 ± 8.67	125.60 ± 10.46
Control group	55	93.71 ± 8.04	114.09 ± 12.20
t		1.163	-5.310
P		0.247	<0.001

3.2. Comparison of swallowing function and psychological status between the two groups

The MDADI score in the observation group was higher than that in the control group, while the Self-Rating Depression Scale and Self-Rating Anxiety Scale scores were lower than those in the control group ($P < 0.05$). See **Table 2**.

Table 2. Comparison of swallowing function and psychological status between the two groups (mean ± SD, scores)

Group	n	MDADI		SDS		SAS	
		Before	After	Before	After	Before	After
Observation group	55	47.67 ± 5.30	71.47 ± 8.93	49.36 ± 6.00	42.53 ± 3.66	51.11 ± 6.60	41.07 ± 4.84
Control group	55	47.05 ± 4.90	62.53 ± 6.01	50.15 ± 5.68	44.73 ± 4.44	52.02 ± 5.12	45.87 ± 3.56
t		-0.636	-6.161	0.702	2.838	0.807	5.927
P		0.526	<0.001	0.484	<0.05	0.421	<0.001

3.3. Comparison of the incidence of home-based adverse events between the two groups

No patients were lost to follow-up during the follow-up period of this study. The total incidence of home-based adverse events in the observation group was lower than that in the control group ($P < 0.05$). See **Table 3**.

Table 3. Comparison of the incidence of home-based adverse events between the two groups [n (%)]

Group	n	Skin infection at tracheostomy site	Airway obstruction	Unplanned extubation	Pulmonary infection	Total incidence
Observation group	55	2 (3.63)	1 (1.82)	1 (1.82)	2 (3.63)	6 (10.9)
Control group	55	4 (7.27)	2 (3.63)	2 (3.63)	3 (5.55)	11 (20.0)
χ^2						4.681
P						0.031

4. Discussion

The anatomical changes caused by laryngeal cancer surgery significantly increase the difficulty of postoperative nursing management. On the one hand, after tracheotomy, the humidification function of the upper respiratory tract is lost, leading to increased risks of thick sputum, sputum crust formation, and pulmonary infection. On the other hand, the loss or alteration of vocal function seriously affects patients' social function, leading to decreased self-identity and causing severe anxiety, depression, and social isolation. Negative emotions not only reduce rehabilitation adherence but are also key independent factors affecting quality of life [7-8]. However, conventional care mostly focuses on acute-phase management in the hospital and

lacks systematic and multidimensional integration, making it difficult to address these complex difficulties. MMHEM uses multimedia audiovisual technology to create an immersive learning experience and activate multiple sensory channels. Compared with traditional single-text or oral education, it is more likely to attract attention, consolidate memory, and promote skill acquisition. Moreover, the intervention design targets not only individuals but also extends to interpersonal relationships, thereby forming an all-round support network [9]. Introducing MMHEM into clinical nursing management, especially for patients with poor adherence, long disease duration, and complex self-management needs, has good clinical application prospects.

The results of this study showed that the total score and all dimension scores of the Exercise of Self-Care Agency Scale in the observation group were higher than those in the control group ($P < 0.05$). Patients after laryngeal cancer surgery face voicelessness and have difficulty learning through verbal feedback, while negative emotions such as anxiety further reduce their willingness to learn and the efficiency of information reception. MMHEM, through multisensory input such as video demonstration (vision), voice guidance or peer demonstration recordings (hearing), and swallowing demonstration (touch), bypasses language communication barriers and directly establishes visual–motor mapping. The results of this study also showed that the quality of life in the observation group was higher than that in the control group. The reason may be that MMHEM uses visual, auditory, tactile, and other sensory inputs, and the integration of consistent multisensory information can improve individual performance, learning, decision-making, and memory, thereby allowing patients to re-establish a sense of control in this process. In addition, by providing rehabilitation experiences of fellow patients, MMHEM offers a "survivor" identity through peer modeling, which helps promote the recovery of patients' social function and social roles, thereby improving quality of life [10]. In this study, the Self-Rating Depression Scale and Self-Rating Anxiety Scale scores in the observation group were lower than those in the control group ($P < 0.05$). Patients after laryngeal cancer surgery need to face expressive deprivation caused by voicelessness, leading to increased anxiety and depression. MMHEM uses a coordinated audiovisual–tactile multisensory system to construct alternative communication and relieve patients' negative emotions. In addition, conventional psychological counseling is difficult to reach the deep fear of "cancer recurrence." MMHEM introduces the experiences of rehabilitation peers and, through empathic identification and role modeling, reshapes patients' cognitive appraisal of illness uncertainty and transforms negative emotions into adaptive coping. Furthermore, the total incidence of home-based adverse events in the observation group was lower than that in the control group. Through multisensory practical transformation, MMHEM converts abstract medical orders into intuitive perceptual–motor memory. At the same time, multisensory integration accelerates the process of skills from unfamiliarity to proficiency, directly reducing airway adverse events caused by operational errors. In addition, relying on digital platforms, MMHEM enables patients to receive continued guidance and real-time consultation outside the hospital through WeChat groups, thereby reducing the occurrence of home-based adverse events. However, this study still has the following limitations: as a single-center study, the sample size is limited, and extrapolation of the results should be done cautiously; secondly, the follow-up time of this study was only 2 months, and the impact of MMHEM on long-term rehabilitation outcomes remains unclear. Future multicenter, large-sample, long-term randomized controlled trials are needed to verify the clinical value of this program further.

5. Conclusion

In summary, the MMHEM-based postoperative transitional care program can improve self-care ability, quality of life, and psychological status in patients after laryngeal cancer surgery and reduce the incidence of

home-based adverse events, providing a reference for transitional management after laryngeal cancer surgery.

Funding

Fund Name: Wenzhou Basic Public Welfare Scientific Research Projects, “Development of a Personalized Predictive Model for the Risk of Pharyngeal Fistula in Patients After Laryngeal Cancer Surgery” (Project No.: Y20220852)

Disclosure statement

The authors declare no conflict of interest.

References

[1] Hoffmann TK, 2021, Total Laryngectomy—Still Cutting-Edge? Cancers (Basel), 13(6): 1405.

[2] Guo A, Nan Y, Zhang A, 2023, Application of a Whole-Process Health Education Program in Home Nursing Safety Management of Patients with Artificial Airway After Laryngeal Cancer Surgery. Guizhou Medical Journal, 47(1): 132–133.

[3] He Y, Tao J, 2021, Effects of Mindfulness-Based Cognitive Therapy on Cancer-Related Fatigue and Emotional Experience in Patients After Laryngeal Cancer Surgery. Journal of Nursing (China), 28(2): 69–72.

[4] Swierad EM, Benson LR, Williams O, 2021, Creating a Scalable Physical Activity Breaks Resource Through the Multisensory Multilevel Health Education Model: H.Y.P.E. The Breaks! Health Promotion Practice, 22(1_suppl): 101S–110S.

[5] Huang C, Cai M, He X, 2017, The Role of Health Education in Ophthalmology Nursing Management. Journal of Traditional Chinese Medicine Management, 25(21): 163–164.

[6] Head and Neck Surgery Group, Editorial Board of the Chinese Journal of Otorhinolaryngology Head and Neck Surgery, Head and Neck Group, Society of Otorhinolaryngology Head and Neck Surgery, Chinese Medical Association, Li X, 2014, Expert Consensus on Surgical and Comprehensive Treatment of Laryngeal Cancer. Chinese Journal of Otorhinolaryngology Head and Neck Surgery, 49(8): 620–626.

[7] Chen Z, Ni X, 2010, Evaluation of the Effects of Individualized Health Education and Collective Health Education. Journal of Nurses Training, 25(9): 828–829.

[8] Yang M, Chen Q, Lou T, 2025, Correlation Analysis Between Postoperative Psychological Resilience and Disability Acceptance, Coping Styles in Patients Undergoing Radical Laryngectomy for Laryngeal Cancer. Journal of Clinical Nursing, 24(6): 17–19.

[9] Li H, Yin M, 2021, Implications of the Multisensory Multilevel Health Education Model for Health Education Programs in China. Chinese Medical Ethics, 34(10): 1342–1346 + 1352.

[10] Wang X, Lian F, Xu F, 2026, Construction of a Transitional Care Program Based on the Multisensory Multilevel Health Education Model for Patients After Laryngeal Cancer Surgery. Pharmaceutical Higher Vocational Education and Modern Nursing, 9(2): 154–158 + 178.

Publisher’s note

Bio-Byword Scientific Publishing remains neutral with regard to jurisdictional claims in published maps and institutional affiliations.

Integrated Services Platform of International Scientific Cooperation

Innoscience Research (Malaysia), which is global market oriented, was founded in 2016.Innoscience Research focuses on services based on scientific research. By cooperating with universities and scientific institutes all over the world, it performs medical researches to benefit human beings and promotes the interdisciplinary and international exchanges among researchers.

Innoscience Research covers biology, chemistry, physics and many other disciplines. It mainly focuses on the improvement of human health. It aims to promote the cooperation, exploration and exchange among researchers from different countries. By establishing platforms, Innoscience integrates the demands from different fields to realize the combination of clinical research and basic research and to accelerate and deepen the international scientific cooperation.

Cooperation Mode



Clinical Workers



In-service Doctors





Foreign Researchers





Hospital



University



Scientific institutions

Our Journals



The *Journal of Architectural Research and Development* is an international peer-reviewed and open access journal which is devoted to establish a bridge between theory and practice in the fields of architectural and design research, urban planning and built environment research.

Topics covered but not limited to:

- Architectural design
- Architectural technology, including new technologies and energy saving technologies
- Architectural practice
- Urban planning
- Impacts of architecture on environment

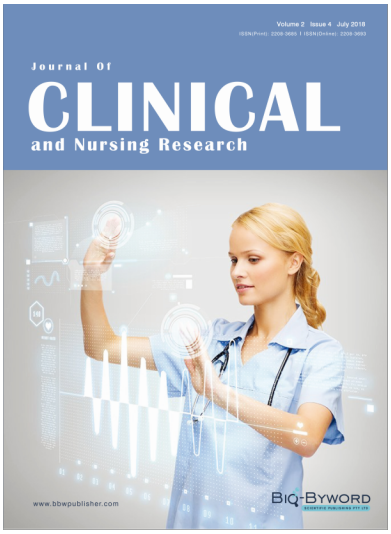

Journal of Clinical and Nursing Research (JCNR) is an international, peer reviewed and open access journal that seeks to promote the development and exchange of knowledge which is directly relevant to all clinical and nursing research and practice. Articles which explore the meaning, prevention, treatment, outcome and impact of a high standard clinical and nursing practice and discipline are encouraged to be submitted as original article, review, case report, short communication and letters.

Topics covered by not limited to:

- Development of clinical and nursing research, evaluation, evidence-based practice and scientific enquiry
- Patients and family experiences of health care
- Clinical and nursing research to enhance patient safety and reduce harm to patients
- Ethics
- Clinical and Nursing history
- Medicine



Journal of Electronic Research and Application is an international, peer-reviewed and open access journal which publishes original articles, reviews, short communications, case studies and letters in the field of electronic research and application.

Topics covered but not limited to:

- Automation
- Circuit Analysis and Application
- Electric and Electronic Measurement Systems
- Electrical Engineering
- Electronic Materials
- Electronics and Communications Engineering
- Power Systems and Power Electronics
- Signal Processing
- Telecommunications Engineering
- Wireless and Mobile Communication